

Monomers and Polymers Based on Renewable Resources for New Photopolymer Coating

Berran Sanay

Univ.-Diss.

**to obtain the academic degree of
"Doctor of Natural Sciences"
(Dr. rer. nat.)
in the discipline Polymer Chemistry**

**submitted to
Faculty of Mathematics and Natural Sciences
University of Potsdam**

Committee

- 1.Prof. Dr. Veronika Strehmel**
- 2.Prof. Dr. André Laschewsky**
- 3.Prof. Dr. Yusuf Yagci**

30.07.2021

Unless otherwise indicated, this work is licensed under a Creative Commons License Attribution-NonCommercial 4.0 International.

This does not apply to quoted content and works based on other permissions.

To view a copy of this license visit:

<https://creativecommons.org/licenses/by-nc/4.0/>

Published online on the

Publication Server of the University of Potsdam:

<https://doi.org/10.25932/publishup-51868>

<https://nbn-resolving.org/urn:nbn:de:kobv:517-opus4-518684>

Foreword

First of all, I would like to thank my supervisor Prof. Veronika Strehmel for giving me the opportunity to continue my studies in Germany. It has been an honour to work as a PhD in her group. She has encouraged me continuously during our work in this period. Her comprehensive knowledge and vast experience helped me to extend my knowledge and skillset. It would be extremely difficult to complete my work without her guidance and encouragement. I am sure she will always be there to support and inspire me whenever I have difficulty or struggle in the rest of my academic life. I would especially like to thank her for initiating this new era in my life with this opportunity.

I am really grateful to Prof. Bernd Strehmel for his inspiring ideas and support. It has been a privilege for me to discuss with him about my research and getting new ideas, suggestions and valuable input for my thesis. He has made a great contribution to finish my PhD study. I would like to thank him for providing his full support and encouragement. I would also like to express my gratefulness to his group members, Dr. Ceren Kütahya, Dennis Oprych, Dr. Christian Schmitz, Dr. Yulian Pang, Paul Hermes, Lukas Appelhoff, Qunying Wang, for their friendship and assistance.

I would also like to thank Prof. André Laschewsky for being my mentor of doctoral study and giving me this opportunity to earn my PhD degree from the University of Potsdam.

I highly appreciate to have Prof. Yusuf Yagci in my PhD committee. His success, perseverance and pioneering publications have always been an inspiration for me.

I would also like to express my sincere thanks to Markus Heinz and Dr. Micheal Schmitt for offering a great working atmosphere and supporting me during this period with their friendship.

Finally, I would like to express my deep and sincere gratitude to my husband and my daughter for being a part of this challenging period and making it possible for me to complete my thesis. He has always been a big supporter of my academic career and does his best for me to pursue my education. Their love, patience, understanding and encouragement are indispensable for me.

Table of Contents

Foreword	II
Table of Contents	III
Abbreviations	VI
List of Schemes	IX
List of Figures	XI
List of Tables	XIV
Abstract	XVI
Kurzfassung	XX
1. Introduction	1
1.1. General Aspects	1
1.2 Motivation of the Thesis	3
2. Fundamentals and State of the Art	6
2.1 Photoinitiated Polymerization	6
2.1.1 Photoinitiated Free Radical Polymerization.....	7
2.1.1.1 Initiation	8
2.1.1.2 Propagation	10
2.1.1.3 Termination	11
2.1.2 Photoinitiated Cationic Polymerization	12
2.1.2.1 Onium Salts.....	12
2.1.2.2 Initiation	13
2.1.2.3 Propagation	14
2.1.2.4 Termination.....	14
2.2 Polymer Network Formation.....	14
3. Materials and Methods	17
3.1 Chemicals.....	17
3.1.1 Solvents.....	17
3.1.2 Reagents	17
3.2 Analytical Methods and Equipment	19
3.2.1 Nuclear Magnetic Resonance Spectroscopy (NMR).....	19
3.2.2 Contact Angle Measurement (CA).....	19
3.2.3 Gel Permeation Chromatography (GPC)	19

3.2.4 Photo Differential Scanning Calorimetry (Photo-DSC).....	19
3.2.5 Differential Scanning Calorimetry (DSC).....	20
3.2.6 Dynamic Mechanical Analysis (DMA).....	20
3.2.7 Thermal Measurement by Thermal Camera	21
3.2.8 Viscosity Measurement	21
3.2.9 Gel Content	21
3.3 Light Source UV-LED at 395 nm	21
4. Experimental Part.....	23
4.1 Sample Preparation.....	23
4.1.1 Photoinitiated Free Radical Polymerization.....	23
4.1.2 Photoinitiated Cationic Polymerization	23
4.2 Film Preparation	24
4.3 Photopolymerization Measurements	24
4.3.1 Temperature Dependent Photo-DSC Measurements.....	25
4.3.2 Time Dependent Photo-DSC Measurements	25
4.4 Thermal Polymerization.....	26
4.5 Synthetic Procedures	26
4.5.1 Synthesis of Ionic Liquids (1a and 1b)	26
4.5.2 Functionalization of Oleic Acid	27
4.5.2.1 Esterification of Oleic Acid with Methanol.....	28
4.5.2.2 Epoxidation of Oleic Acid Methyl Ester.....	28
4.5.2.3 Functionalization of 9,10-Epoxystearic Acid Methyl Ester by Ring Opening Reaction of the Oxirane Group with (Meth)acrylic Acid (2 and 3).....	29
4.5.2.4 Synthesis of the Isomer Mixture Comprising Methyl 9-(1H-imidazol-1-yl)-10- (methacryloyloxy)octadecanoate and Methyl 9-(Methacryloyloxy)-10-(1H-imidazol-1- yl)octadecanoate (4).....	30
4.5.3 Synthesis of 4-(4-Methacryloyloxyphenyl)-butan-2-one (7).....	31
4.5.4 Esterification of Oleic Acid with Ethylene Glycol	32
4.5.4.1 Epoxidation of Oleic Acid 1,2-Ethanedyl Ester	32
4.5.4.2 Ring Opening Reaction of Bis-(9,10-epoxystearic acid) 1,2-Ethanedyl Ester.....	33
5. Results and Discussion.....	36
5.1 Photoinitiated Polymerization of Monomers Modified from Oleic Acid Mix and Ionic Liquids	39
5.1.1 Comparison of Photopolymerization of Ionic Liquid Monomers (1a, 1b), Methyl 9- (Acryloyloxy)-10-hydroxyoctadecanoate / Methyl 9-Hydroxy-10-(acryloyloxy)octadecanoate (2) with 1,6-Hexanediol Diacrylate (5).....	40

5.1.2 Comparison of Photopolymerization of Methyl 9-(Methacryloyloxy)-10-hydroxyoctadecanoate / Methyl 9-Hydroxy-10-(methacryloyloxy)octadecanoate (3), Methyl 9-(1H-imidazol-1yl)-10-(methacryloyloxy)octadecanoate / Methyl 9-(Methacryloyloxy)-10-(1H-imidazol-1yl)octadecanoate (4) with 1,6-Hexanediol Dimethacrylate (6)	43
5.2 Comparison of Photopolymerization Kinetic of Monomers Bearing Methacrylate and Phenyl Groups (7, 8 and 9)	46
5.2.1 Photoinitiated Polymerization of 4-(4-Methacryloyloxyphenyl)-butan-2-one (7) at 40°C.....	46
5.2.2 Photoinitiated Polymerization of 4-(4-Methacryloyloxyphenyl)-butan-2-one (7) at Elevated Temperature	55
5.2.3 Comparison of 4-(4-Methacryloyloxyphenyl)-butan-2-one (7) with Further Methacrylates Comprising a Phenyl Moiety	58
5.3 Design of New Polymeric Networks Based on Green Methacrylates.....	61
5.3.1 Photoinitiated Homopolymerization of the Biobased Dimethacrylate (10)	62
5.3.2 Photoinitiated Copolymerization of the Biobased Dimethacrylate (10) with Methacrylate 7 and 4, Respectively.....	65
5.3.3 Crosslinked Films Derived by Photoinitiated Homopolymerization of the Biobased Dimethacrylate (10) and Copolymerization with Methacrylate 7 and 4, Respectively	70
5.4 Photoinitiated Cationic Polymerization of Biobased Epoxides in Comparison with Commercial Epoxides.....	74
5.4.1 Photoinitiated Polymerization of 9,10-Epoxy Stearates 11 and 12 in Comparison with the Commercial Cycloaliphatic Diepoxide 13 and Aliphatic Diepoxide 14	77
5.4.2 Photoinitiated Copolymerization of Bis-(9,10-epoxystearic acid) 1,2-Ethanediy Ester (12) with Bisphenol-A-diglycidylether (15).....	81
5.5 Surface-Wetting Characterization for Crosslinked Polymers by Contact Angle Measurement.....	85
6.Conclusion	92
References	98
Curriculum Vitae	111
Attachment	114

Abbreviations

DSC	Differential scanning calorimetry
Photo-DSC	Photo differential scanning calorimetry
GPC	Gel permeation chromatography
NMR	Nuclear magnetic resonance
DMA	Dynamic mechanical analysis
UV	Ultraviolet
ITX	Isopropylthioxanthone
Sens	Sensitizer
LED	Light emitting diode
Hg	Mercury
3D	Three dimensional
Vis	Visible
M_n	Number average molecular weight
M_w	Weight average molecular weight
\bar{D}	Dispersity
PI	Photoinitiator
PIS	Photoinitiating system
R	Radical
P	Polymer
ISC	Intersystem crossing
M	Monomer
IL	Ionic Liquid
R_p^{\max}	Maximum of the polymerization rate
t_{\max}	Time to obtain the maximum of the polymerization rate
COI	Coinitiator
k_d	Rate constant of decomposition
k_i	Rate constant of initiation
k_p	Rate constant of propagation
k_{tc}	Rate constant of termination by combination
k_{td}	Rate constant of termination by disproportionation
VOC	Volatile Organic Compound
Ivocerin®	Di(4-methoxybenzoyl)diethylgermane

Irgacure® TPO-L	Ethyl (2,4,6-trimethylbenzoyl) phenylphosphinate
S2617	Bis(<i>t</i> -butyl)-iodonium-tetrakis(perfluoro- <i>t</i> -butoxy)aluminate
ppm	Parts per million
PS	Photosensitizer
t	Time
h	Hour
min	Minute
sec	Second
M_c	Molecular weight between two crosslink points
E'	Storage modulus
E''	Loss modulus
CA	Contact angle
DABCO	1,4-Diazabicyclo(2.2.2)octane
DMAP	4- <i>N,N</i> -dimethyl amino pyridine
C_3H_6O	Acetone
$(CH_3)_3COCH_3$	<i>t</i> -Butyl methylether
Et_2O	Diethyl ether
CH_2Cl_2	Dichloromethane
MeOH	Methanol
<i>n</i> -Hex	<i>n</i> -Hexane
EtOAc	Ethyl acetate
C_4H_8O	Tetrahydrofuran
$CaCl_2$	Calcium chloride
$MgSO_4$	Magnesium sulfate
$NaHCO_3$	Sodium bicarbonate
NaOH	Sodium hydroxide
K_2CO_3	Potassium carbonate
HCl	Hydrochloric acid
H_2SO_4	Sulphuric acid
$LiNTf_2$	Lithium bis(trifluoromethylsulfonyl)imide
HQ	Hydroquinone
MEHQ	Monomethyl ether hydroquinone
BHT	Butylated hydroxytoluene
NA	Not analyzed

List of Schemes

Scheme 1: General illustration of the photopolymerization process.	6
Scheme 2: General presentation of photoinitiated free radical polymerization.	7
Scheme 3: Representation of intramolecular cyclization and intermolecular crosslinking	15

List of Figures

- Figure 1: Polymerization rate (R_p (s⁻¹)) as function of irradiation time (s) for photoinitiated polymerization of 1,6-hexanediol diacrylate (5), methyl 9-(acryloyloxy)-10-hydroxyoctadecanoate /methyl 9-hydroxy-10-(acryloyloxy)octadecanoate (2), N-octyl-N'-vinylimidazolium NTf2 (1a), and N-decyl-N'-vinylimidazolium NTf2 (1b) containing 1 wt % Irgacure® TPO-L. Irradiation was carried out at 40 °C for 10 min, adapted from [64].41
- Figure 2: Conversion as function of irradiation time (s) for photoinitiated polymerization of 1,6-hexanediol diacrylate (5), methyl 9-(acryloyloxy)-10-hydroxyoctadecanoate / methyl 9-hydroxy-10-(acryloyloxy)octadecanoate (2), N-octyl-N'-vinylimidazolium NTf2 (1a), and N-decyl-N'-vinylimidazolium NTf2 (1b) containing 1 wt % Irgacure® TPO-L. Irradiation was carried out at 40 °C for 10 min adapted from [64].43
- Figure 3: Polymerization rate (R_p (s⁻¹)) as function of irradiation time (s) for photoinitiated polymerization of 1,6-hexanediol dimethacrylate (6), methyl 9-(1H-imidazol-1yl)-10-(methacryloyloxy)octadecanoate / methyl 9-(methacryloyloxy)-10-(1H-imidazol-1yl)octadecanoate (4), methyl 9-(methacryloyloxy)-10-hydroxyoctadecanoate / methyl 9-hydroxy-10-(methacryloyloxy)octadecanoate (3), containing 1 wt % Irgacure® TPO-L. Irradiation was carried out at 40 °C for 10 min, adapted from [64].44
- Figure 4: Conversion as function of irradiation time (s) for photoinitiated polymerization of 1,6-hexanediol dimethacrylate (6), methyl 9-(1H-imidazol-1yl)-10-(methacryloyloxy)octadecanoate / methyl 9-(methacryloyloxy)-10-(1H-imidazol-1yl)octadecanoate (4), methyl 9-(methacryloyloxy)-10-hydroxyoctadecanoate / methyl 9-hydroxy-10-

(methacryloyloxy)octadecanoate (3) containing 1 wt % TPO-L. Irradiation was carried out at 40 °C for 10 min, adapted from [64].45

Figure 5: Polymerization rate (R_p (s⁻¹)) as function of irradiation time (s) for photoinitiated polymerization of 4-(4-methacryloyloxyphenyl)-butan-2-one (7) containing Irgacure® TPO-L (1 wt % and 3 wt %, respectively) or Ivocerin® (1 wt %) at 40 °C for 10 min, adapted from [112].47

Figure 6: Conversion as function of irradiation time (s) for photoinitiated polymerization of 4-(4- methacryloyloxyphenyl)-butan-2-one (7) containing Irgacure® TPO-L (1 wt % and 3 wt %, respectively) or Ivocerin® (1 wt %) at 40 °C for 10 min, adapted from [112].48

Figure 7: Temperature measured during irradiation of a pure glass substrate (blank) and glass substrates coated with monomer (7, 8, or 9) containing photoinitiator (Irgacure® TPO-L 1 wt % or 3 wt % or Ivocerin® 1wt%) with light of 395 nm for 10 min. The films were prepared on a glass substrate using the 120 µm side of a four-way film applicator to maintain comparable thickness for all films. The films on glass substrates were purged with nitrogen in a plastic box equipped with a quartz glass window before irradiation for 5 min. Then, irradiation was carried out in the nitrogen atmosphere using a 395 nm light source for 10 min, and the temperature changes were recorded during irradiation using a thermal camera (testo 0563 0885 V7), adapted from [112].49

Figure 8: DSC curves of photopolymerizing mixtures containing 1 wt % Irgacure® TPO-L and monomer 7 (T_g = -62 °C; $T_{recryst}$ = -12 °C; T_m = 26 °C), 8 (T_g = -71 °C), or 9 (T_m = 21 °C) after 6 s irradiation at 40°C in the photo-DSC, adapted from [112].50

Figure 9: DSC curves of photopolymerizing mixtures containing monomer and 1 wt % Irgacure® TPO-L (monomer 7: $T_g = -44\text{ }^\circ\text{C}$; 8: $T_g = -65\text{ }^\circ\text{C}$, and 9: $T_g = -81\text{ }^\circ\text{C}$; $T_{\text{ecryst}} = -33\text{ }^\circ\text{C}$; $T_m = 13\text{ }^\circ\text{C}$) after 15 s (7) or 20 s (8 and 9, respectively) irradiation at $40\text{ }^\circ\text{C}$ in the photo-DSC, adapted from [112].51

Figure 10: An overlay of GPC chromatograms (RI detector) of photopolymers obtained by photoinitiated polymerization of 4-(4-methacryloyloxyphenyl)-butan-2-one (7) containing 1 wt % Irgacure® TPO-L; a) in the photo-DSC pan at $40\text{ }^\circ\text{C}$ after irradiation for 6 s, 10 s, 15 s, 25 s, 30 s, and 10 min; b) after irradiation on a glass substrate outside of the photo-DSC at room temperature for 6 s and 10 min, respectively to isolate higher amount on purified polymer, adapted from [112].52

Figure 11: An overlay of GPC chromatograms (RI detector) of photopolymers obtained by photoinitiated polymerization of 4-(4-methacryloyloxyphenyl)-butan-2-one (7) containing 1 wt % Irgacure® TPO-L after an irradiation time at $85\text{ }^\circ\text{C}$ for 6 s, 20 s, 25 s, 30 s, and 10 min, adapted from [112].57

Figure 12: An overlay of GPC chromatograms (RI detector) of polymers obtained by photoinitiated polymerization of 4-(4-methacryloyloxyphenyl)-butan-2-one (7) containing 1 wt % Irgacure® TPO-L after irradiation at $85\text{ }^\circ\text{C}$ for 10 min (black line) compared with a polymer received by thermal polymerization in the presence of the photoinitiator at $85\text{ }^\circ\text{C}$ in the absence of light for 3 hours (red line), adapted from [112].57

Figure 13: Polymerization rate (R_p (s^{-1})) as function of irradiation time (s) for photoinitiated polymerization of 4-(4-methacryloyloxyphenyl)-butan-2-one (7), 2-phenoxyethyl methacrylate (8) and phenyl methacrylate (9) containing 1 wt % Irgacure® TPO-L at $40\text{ }^\circ\text{C}$ for 10 min, adapted from [112].58

- Figure 14: Conversion as function of irradiation time (s) for photoinitiated polymerization of 4-(4-methacryloyloxyphenyl)-butan-2-one (7), 2-phenoxyethyl methacrylate (8) and phenyl methacrylate (9) containing 1 wt % Irgacure® TPO-L at 40 °C for 10 min, adapted from [112].59
- Figure 15: Polymerization rate (R_p (s⁻¹)) as function of irradiation time (s) for photoinitiated polymerization of ethane-1,2-diyl bis(9-methacryloyloxy-10-hydroxy octadecanoate) / ethane-1,2-diyl 9-hydroxy-10-methacryloyloxy-9'-methacryloyloxy-10'-hydroxy octadecanoate / ethane-1,2-diyl bis(9-hydroxy-10-methacryloyloxy octadecanoate) (10) containing Irgacure® TPO-L (1 wt % and 3 wt %, respectively) or Ivocerin® (1 wt %) at 40 °C for 10 min, adapted from [113]......63
- Figure 16: Conversion as function of irradiation time (s) for photoinitiated polymerization of ethane-1,2-diyl bis(9-methacryloyloxy-10-hydroxy octadecanoate) / ethane-1,2-diyl 9-hydroxy-10-methacryloyloxy-9'-methacryloyloxy-10'-hydroxy octadecanoate / ethane-1,2-diyl bis(9-hydroxy-10-methacryloyloxy octadecanoate) (10) containing Irgacure® TPO-L (1 wt % and 3 wt %, respectively) or Ivocerin® (1 wt %) at 40 °C for 10 min, adapted from [113]......63
- Figure 17: Polymerization rate (R_p (s⁻¹)) as function of irradiation time (s) for photoinitiated copolymerization of ethane-1,2-diyl bis(9-methacryloyloxy-10-hydroxy octadecanoate) / ethane-1,2-diyl 9-hydroxy-10-methacryloyloxy-9'-methacryloyloxy-10'-hydroxy octadecanoate / ethane-1,2-diyl bis(9-hydroxy-10-methacryloyloxy octadecanoate) (10) and 4-(4-methacryloyloxyphenyl)-butan-2-one (7) (1:1, mol:mol) containing Irgacure® TPO-L (1 wt % and 3 wt %, respectively) or Ivocerin® (1 wt %) at 40 °C for

10 min, adapted from [113].....66

Figure 18: Conversion as function of irradiation time (s) for photoinitiated copolymerization of the ethane-1,2-diyl bis(9-methacryloyloxy-10-hydroxy octadecanoate) / ethane-1,2-diyl 9-hydroxy-10-methacryloyloxy-9'-methacryloyloxy-10'-hydroxy octadecanoate / ethane-1,2-diyl bis(9-hydroxy-10-methacryloyloxy octadecanoate) (10) and 4-(4-methacryloyloxyphenyl)-butan-2-one (7) (1:1, mol:mol) containing Irgacure® TPO-L (1 wt % and 3 wt %, respectively) or Ivocerin® (1 wt %) at 40 °C for 10 min, adapted from [113].....66

Figure 19: Polymerization rate (R_p (s⁻¹)) as function of irradiation time (s) for photoinitiated copolymerization of ethane-1,2-diyl bis(9-methacryloyloxy-10-hydroxy octadecanoate) / ethane-1,2-diyl 9-hydroxy-10-methacryloyloxy-9'-methacryloyloxy-10'-hydroxy octadecanoate / ethane-1,2-diyl bis(9-hydroxy-10-methacryloyloxy octadecanoate) (10) and 4-(4-methacryloyloxyphenyl)-butan-2-one (7) (1:9, mol:mol) containing Irgacure® TPO-L (1 wt % and 3 wt %, respectively) or Ivocerin® (1 wt %) at 40 °C for 10 min, adapted from [113].....67

Figure 20: Conversion as function of irradiation time (s) for photoinitiated copolymerization of ethane-1,2-diyl bis(9-methacryloyloxy-10-hydroxy octadecanoate) / ethane-1,2-diyl 9-hydroxy-10-methacryloyloxy-9'-methacryloyloxy-10'-hydroxy octadecanoate / ethane-1,2-diyl bis(9-hydroxy-10-methacryloyloxy octadecanoate) (10) and 4-(4-methacryloyloxyphenyl)-butan-2-one (7) (1:9, mol:mol) containing Irgacure® TPO-L (1 wt % and 3 wt %, respectively) or Ivocerin® (1 wt %) at 40 °C for 10 min, adapted from [113].....68

Figure 21: Polymerization rate (R_p (s⁻¹)) as function of irradiation time (s) for photoinitiated copolymerization of ethane-1,2-diyl bis(9-methacryloyloxy-10-hydroxy octadecanoate) / ethane-1,2-diyl 9-hydroxy-10-methacryloyloxy-9'-methacryloyloxy-10'-hydroxy octadecanoate / ethane-1,2-diyl bis(9-hydroxy-10-methacryloyloxy octadecanoate) (10) and methyl 9-(1H-imidazol-1-yl)-10-(methacryloyloxy)octadecanoate / methyl 9-(methacryloyloxy)-10-(1H-imidazol-1-yl)octadecanoate (4) (1:9, mol:mol) containing Irgacure® TPO-L (1 wt % and 3 wt %, respectively) or Ivocerin® (1 wt %) at 40 °C for 10 min, adapted from [113].69

Figure 22: Conversion as function of irradiation time (s) for photoinitiated copolymerization of the ethane-1,2-diyl bis(9-methacryloyloxy-10-hydroxy octadecanoate) / ethane-1,2-diyl 9-hydroxy-10-methacryloyloxy-9'-methacryloyloxy-10'-hydroxy octadecanoate / ethane-1,2-diyl bis(9-hydroxy-10-methacryloyloxy octadecanoate) (10) and methyl 9-(1H-imidazol-1-yl)-10-(methacryloyloxy)octadecanoate / methyl 9-(methacryloyloxy)-10-(1H-imidazol-1-yl)octadecanoate (4) (1:9, mol:mol) containing Irgacure® TPO-L (1 wt % and 3 wt %, respectively) or Ivocerin® (1 wt %) at 40 °C for 10 min, adapted from [113].69

Figure 23: Overlay of loss modulus (MPa) as function of temperature (°C) measured by DMA on homopolymer (poly-10) and copolymer (co-(10-7)) (stiochiometric ratio of the monomers and molar ratio=1:9) an co-(10-4) (molar ratio=1:9) films, adapted from [113].71

Figure 24: Polymerization rate (R_p (s⁻¹)) as function of irradiation time (s) for photoinitiated polymerization of 9,10-epoxystearic acid methyl ester (11), bis-(9,10-epoxystearic acid) 1,2-ethanediyl ester (12), 3',4'-

epoxycyclohexylmethyl-3',4'-epoxycyclohexane carboxylate (13) and 1,4-butanediol diglycidyl ether (14) containing ITX and S2617 by constant radiation power of 180 mW.cm⁻² for 20 min irradiation at 60 °C, adapted from [114].78

Figure 25: Conversion as function of irradiation time (s) for photoinitiated polymerization of 9,10-epoxystearic acid methyl ester (11), bis-(9,10-epoxystearic acid) 1,2-ethanediyl ester (12), 3',4'-epoxycyclohexylmethyl 3',4'-epoxycyclohexane carboxylate (13) and 1,4-butanediol diglycidyl ether (14) containing ITX and S2617 by constant radiation power of 180 mW.cm⁻² for 20 min irradiation at 60 °C, adapted from [114].78

Figure 26: Polymerization rate (R_p (s⁻¹)) as function of irradiation time (s) for photoinitiated polymerization of 15, 12:15 (1:1, mol:mol), 12:15 (1:5, mol:mol) and 12:15 (1:9, mol:mol) containing ITX and S2617 by constant radiation power of 180 mW.cm⁻² for 20 min irradiation at 60 °C, adapted from [114]. .83

Figure 27: Conversion as function of irradiation time (s) for photoinitiated polymerization of 15, 12:15 (1:1, mol:mol), 12:15 (1:5, mol:mol) and 12:15 (1:9, mol:mol) containing ITX and S2617 by constant radiation power of 180 mW.cm⁻² for 20 min irradiation at 60 °C, adapted from [114].83

List of Tables

Table 1: Structure of type I photoinitiators.....	18
Table 2: Structure of onium salt.....	18
Table 3: Structure of the monomers used in the following sections. Two isomers of 2, 3, and 4 and three isomers of 10 were drawn, respectively.....	37
Table 4: Maximum of the polymerization rate (R_{pmax}) , time (t_{max}) to obtain the maximum of polymerization rate, and final conversion for photoinitiated polymerization of the ionic liquids 1a and 1b, methyl 9-((meth)acryloyloxy)-10-hydroxyoctadecanoate / methyl 9-hydroxy-10-((meth)acryloyloxy)octadecanoate 2 and 3, methyl 9-(1H-imidazol-1yl)-10-(methacryloyloxy)octadecanoate / methyl 9-(methacryloyloxy)-10-(1H-imidazol-1yl)octadecanoate 4, and the commercial di(meth)acrylates 5 and 6 containing either Irgacure® TPO-L (1 wt % and 3 wt %, respectively) and Ivocerin® (1 wt %) as photoinitiator for 10 min irradiation time at 40 °C , adapted from [64]).	42
Table 5: Maximum polymerization rate (R_{pmax}) , time (t_{max}) to obtain the maximum polymerization rate and final conversion for photoinitiated polymerization of 4-(4-methacryloyloxyphenyl)-butan-2-one (7) in the presence of Irgacure® TPO-L (1 wt % and 3 wt %, respectively) or Ivocerin® (1 wt %), and 2-phenoxyethyl methacrylate (8) as well as phenyl methacrylate (9) containing each TPO-L (1 wt %) for 10 min irradiation time at 40 °C , adapted from [112].....	48

Table 6: Temperature measured after irradiation of a pure glass substrate (blank) and glass substrates coated with monomer (7, 8, or 9) containing photoinitiator (1 wt % or 3 wt % Irgacure® TPO-L or 1 wt % Ivocerin®) with light of 395 nm after 10 min of irradiation, adapted from [112].50

Table 7: Monomer conversion obtained from both photo-DSC and ¹H-NMR measurements, number average molecular weight (M_n), weight average molecular weight (M_w), and dispersity (\mathcal{D}) of the polymer obtained during photoinitiated polymerization of 7, 8, and 9 using 1 wt % Irgacure® TPO-L at a given temperature (T) after selected irradiation time (t), adapted from [112].52

Table 8: Glass transition temperature (T_g), number average molecular weight (M_n), weight average molecular weight (M_w), and dispersity (\mathcal{D}) of purified polymers obtained either by photoinitiated polymerization of 7, 8, and 9 using 1 wt % Irgacure® TPO-L at a given temperature (T) after selected irradiation time (t) on a glass substratea) or thermal initiated polymerization in the presence of the photoinitiator at 85 °C in the absence of lightb) adapted from [112].53

Table 9: Polymerization temperature (T), irradiation time (t), glass transition temperature (T_g), recrystallization temperature during heating ($T_{recryst}$), melting temperature (T_m), enthalpy of recrystallization ($\Delta H_{recryst}$), enthalpy of melting (ΔH_m) obtained during photoinitiated polymerization of 7, 8, and 9 using 1 wt % Irgacure® TPO-L at a given temperature (T) after selected irradiation time (t), adapted from [112]. ..54

Table 10: Polymerization temperature (T), maximum of the polymerization rate (R_{pmax}), time (t_{max}) to obtain the maximum of the polymerization rate,

and final monomer conversion (%) for photoinitiated polymerization of 4-(4-methacryloyloxyphenyl)-butan-2-one (7), 2-phenoxyethyl methacrylate (8), and phenyl methacrylate (9) containing 1 wt % Irgacure® TPO-L each after 10 min irradiation at various temperatures, adapted from [112].55

Table 11: Maximum of the polymerization rate (R_{pmax}), time (t_{max}) to obtain the maximum of the polymerization rate, and final conversion for photoinitiated polymerization of the ethane-1,2-diyl bis(9-methacryloyloxy-10-hydroxy octadecanoate) / ethane-1,2-diyl 9-hydroxy-10-methacryloyloxy-9'-methacryloyloxy-10'-hydroxy octadecanoate / ethane-1,2-diyl bis(9-hydroxy-10-methacryloyloxy octadecanoate) (10), 4-(4-methacryloyloxyphenyl)-butan-2-one (7), methyl 9-(1H-imidazol-1yl)-10-(methacryloyloxy)octadecanoate / methyl 9-(methacryloyloxy)-10-(1H-imidazol-1yl)octadecanoate (4), as well as the mixtures of 10 and 7 (molar ratio= 1:1 and 1:9, respectively) as well as 10 and 4 (molar ratio= 1:9) using either Irgacure® TPO-L (1 wt % and 3 wt %, respectively) or Ivocerin® (1 wt%) as photoinitiator and 10 min irradiation time at 40°C, adapted from [113].64

Table 12: Glass transition temperatures of the homopolymer (poly-10), and copolymers (co-10-7) (1:1, mol:mol), co-(10-7) (1:9, mol:mol) and co-(10-4) (1:9, mol:mol) films, adapted from [113].72

Table 13: Density of the crosslinked films, temperature used for calculation of the crosslink density (Trubbery) using both the real part of the elastic modulus (E') and density of the films, crosslinks density, and molecular weight between crosslink points (M_c) for poly-10, co-(10-7) (1:1,

mol:mol), co-(10-7) (1:9, mol:mol) and co-(10-4) (1:9, mol:mol) films, adapted from [113].74

Table 14: Structure of the monomers used in this section, adapted from [114].75

Table 15: Melting temperature (T_m , °C) and glass transition temperature (T_g , °C) obtained by DSC measurements of 9,10-epoxystearic acid methyl ester (11), bis-(9,10-epoxystearic acid) 1,2-ethanediyl ester (12), 3',4'-epoxycyclohexylmethyl-3',4'-epoxycyclohexane carboxylate (13), 1,4-butanediol diglycidyl ether (14) and bisphenol-A-diglycidylether (15) as well as the mixtures of 12:15 (molar ratio of 12:15 = 1:1, 1:5 and 1:9) and additionally viscosity (η , mPa.s) of the monomers and monomer mixtures (molar ratio of 12:15 = 1:1, 1:5 and 1:9) at 60 °C at a given shear rate ($\dot{\gamma}$, 1/s) where the viscosity becomes independent on the shear rate or if the viscosity is independent on the shear rate at all (*) and viscosity (η , mPa.s) at 23 °C for liquid monomers at room temperature, adapted from [114].76

Table 16: Maximum of the polymerization rate (R_{pmax}), time (t_{max}) to obtain the maximum of the polymerization rate, and final conversion for photoinitiated polymerization of 9,10-epoxystearic acid methyl ester (11), bis-(9,10-epoxystearic acid) 1,2-ethanediyl ester (12), and 3',4'-epoxycyclohexylmethyl 3',4'-epoxycyclohexane carboxylate (13) and 1,4-butanediol diglycidyl ether (14) using ITX and S2617 and 20 min irradiation time at 60°C, adapted from [114].79

Table 17: Glass transition temperature (T_g , °C) and gel content of the polymers derived from 9,10-epoxystearic acid methyl ester (11), 9,10-epoxystearic acid 1,2-ethane diyl ester (12), and 3',4'-

epoxycyclohexylmethyl-3',4'-epoxycyclohexane carboxylate (13), 1,4-butanediol diglycidyl ether (14) and bisphenol-A-diglycidylether (15), adapted from [114].80

Table 18: Maximum of the polymerization rate (R_{pmax}), time (t_{max}) to obtain the maximum of the polymerization rate, and final conversion for photoinitiated polymerization of 15, 12:15 (1:1, mol:mol), 12:15 (1:5, mol:mol) and 12:15 (1:9, mol:mol) using ITX and aluminate and 20 min irradiation time at 60 °C, adapted from [114].83

Table 19: Glass transition temperature and secondary relaxation* (e. g. β relaxation) of the isolated polymers made of the samples of 15, 12:15 (1:1, mol:mol), 12:15 (1:5, mol:mol) and 12:15 (1:9, mol:mol) containing ITX and S2617. *secondary relaxation in the $\tan \delta$ curve and loss modulus curve, respectively may be attributed to non-reacted monomer (in case of poly-13) or β relaxation (in case of poly-15 and poly-(12-15)), adapted from [114].84

Table 20: Crosslink density of the isolated polymers made from 15,13, and 12:15 mixtures (molar ratio 12:15 = 1:1; 1:5; 1:9), respectively using ITX and S2617 for photoinitiated polymerization, adapted from [114].85

Table 21: Contact angles for distilled water, ethylene glycol and diiodomethane measured on the crosslinked films of poly-10, co-(10-7) (1:1, mol:mol), co-(10-7) (1:9, mol:mol), co-(10-4) (1:9, mol:mol), poly-12, poly-13, poly-14, poly-15, co-(12-15) (1:1, mol:mol), co-(12-15) (1:5, mol:mol) and co-(12-15) (1:9, mol:mol) made by photoinitiated polymerization. Toluene is also used as an additional solvent for the films modified from

epoxies(12,13,14,15), adapted from [113, 114].86

Table 22: Surface free energy (σ_s), polar (σ_{sp}) and dispersion (σ_{sd}) components of

the surface free energy for the films of poly-10, co-(10-7) (1:1, mol:mol), co-(10-7) (1:9, mol:mol), co-(10-4) (1:9, mol:mol), poly-12, poly-13, poly-14, poly-15, co-(12-15) (1:1, mol:mol), co-(12-15) (1:5, mol:mol) and co-(12-15) (1:9, mol:mol) made by photoinitiated polymerization, adapted from [113, 114].89

Abstract

The present work focuses on minimising the usage of toxic chemicals by integration of the biobased monomers, derived from fatty acid esters, to photopolymerization processes, which are known to be nature friendly. Internal double bond present in the oleic acid was converted to more reactive (meth)acrylate or epoxy group. Biobased starting materials, functionalized by different pendant groups, were used for photopolymerizing formulations to design of new polymeric structures by using ultraviolet light emitting diode (UV-LED) (395 nm) via free radical polymerization or cationic polymerization.

New (meth)acrylates (**2,3** and **4**) consisting of two isomers, methyl 9-((meth)acryloyloxy)-10-hydroxyoctadecanoate / methyl 9-hydroxy-10-((meth)acryloyloxy)octadecanoate (**2** and **3**) and methyl 9-(1H-imidazol-1-yl)-10-(methacryloyloxy)octadecanoate / methyl 9-(methacryloyloxy)-10-(1H-imidazol-1-yl)octadecanoate (**4**), modified from oleic acid mix, and ionic liquid monomers (**1a** and **1b**) bearing long alkyl chain were polymerized photochemically. New (meth)acrylates are based on vegetable oil, and ionic liquids (ILs) have nonvolatile behaviour. Therefore, both monomer types have green approach. Photoinitiated polymerization of new (meth)acrylates and ionic liquids was investigated in the presence of ethyl (2,4,6-trimethylbenzoyl) phenylphosphinate (Irgacure® TPO-L) or di(4-methoxybenzoyl)diethylgermane (Ivocerin®) as photoinitiator (PI). Additionally, the results were discussed in comparison with those obtained from commercial 1,6-hexanediol di(meth)acrylate (**5** and **6**) for deeper investigation of biobased monomer's potential to substitute petroleum derived materials with renewable resources for possible coating applications. Kinetic study shows that methyl 9-(1H-imidazol-1-yl)-10-(methacryloyloxy)octadecanoate / methyl 9-(methacryloyloxy)-10-(1H-imidazol-1-yl)octadecanoate (**4**) and ionic liquids (**1a** and **1b**) have quantitative conversion after irradiation process which is important for practical applications. On the other hand, heat generation occurs in a longer time during the polymerization of biobased systems or ILs.

The poly(meth)acrylates modified from (meth)acrylated fatty acid methyl ester monomers generally show a low glass transition temperature because of the presence of long aliphatic chain in the polymer structure. However, poly(meth)acrylates containing aromatic group have higher glass transition temperature. Therefore, new 4-(4-methacryloyloxyphenyl)-butan-2-one (**7**) was synthesized which can be a promising candidate for the green techniques, such as light induced polymerization. Photokinetic

investigation of the new monomer, 4-(4-methacryloyloxyphenyl)-butan-2-one (**7**), was discussed using Irgacure® TPO-L or Ivocerin® as photoinitiator. The reactivity of that monomer was compared to commercial 2-phenoxyethyl methacrylate (**8**) and phenyl methacrylate (**9**) basis of the differences on monomer structures. The photopolymer of 4-(4-methacryloyloxyphenyl)-butan-2-one (**7**) might be an interesting candidate for the coating application with the properties of quantitative conversion and high molecular weight. It also shows higher glass transition temperature.

In addition to the linear systems based on renewable materials, new crosslinked polymers were also designed in this thesis. Therefore, isomer mixture consisting of ethane-1,2-diyl bis(9-methacryloyloxy-10-hydroxy octadecanoate), ethane-1,2-diyl 9-hydroxy-10-methacryloyloxy-9'-methacryloyloxy-10'-hydroxy octadecanoate and ethane-1,2-diyl bis(9-hydroxy-10-methacryloyloxy octadecanoate) (**10**) was synthesized by derivation of the oleic acid which has not been previously described in the literature. Crosslinked material based on this biobased monomer was produced by photoinitiated free radical polymerization using Irgacure® TPO-L or Ivocerin® as photoinitiator. Furthermore, material properties were diversified by copolymerization of **10** with 4-(4-methacryloyloxyphenyl)-butan-2-one (**7**) or methyl 9-(1H-imidazol-1-yl)-10-(methacryloyloxy)octadecanoate / methyl 9-(methacryloyloxy)-10-(1H-imidazol-1-yl)octadecanoate (**4**). In addition to this, influence of comonomer with different chemical structure on the network system was investigated by analysis of thermo-mechanical properties, crosslink density and molecular weight between two crosslink junctions. An increase in the glass transition temperature caused by copolymerization of biobased monomer **10** with the excess amount of 4-(4-methacryloyloxyphenyl)-butan-2-one (**7**) was confirmed by both techniques, differential scanning calorimetry (DSC) and dynamic mechanical analysis (DMA). On the other hand, crosslink density decreased as a result of copolymerization reactions due to the reduction in the mean functionality of the system. Furthermore, surface characterization has been tested by contact angle measurements using solvents with different polarity.

This work also contributes to the limited data reported about cationic photopolymerization of the epoxidized vegetable oils in the literature in contrast to the widely investigation of thermal curing of the biorenewable epoxy monomers. In addition to the 9,10-epoxystearic acid methyl ester (**11**), a new monomer of bis-(9,10-epoxystearic acid) 1,2-ethanediyl ester (**12**) has been synthesized from oleic acid. These two biobased epoxies have been polymerized via cationic photoinitiated polymerization in the presence of bis(*t*-butyl)-

iodonium-tetrakis(perfluoro-*t*-butoxy)aluminate ($[\text{Al}(\text{O}-t\text{-C}_4\text{F}_9)_4]^+$) and isopropylthioxanthone (ITX) as photoinitiating system. Polymerization kinetic of 9,10-epoxystearic acid methyl ester (**11**) and bis-(9,10-epoxystearic acid) 1,2-ethanediyl ester (**12**) was investigated and compared with the kinetic of commercial monomers being 3,4-epoxycyclohexylmethyl-3',4'-epoxycyclohexane carboxylate (**13**), 1,4-butanediol diglycidyl ether (**14**), and diglycidylether of bisphenol-A (**15**). Both biobased epoxies (**11** and **12**) showed higher conversion than cycloaliphatic epoxy (**13**), and lower reactivity than 1,4-butanediol diglycidyl ether (**14**). Additional network systems were designed by copolymerization of bis-(9,10-epoxystearic acid) 1,2-ethanediyl ester (**12**) and diglycidylether of bisphenol-A (**15**) in different molar ratios (1:1; 1:5; 1:9). It addresses that, final conversion is dependent on polymerization rate as well as physical processes such as vitrification during polymerization. Moreover, low glass transition temperature of homopolymer derived from bis-(9,10-epoxystearic acid) 1,2-ethanediyl ester (**12**) was successfully increased by copolymerization with diglycidylether bisphenol-A (**15**). On the other hand, the surface produced from bis-(9,10-epoxystearic acid) 1,2-ethanediyl ester (**12**) shows hydrophobic character. Higher concentration of biobased diepoxy (**12**) in the copolymerizing mixture decreases surface free energy. Network systems were also investigated according to the rubber elasticity theory. Crosslinked polymer derived from the mixture of bis-(9,10-epoxystearic acid) 1,2-ethanediyl ester (**12**) and diglycidylether of bisphenol-A (**15**) (molar ratio=1:5) exhibits almost ideal polymer network.

Kurzfassung

Die vorliegende Arbeit konzentriert sich auf die Minimierung des Einsatzes von giftigen Chemikalien durch die Integration von biobasierten Monomeren, die aus Fettsäureestern gewonnen werden, in Photopolymerisationsprozessen, die als naturfreundlich bekannt sind. Die in der Ölsäure vorhandene interne Doppelbindung wurde in eine reaktivere (Meth)acrylat- oder Epoxidgruppe umgewandelt. Biobasierte Ausgangsmaterialien, funktionalisiert durch verschiedene Seitengruppen, wurden für photopolymerisierende Formulierungen verwendet, um neue polymere Strukturen unter Verwendung einer ultravioletten lichtemittierenden Diode (UV-LED) (395 nm) über freie radikalische Polymerisation oder kationische Polymerisation zu entwickeln.

Neue (Meth)acrylate, Methyl-9-((meth)acryloyloxy)-10-hydroxyoctadecanoat / Methyl-9-hydroxy-10-((meth)acryloyloxy)octadecanoat (**2** und **3**) und Methyl-9-(methacryloyloxy)-10-(1H-imidazol-1yl)octadecanoat / Methyl-9-(1H-imidazol-1yl)-10-(methacryloyloxy)octadecanoat (**4**), modifiziert aus einem Ölsäuregemisch und ionischen flüssigen Monomeren mit einer langen Alkylkette wurden photochemisch polymerisiert. Die neuen (Meth)acrylate basieren auf Pflanzenöl. Die ionischen Flüssigkeiten (ILs) haben ein nichtflüchtiges Verhalten. Daher haben beide Monomertypen einen grünen Ansatz. Photoinitierte Polymerisationen von neuen (Meth)acrylaten und ionischen Flüssigkeiten wurden in Gegenwart von Ethyl-(2,4,6-trimethylbenzoyl)phenylphosphinat (Irgacure® TPO-L) oder Di(4-methoxybenzoyl)diethylgerman (Ivocerin®) als Photoinitiator untersucht. Zusätzlich wurden die Ergebnisse im Vergleich mit denen von kommerziellem 1,6-hexandiol di(meth)acrylat (**5** und **6**) diskutiert, um das Potenzial von biobasierten Monomeren zur Substitution von erdölbasierten Materialien durch erneuerbare Ressourcen für mögliche Beschichtungsanwendungen genauer zu untersuchen. Die kinetische Studie zeigt, dass Methyl-9-(1H-imidazol-1yl)-10-(methacryloyloxy)octadecanoat / Methyl-9-(methacryloyloxy)-10-(1H-imidazol-1yl)octadecanoat (**4**) und die ionischen Flüssigkeiten (**1a** und **1b**) eine quantitative Umsetzung nach dem Bestrahlungsprozess aufweisen, was für praktische Anwendungen wichtig ist. Andererseits erfolgt die Wärmeentwicklung bei der Polymerisation von biobasierten Systemen oder ILs in einem längeren Zeitraum.

Die aus Fettsäuren hergestelltem modifizierten Poly(meth)acrylate zeigen im Allgemeinen eine niedrige Glasübergangstemperatur aufgrund der Anwesenheit einer langen aliphatischen Kette in der Polymerstruktur. Poly(meth)acrylate, die eine aromatische

Gruppe enthalten, haben jedoch eine höhere Glasübergangstemperatur. Daher wurde das neue 4-(4-Methacryloyloxyphenyl)-butan-2-on (**7**) synthetisiert, das ein vielversprechender Kandidat für die grünen Techniken, wie zum Beispiel die lichtinduzierte Polymerisation, sein kann. Die photokinetische Untersuchung des neuen Monomers, 4-(4-Methacryloyloxyphenyl)-butan-2-on (**7**), wurde unter Verwendung von Irgacure® TPO-L oder Ivocerin® als Photoinitiator diskutiert. Die Reaktivität dieses Monomers wurde mit kommerziellem 2-Phenoxyethylmethacrylat (**8**) und Phenylmethacrylat (**9**) aufgrund der Unterschiede in der Monomerstruktur verglichen. Das Photopolymer von 4-(4-Methacryloyloxyphenyl)-butan-2-on (**7**) könnte ein interessanter Kandidat und eine Alternative zu den herkömmlichen Monomeren für die Beschichtungsanwendung sein aufgrund der quantitativen Umsetzung des Monomeren und des hohen Molekulargewichts sowie einer höheren Glasübergangstemperatur des resultierenden Photopolymeren.

Neben den linearen Systemen auf Basis nachwachsender Rohstoffe wurden in dieser Arbeit auch neue vernetzte Polymere entwickelt. So wurde ein Ethan-1,2-diyl bis(9-methacryloyloxy-10-hydroxy octadecanoate), Ethane-1,2-diyl 9-hydroxy-10-methacryloyloxy-9'-methacryloyloxy-10'-hydroxy octadecanoat und Ethane-1,2-diyl bis(9-hydroxy-10-methacryloyloxy octadecanoat) (**10**) Monomer mit zwei funktionellen Gruppen durch weitere Derivatisierung der Ölsäure synthetisiert, das bisher in der Literatur nicht beschrieben wurde. Ein vernetztes Material auf Basis dieses biobasierten Monomers wurde durch photoinitierte, radikalische Polymerisation unter Verwendung von Irgacure® TPO-L oder Ivocerin® als Photoinitiator hergestellt. Darüber hinaus wurden die Materialeigenschaften durch Copolymerisation des **10** mit 4-(4-Methacryloyloxyphenyl)-butan-2-on (**7**) oder Methyl-9-(1H-imidazol-1yl)-10-(methacryloyloxy)-octadecanoat / Methyl-9-(methacryloyloxy)-10-(1H-imidazol-1yl)-octadecanoat (**4**) variiert. Darüber hinaus wurde der Einfluss von Comonomeren mit unterschiedlicher chemischer Struktur auf das Netzwerksystem durch Analyse der mechanischen Eigenschaften, der Glasübergangstemperaturen, der Vernetzungsdichte und des Molekulargewichts zwischen zwei Vernetzungsstellen untersucht. Eine Erhöhung der Glasübergangstemperatur durch die Copolymerisation von **10** mit einem Überschuss von 4-(4-Methacryloyloxyphenyl)-butan-2-on (**7**) wurde durch DSC und DMA bestätigt. Andererseits verringerte sich die Vernetzungsdichte aufgrund der Verringerung der mittleren Funktionalität des Systems. Darüber hinaus wurde die Oberflächencharakterisierung durch Kontaktwinkelmessungen unter Verwendung von Lösungsmitteln mit unterschiedlicher Polarität getestet.

Diese Arbeit trägt auch zur Erweiterung der in der Literatur über die kationische Photopolymerisation der epoxidierten Pflanzenöle berichteten Erkenntnisse bei, die, im Gegensatz zu den weit verbreiteten Untersuchungen zur thermischen Härtung der biobasierten Epoxidmonomere nur begrenzt verfügbar sind. Zusätzlich zum 9,10-Epoxystearinsäuremethylester (**11**) wurde ein neues Monomer Bis-(9,10-epoxystearinsäure)-1,2-ethandylester (**12**) auf der Basis von Ölsäure synthetisiert. Diese beiden biobasierten Epoxide wurden durch kationische photoinitierte Polymerisation in Gegenwart von Bis(*t*-butyl)-iodonium-tetrakis(perfluor-*t*-butoxy)aluminat ($[Al(O-t-C_4F_9)_4]$ -) und Isopropylthioxanthon (ITX) als photostimulierendes System polymerisiert. Die Polymerisationskinetik von 9,10-Epoxystearinsäuremethylester (**11**) und Bis-(9,10-epoxystearinsäure)-1,2-ethandylester (**12**) wurde untersucht und mit der Kinetik der kommerziellen Monomere 3,4-Epoxycyclohexylmethyl-3',4'-epoxycyclohexancarboxylat (**13**), 1,4-Butandiol diglycidylether (**14**) und Diglycidylether von Bisphenol-A (**15**) verglichen. Beide biobasierten Epoxide (**11** und **12**) zeigten eine höhere Umwandlung als das cycloaliphatische Epoxid (**13**) und eine geringere als 1,4-Butandiol diglycidylether (**14**). Weitere Netzwerksysteme wurden durch Copolymerisation von Bis-(9,10-epoxystearinsäure)-1,2-ethandylester (**12**) und Diglycidylether von Bisphenol-A (**15**) in verschiedenen molaren Verhältnissen (1:1; 1:5; 1:9) hergestellt. Es wird angesprochen, dass der endgültige Umsatz sowohl von der Polymerisationsgeschwindigkeit als auch von physikalischen Prozessen wie der Verglasung während der Polymerisation abhängig ist. Darüber hinaus wurde die niedrige Glasübergangstemperatur des Homopolymers aus Bis-(9,10-epoxystearinsäure)-1,2-ethandylester (**12**) durch Copolymerisation mit Diglycidylether von Bisphenol-A (**15**) erfolgreich erhöht. Andererseits zeigt die aus Bis-(9,10-epoxystearinsäure) 1,2-ethandylester (**12**) hergestellte Oberfläche einen hydrophoben Charakter. Eine höhere Konzentration des biobasierten difunktionellen Epoxids (**12**) in der Copolymerisationsmischung verringert die freie Oberflächenenergie. Die Netzwerksysteme wurden auch unter Einsatz der Gummielastizitätstheorie untersucht. Das vernetzte Polymer, das aus der Mischung von Bis-(9,10-epoxystearinsäure) 1,2-ethandylester (**12**) und Diglycidylether von Bisphenol-A (**15**) (Molverhältnis=1:5) hergestellt wurde, zeigt ein nahezu ideales Polymernetzwerk.

1. Introduction

1.1. General Aspects

There has been a growing interest in the research conducted to ensure that the standards of chemical processes and production of chemicals meet the requirements of the green chemistry in the past decade. It is due to both depletion of the fossil reserves and an increase in environmental awareness. The basis of the technologies for manufacturing polymeric materials has been focused on systems activated by light. Designing polymeric materials derived by photopolymerization is a highly effective and widespread technique, and it is still developing rapidly [1-2]. The photopolymerizing formulations are usually prepared from petroleum derived materials. However, there has been an increasing demand in alteration of renewable feedstocks because of the environmental concerns [3-5]. Vegetable oils are promising candidates to replace petroleum based products with sustainable sources because they are environmental friendly, inexpensive and abundant. Additionally, they bear functional groups such as hydroxy, epoxy, carboxyl and C=C, which enable to increase reactivity by functionalization.

Chemists have integrated photochemical strategies on different chemical syntheses in consideration of the self-generated reactions in nature [6-8]. Thus, light is one of the reagent that is employed in the area of chemistry in various techniques [1,8-9]. Photochemistry is a technique that works on the basis of the interaction of light with light sensitive chemicals in chemistry, biology and materials science. Photochemical technique has been presented as environmentally friendly due to the properties of low-energy requirement, volatile organic compound (VOC) free formulations and room temperature operation [10-13]. Moreover, employment of light to initiate the reaction highlights one type of energy efficient method that addresses to one principle of green chemistry.

In principal, light supplies activation energy, which is required for various reactions. Light sensitive molecule is excited by absorption of light and initiates the photochemical reaction. Reactive species are produced as a result of a photochemical reaction in the excited state of the molecule after the absorption of light, which efficiently initiates the polymerization reaction [1].

Photoinduced polymerization has been widely used in polymer chemistry. In principle, polymerization is induced by a light source. Photopolymerization processes have been met growth interest in different conventional applications in coatings, inks, adhesives, and microelectronics [14]. Furthermore, this technique has been effectively applied in dentistry, 3D printings, laser printing images, as well as bioapplications such as drug delivery

systems, tissue engineering and implants [14-16]. Since its benefits over to the conventional polymerization technique have been explored, photopolymerization has also been widely used for synthetic polymer chemistry. Liquid or viscous monomers are chemically converted to the solid polymers after initiation of the photopolymerization with light-sensitive initiator. Polymer networks are produced by linkage of the growing chains bearing different functional groups. Network systems exhibit improvements in both thermal and mechanical properties, which play a key role in applications as a material or coating. Polymer networks show high hardness, shock resistance and low solubility or swelling capacity which depend on the degree of crosslinking [17-19]. Three dimensional structures are designed from the monomers or prepolymers containing at least two functional groups. Crosslinked polymers are insoluble in organic solvents which enables the resistance to various surfaces from chemical and/or mechanical wear. Moreover, properties of the coated surfaces can be controlled by network density for the desired applications [20]. Although these involve mechanical properties which mostly present a greater hardness and therefore higher tensile strength, this may also cause a highly brittle crosslinked films [21]. High degree of brittleness of the final material is generally avoided in order to cause a break and loss in the adhesive strength.

Photoinitiators, which have an absorption in UV region, have been widely preferred in coating applications [22, 23]. These compounds, that belong to the Norrish type I class [24], form initiating radicals after photolytic cleavage and initiate the polymerization reaction. UV-LED technologies display characteristic features such as low energy consumption, low heat generation, long life-times, easy to manage and compact. LEDs supply almost monochromatic light with a narrow bandwidth. On the other hand, mercury (Hg) lamps are harmful for operator because of the presence of UV rays and ozone release. Hg lamps have a wide emission spectrum, which leads the partially absorption of the generated light by initiator. It causes a reduction in the efficiency of the system [25].

Absorption can be shifted into the visible range (Vis) by photosensitization. A two-components photoinitiator system is often employed where photosensitizer is excited by absorption of light. Since the energy absorbed by photosensitizer is not adequate, bonds can not be broken directly [26]. Initiating species are produced as a result of electron transfer between sensitizer and initiator.

The main advantage of LED sources delivers light in the narrow wavelength range which allows targeted selection of photoinitiators for desired region. Thus, total energy-costs can be reduced and process improved.

The light has been used in different polymerization mechanisms involving ionic, radical and step-growth polymerization. Conventional radical, anionic and/or cationic polymerization processes are highly practical and convenient to form polymeric structures with high molecular weights and broad molecular weight distributions. From industrial aspect, radical and cationic polymerization initiated by light are commonly used techniques. There are still rapid development of these techniques in terms of designing new types of photoinitiator systems, synthesis of biobased starting materials, and new light source technologies [25-28].

1.2 Motivation of the Thesis

This work focuses on modification of biobased materials to substitute for conventional monomers in photopolymerizing systems, which are formulated for different coating applications.

The motivation of this thesis is to display further alternatives for the modification of the vegetable oil, which improve the reactivity for polymerization reaction. In particular, (meth)acrylate or epoxy groups can be polymerized radically or cationically. Utilization of the biobased monomers derived from renewable resources into synthetic polymer chemistry have been adapted in photoinitiated polymerization.

A critical aspect of this work deals with the challenge to present the new possibilities for modification of unsaturated fatty acid esters where (meth)acrylate or epoxy groups are to be introduced. Different functionalization methods have been described for oleic acid as a model material in the literature. In this work, bis-(9,10-epoxystearic acid) 1,2-ethanediyl ester (**12**) and the isomer mixture of ethane-1,2-diyl bis(9-methacryloyloxy-10-hydroxy octadecanoate), ethane-1,2-diyl 9-hydroxy-10-methacryloyloxy-9'-methacryloyloxy-10'-hydroxy octadecanoate and ethane-1,2-diyl bis(9-hydroxy-10-methacryloyloxy octadecanoate) (**10**) were derived from the oleic acid and transferred to the network structure by photochemically.

The aim of this work is to characterize the final properties of the models, derived from biobased starting materials, in order to investigate the comparability of the properties of the materials made from commercial and biobased monomers. In the course of this, new monomers have been synthesized and photochemical properties of the systems investigated by using 395 nm light source. A comparison of the polymerization rate, the curing time and final conversion of the polymerizable group have been studied by using different photoinitiators and concentration, which are Irgacure® TPO-L 1 wt %, Irgacure® TPO-L 3 wt %, Ivocerin® 1 wt % for free radical polymerization.

The materials produced by cationic polymerization of epoxide monomers show generally lower volumetric shrinkage and also improved adhesion properties to the surface in comparison with the photopolymers obtained via free radical route [28-30]. Newly developed bis-(9,10-epoxystearic acid) 1,2-ethanediyl ester monomer (**12**) was cured via cationic route in the presence of bis(*t*-butyl)-iodonium-tetrakis(perfluoro-*t*-butoxy)aluminate ($[\text{Al}(\text{O}-t\text{-C}_4\text{F}_9)_4]^+$) and isopropylthioxanthone (ITX) as photoinitiating system. Final material properties have been varied by incorporation of the comonomer with more rigid structure into the network structure and analyzed by different techniques.

Even if there are some researches of light induced cationic polymerization of epoxy monomers functionalized from renewable resources such as epoxidized castor oil, trisepoxy phloroglucinol, diglycidylether of vanillyl alcohol, epoxidized soybean oil and limonene dioxide in the literature [27, 31-33], the data are still limited in contrast to the reports about thermal polymerization of the biobased epoxy monomers. This work also focuses on the photoinitiated curing of the epoxy monomers via cationic route. In the course of this, polymer networks from the epoxy monomers bearing different pendant groups have been developed and deeply investigated in this work.

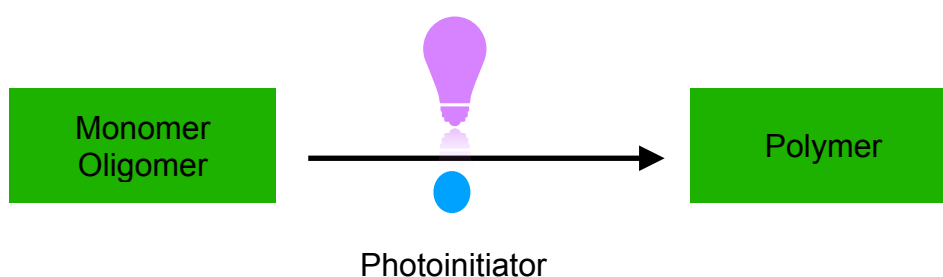
Publications as First Author or shared First Authorship:

1. B. Sanay, B. Strehmel, V. Strehmel, "Manufacturing and Photocrosslinking of a New Bio-based Dimethacrylate for Application in Water-Repellent Coating", *Applied Research*, **2021** (submitted).
2. B. Sanay, B. Strehmel, V. Strehmel, "Formation of Highly Crosslinked Polymer Films in the Presence of Bio-based Epoxy by Photoinitiated Cationic Polymerization", *Progress in Organic Coatings*, **158**, **2021**, 106377.
3. B. Sanay, B. Strehmel, V. Strehmel, "Photoinitiated Polymerization of Methacrylates Comprising Phenyl Moieties", *Journal of Polymer Science*, **58**, **2020**, 1-13.
4. B. Sanay, B. Strehmel, V. Strehmel, "Green Approach of Photoinitiated Polymerization Using Monomers Derived from Oleic Acid and Ionic Liquid", *ChemistrySelect*, **4**, **2019**, 10214-10218.

2. Fundamentals and State of the Art

2.1 Photoinitiated Polymerization

Depending on the way of the radical generation, free radical polymerization can be initiated by photochemically, thermally, chemical redox initiators, voltage and mechanical force [34]. Light beam is used to trigger the reaction in chemical materials such as polymers, oligomers or monomers, to produce a new formed materials, in the principle of light induced polymerization. The polymerization initiated by light with the proper wavelength is called photoinitiated polymerization where polymer are formed from monomers/oligomers (Scheme 1).



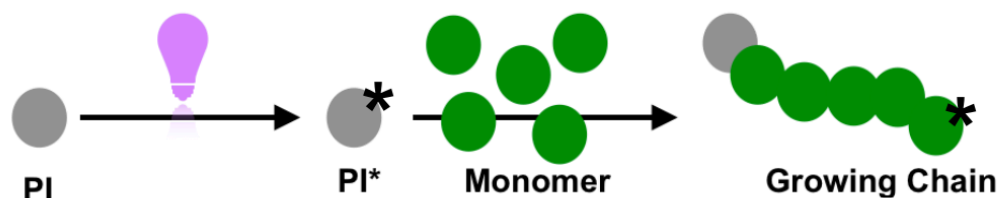
Scheme 1: General illustration of the photopolymerization process.

It has nature friendly benefits in comparison with conventional thermal polymerization technique with the properties of low energy consumption, solvent free formulation, fast curing, and room temperature operation [35-38]. Therefore, this method is called environmental friendly. The interest of this technique has been gradually increased by extension of the application areas such as coating manufacturing, varnishes, laser imaging, inks, stereolithography, 3D printing, adhesive and dental composites for more than 40 years [2,12, 39-43]. Photopolymerization also satisfies the expectations in the biomedical applications. For instance, immobilisation of the enzymes requires the low temperature operation, which is one of the benefits offered by photoinitiated polymerization. Moreover, less side reactions take place in the photoinitiated polymerization of the monomer bearing monofunctional group compared to the thermal polymerization of the monomer that may be accompanied by a higher amount of side reactions [44-47]. Methacrylate and acrylate monomers are generally preferred starting materials to generate crosslinked or linear polymer via photoinitiated free radical polymerization. The formulation to obtain the photopolymer generally comprises monomer, photoinitiator or photoinitiating system (PIS) and other additives depending on the application areas. Besides the other factors which affect the efficiency of the

photopolymerization, photoinitiator plays a key role in the formulation, which directs polymerization rate, surface properties such as hardness, transparency or tack-free index, etc [43-44]. Furthermore, compatibility of the emission spectrum of the radiation with the absorption region of the photoinitiator/PIS and number of available incident photons, I_0 , are significant parameters as well. The spectral parameters such as molar extinction coefficients (ϵ) and ground state spectra of the photoinitiator/PS/PIS have a decisive impact on the polymerization efficiency [12,46] because of the direct relation between polymerization rate and the light absorption.

2.1.1 Photoinitiated Free Radical Polymerization

The key component of the polymerization formulation is the light sensitive photoinitiator, which decomposes by light into free radical species. Free radicals formed in the initiation step add to the double bond in the monomer molecules to grow the polymer chain (Scheme 2). Photoinitiated polymerization is generally mentioned as a chain growing reaction initiated by light. Formation of the radicals from the photoinitiator by exposure light is necessary for the initiation step of the polymerization. Though the polymerization rate can be altered by changing the photoinitiator type or concentration, free radical polymerization generally proceeds fast.



Scheme 2: General presentation of photoinitiated free radical polymerization.

On the other hand, photopolymerization involves complicated chemical and physical processes, which convert the liquid photopolymerizing mixture to the solid photopolymer after short irradiation time and the final material properties such as glass transition temperature, mechanical strength and deformation etc. are evolved with the conversion degree in this curing time. For this reason, it is really important to study the final material properties of the polymer obtained after irradiation [48-50]. Kinetic study of the photopolymerization provides the information about conversion degree, rate of polymerization and helps to link these information obtained with the changes on the physical properties of the resulting photopolymer depending on the irradiation.

Photopolymerization kinetic has been widely investigated to get further information [51-55]. Photokinetic investigation was done through the calculation of the polymerization rate and conversion degree of the monomers from the data obtained by differential scanning calorimetry using light (Photo-DSC) in this work.

Free radical polymerization is formulated with the monomer bearing double bond which forms the covalent bond. Functionality of the monomer influences the formation of network structure as well as degree of crosslinking. Higher number of the polymerizable groups in the monomer structure results in a crosslinked polymer with higher crosslink density after photopolymerization [56]. Photoinitiated polymerization proceeds with the same steps of the typical free radical polymerization pathway of initiation, propagation, and termination as described below [57]:

2.1.1.1 Initiation

Generation of the radicals by photodecomposition of the photoinitiator is the first step of the photopolymerization to initiate the reaction. The reactive species formed by light absorption of the photoinitiator attack to the region with high electron density, which is the carbon-carbon double bond of the monomer. The initiation step includes two main steps as described in (2.1) and (2.2): the generation of the radicals from PI followed by the addition of the radical to the monomer to form the primary radicals [58]. Emission spectrum of the light source should overlap with the specific wavelength range of the photoinitiator to convert into the radical species [59-60]. Radicals from photoinitiators are generated by photochemical cleavage of aldehydes or ketones, which is called Norrish-type reactions. Radical photoinitiators can be considered into two main classes of: type I and type II PIs.



Type I Photoinitiators :

Type I photoinitiators (PI) form radicals through α -cleavage of the C-C bond and it is referred to Norrish Type I reaction. Aromatic carbonyl compounds are known to undergo into a homolytic C-C bond-cleavage under UV irradiation. Type I PIs have generally high reactivity and quantum yield for dissociation. They have a wide range of structural diversity. Benzoin, benzil, α -hydroxy ketones, oxime ester, sulfonyl ketone, thiobenzoate, bisacylgermane and bisacylphosphane oxide etc. are some of the type I PIs.

Irgacure® TPO-L ((ethyl (2,4,6-trimethylbenzoyl) phenylphosphinate) and Ivocerin® (di(4-methoxybenzoyl)diethylgermane) are Norrish type I photoinitiators, which were used in this work.

Acylgermanes such as di(4-methoxybenzoyl)diethylgermane are reported as highly reactive PIs under visible light, which produce benzoyl and metal centered reactive species. It was already reported that di(4-methoxybenzoyl)diethylgermane (Ivocerin®) is highly efficient which undergoes primarily α -cleavage reaction [60-62]. It is mainly used in dental and composite applications. Primary germyl and benzoyl radicals are produced as a result of excitation of Ivocerin®.

Irgacure® TPO-L is fast and efficient photoinitiator, which gives benzoyl and phosphinyl radicals that initiate the polymerization reaction of formulations comprising acrylates, unsaturated polyesters and styrene [63-64].

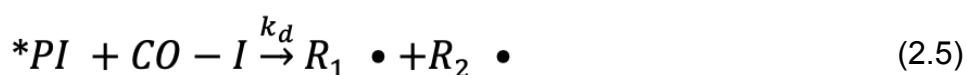
The generation of radicals ($R\cdot$) during this type of reactions shows first-order kinetics since only one species is involved in the photo-cleavage step ((2.3) and (2.4)).



$$\frac{dR_1 \cdot}{dt} = \frac{dR_2 \cdot}{dt} = R_i = k_d \cdot *PI \quad (2.4)$$

Type II Photoinitiators:

Type II PIs produce initiating radicals in combination with coinitiator (COI). Initiation of the photoinitiated radical polymerization can be carried out by -H abstraction or electron transfer. In contrast to Norrish type I PIs, type II PIs form radicals through a bimolecular process. The initiation step of the polymerization is generally slower for bimolecular system in comparison with the system initiated by Type I PIs due to the bimolecular reaction. They need a co-initiator to produce radicals because of their low excitation energy [61].



$$\frac{dR_1 \cdot}{dt} = \frac{dR_2 \cdot}{dt} = R_i = k_d \cdot *PI \cdot CO - I \quad (2.6)$$

Radicals ($R\cdot$) can be formed as a result of the reaction of the PIs and co-initiator (CO-I) as shown in (2.5). It is the second-order kinetic because two species of radicals ($(R_1\cdot)$ and $(R_2\cdot)$) formed in the initiation step via hydrogen abstraction or e⁻ transfer (2.6) [42].

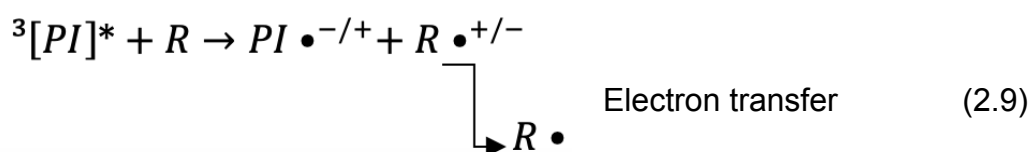
The interaction of the PI excited by light with the co-initiator may occur through two different pathways.

Hydrogen Abstraction: Co-initiator donates a suitable hydrogen from its functional group (carbonyl group) to the PI that is in the excited state after the absorption of UV light and it leads the radical formation as defined in (2.7) and (2.8).



Electron Transfer: is the another possibility to generate initiating species. In the case of amine as a co-initiator, an electron is transferred to type II PI when it is in the triplet state after excitation which leads to generation of the radicals (2.9) [37]. This species may be a radical as well as cations or anions.

Benzophenone, camphorquinone and thioxanthone are the typical examples of type II photoinitiators. Thioxanthenes and its derivatives are the most common used type II PIs since they have high quantum efficiency [37]. Amines, thiols, phosphorous compounds, and silanes are a few examples of co-initiators used for the type II PIS, whereby the highest efficiency for hydrogen donation is shown in tertiary amines.



2.1.1.2 Propagation

The next step after initiation is the propagation where the functional groups of the monomer are consumed by addition to the radical site at the growing chain (2.10). After the activation of the radicals in the initiation step, double bond in the monomer structure will be activated and lead to generation of growing radical chain by further addition of the monomers to the active part of the chain [58-60]. In this step, the monomer concentration reduces by combination of the monomer to the polymer chain, leading to the growth of the

polymer chain (2.11). The growing polymer chain generally involves a radical end group. The double bonds are consumed in the propagation process [65-68].



$$-\frac{d[M]}{dt} = R_p = k_p \cdot [M] \cdot [M \bullet] \quad (2.11)$$

2.1.1.3 Termination

Termination can occur as a result of the reaction of two radicals and dead polymer forms. The polymerization reaction can be terminated by two possible pathways: either combination or disproportionation. One dead polymer chain can be produced by the reaction of the two radical polymer chains as shown in (2.12). On the other hand, chain growth of the polymer chain can be terminated through disproportionation reaction (2.13) by abstraction of a hydrogen atom from the other polymer chain resulting in one dead polymer chain and one polymer chain bearing double bond [68-70]. Rate of termination is expressed as defined in (2.14). Oxygen in the reaction environment can react with radical and inhibit the polymerization. It is highly reactive to the excited state and initiating radicals. For this reason, oxygen causes a decrease in the polymerization rate [22, 71-72].



$$R_t = 2k_t \cdot [M \bullet]^2 \quad (2.14)$$

In some cases, rate of polymerization can be controlled by the diffusion of the species in the reaction system in case of an increase of the viscosity in the medium during irradiation. It causes a reduction in the movement of the large polymer chains and mobility of the active polymer chains is hindered [73-75]. It results in a decrease in the termination rate of the reactive polymer chains. In this case, diffusion-controlled termination takes place for the polymerization reaction. It is called Trommsdorff effect or auto acceleration [76]. When the viscosity of the reaction medium gets too high, diffusion of the small molecules is limited as well, that leads to a reduction in the propagation rate and limits the conversion.

2.1.2 Photoinitiated Cationic Polymerization

Epoxide or oxirane monomers can undergo cationic ring opening polymerization initiated by light [2, 38, 42, 77-84]. The absence of the stable cationic photoinitiator restricted the development of the cationic photopolymerization before 1970s. Aryldiazonium salts were shown as a possible compound to induce the cationic polymerization reaction of the epoxide compounds by *Schlessinger et al* but they did not have the thermal stability [85]. *Crivello and co-workers* discovered the onium salts (diaryliodonium or triphenylsulfonium) activated by UV-irradiation in the late 1970s and application areas of the cationic photopolymerization has been expanded such as inks, coating or adhesives *etc* since this discovery [86-90]. These compounds are highly photosensitive and thermally stable. In addition to this, cationic photopolymerization of epoxy monomers has attracted a wide range of industrial areas from aerospace to electronic applications by providing multifunctionality to the surfaces such as scratch resistance, antistatic coating, high abrasion resistance, and chemical stability [91-92].

It has other decisive plusses such as low volume shrinkage, dark post-reaction and adhesion to the surface compared to the free radical polymerization [30,92]. Cationic polymerization formulations of epoxide monomers are categorized by less-toxic compared to the free radical formulations containing (meth)acrylate monomers. Therefore, it may be an alternative to the systems containing (meth)acrylate monomer used in radical polymerizations. However, the cationic ring opening polymerization is sensitive to the moisture and water even if oxygen does not effect the polymerization. Water or other species bearing hydroxy group, as a transfer agent, may change the polymerization rate and degree of polymerization [93-94]. Polymerization rate of the cationic polymerization is generally slower than that of free radical polymerization [37,95].

2.1.2.1 Onium Salts

Photoacid generation from the onium salt by UV radiation to initiate the cationic polymerization was first investigated by Crivello in 1978 [85-86]. Onium salts (iodonium or sulfonium) can be classified as most commonly applied cationic photoinitiators [96]. They correspond to the requirements of the photopolymerization formulations with the properties of thermal stability and nonreactivity to the monomer in the system at room temperature [90].

The light absorbing part of the cationic photoinitiator is the cation in its structure, and it defines not only the absorption capacity but also photochemistry of the initiator. Accordingly, typical UV-absorption is governed by nature of cation in the structure. The

anion moiety plays a role to control the acidity of the photogenerated acid during photolysis which is related with the initiation efficiency. Anion also affects the polymerization kinetic due to its role on the characterization of the propagating ionic species [90,97-98]. The counter ion nature plays a significant role in the polymerization reaction since it may react with the active cationic centre causing a decrease in the polymerization rate or inhibition of the polymerization reaction [90].

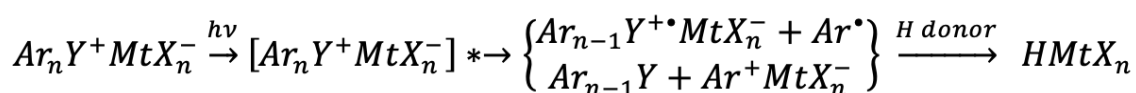
Although some photoinitiators show high efficiency, they have a limitation in the absorption wavelength region up to 300 nm to be activated. (BF_4^- , PF_6^- , AsF_6^- , SbF_6^-) [99]. It was deeply studied and presented that derivatization of the aromatic ring by incorporation of the chromophoric group shifts the absorption wavelength to the broaden spectral range [47,86-91,100-103]. Alternatively, this limitation can be overcome by indirect paths which are electron transfer, energy transfer or oxidation of free radicals to activate the IS (initiating system).

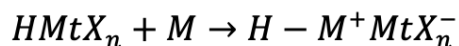
An electron transfer occurs from the excited photosensitizer to onium salt in photosensitization mechanism. Onium salt decomposes by electron transfer and initiate the polymerization. Another indirect way to initiate the cationic polymerization is charge transfer mechanism which radical cations with aromatic structure are generated as a result of intermolecular electron transfer between an electron acceptor (onium salt, such as pyridinium) and an electron donor. In free radical promoted mechanism, oxidation of the free radicals by onium salt produces active species which can basically trigger the cationic polymerization [104-106].

In this work, system was operated by onium salt in combination with sensitizer, which leads to the cation formation to initiate cationic polymerization. Aluminate $[\text{Al}(\text{O}-t\text{-C}_4\text{F}_9)_4]^-$ was selected as a counter ion of the iodonium salt due to its efficiency reported previously [107-108]. It is a promising alternative to hexafluorophosphate with the properties of well solubility in the many photopolymerizing mixture as well as free of HF release.

2.1.2.2 Initiation

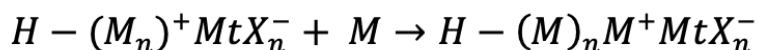
Reactive Brønsted acid is formed as a result of excitation of the onium salt by irradiation and initiates the reaction [90,99,109]. It is shown photolysis of an onium salt ($\text{Ar}_n\text{Y}^+\text{MtX}_n^-$) where Ar_nY^+ is cationic part (such as diaryliodonium, $\text{Y} = \text{I}, \text{S} \dots$) and MtX_n^- is counterion (SbF_6^- , PF_6^- or BF_6^-).





2.1.2.3 Propagation

Monomers add to the macromolecular chains leading to the growing chain and polymer formation [90,99,109].



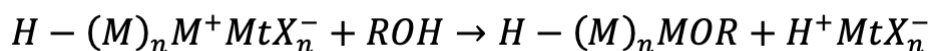
2.1.2.4 Termination

Recombination does not occur in termination step of the cationic polymerization. Occlusion, reaction with impurities such as water or transfer reactions (with counter ion or cyclization) can terminate the polymerization as described below:

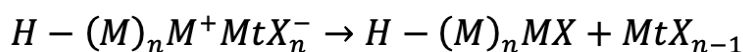
Occlusion



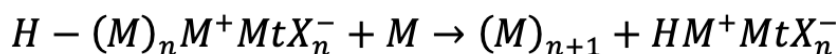
Reaction with compound involving -OH group (or impurities)



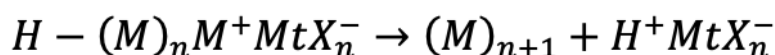
Reaction with counter ion



Reaction with monomer



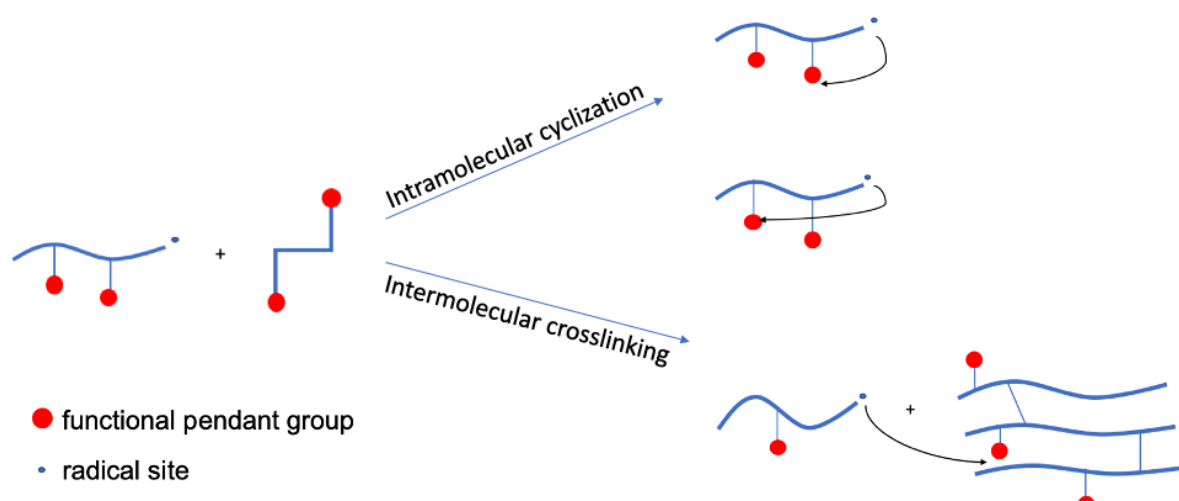
Chain transfer



2.2 Polymer Network Formation

Besides the common reaction steps of crosslinking and linear polymerization, multifunctional monomers bearing two or more functional groups show different

phenomena from the monofunctional monomers in polymerization reaction. The presence of more than one functional group in the monomer structure gives a three dimensional network system as a result of polymerization in contrast to the linear polymerization of monomer with one polymerizable group. Firstly, multifunctional monomers react with the growing radical chain which leads to radical polymer units containing functional group moieties. As the reaction can continue by the addition of the other monomer molecule to the growing polymer chain, intramolecular cyclization or intermolecular crosslinking can also occur in propagation step. The reaction between two functional groups on the different polymer molecules is called intermolecular crosslinking (Scheme 3). Intramolecular cyclization occurs when the radical part of the growing chain reacts with the pendant functional group on the same polymer chain. As a result of cyclization reaction, microgel formation occurs, which leads to structurally inhomogeneity in the network and a delay in the gel point due to the unreacted functional group trapping in the microgel regions [110].



Scheme 3: Representation of intramolecular cyclization and intermolecular crosslinking .

Formation of the polymer networks inhibits the mobility of the polymer chains and growing macromolecules can mainly diffuse each other by segmental diffusion or propagation.

When the crosslinking density of the network system increases, segmental diffusion is limited and termination is dominated by reaction diffusion [110-111]. Therefore, termination rate constant decreases by diffusion limitations which causes autoacceleration or Trommsdorff effect that is generally the case for radical crosslinking polymerization of multifunctional monomers. Limited conversion of polymerizing group can be caused due to both topological or vitrification effects [110-111].

3. Materials and Methods

This chapter briefly discloses the experimental conditions used in this thesis. The conditions explained in this subchapter were previously published or submitted [64,112, 113, 114].

3.1 Chemicals

3.1.1 Solvents

The following solvents used in synthetic procedures and purification processes are commercially available: Acetone (C₃H₆O), *t*-butyl methylether ((CH₃)₃COCH₃), diethyl ether (Et₂O), dichloromethane, (CH₂Cl₂), methanol (MeOH), rotidry methanol, *n*-hexane (*n*-Hex), ethyl acetate (EtOAc), tetrahydrofuran (THF) (C₄H₈O), 1,4-dioxan were bought from Carl Roth. Deuterated solvents were purchased from ARMAR AG.

3.1.2 Reagents

Oleic acid (abcr, tech., 90 %), oleic acid (VWR, tech., 81 %), ethylene glycol (Carl Roth, ≥99 %), formic acid (Sigma Aldrich, ≥95%), sulfuric acid (H₂SO₄), hydrochloric acid (HCl), methacrylic acid (250 ppm MEHQ as inhibitor, Sigma Aldrich, 99.9 %), acrylic acid (200 ppm MEHQ as inhibitor, Sigma Aldrich, 99.9 %), diazobicyclo[2.2.2]octane (DABCO, Alfa Aesar, 98 %), hydrogen peroxide solution (50 %, Sigma Aldrich), imidazole (Carl Roth, ≥99 %), methacrylic anhydride (2,000 ppm topanol A as inhibitor, Sigma Aldrich, 94 %), 4-*N,N*-dimethyl amino pyridine (DMAP, Sigma Aldrich), hydroquinone (Sigma Aldrich, ≥99%), 4-(4-hydroxyphenyl)butan-3-one (Acros, ≥99.0 %), methacryloyl chloride (0.02 % 2,6-di-*tert*-butyl-4-methylphenol as stabilizer, Sigma Aldrich, ≥97.0 %), triethylamine (Carl Roth, ≥99.5 %), isopropyl thioxanthone (ITX, Sigma Aldrich), di(4-methoxybenzoyl)diethylgermane (Ivocerin®, Ivoclar Vivadent AG), ethyl (2,4,6-trimethylbenzoyl) phenylphosphinate (Irgacure® TPO-L, BASF), bis(*t*-butyl)-iodonium-tetrakis(perfluoro-*t*-butoxy)aluminate (S2617) (FEW Chemicals) were used as received.

2-Phenoxyethyl methacrylate (**8**) ((stabilized with HQ + MEHQ), TCI, >85.0%), phenyl methacrylate (**9**) ((stabilized with BHT), TCI, >97.0 %), 1,6-hexanediol diacrylate (**5**) ((stabilized with MEHQ), TCI, >85.0 %), and 1,6-hexanediol dimethacrylate (**6**) ((stabilized with MEHQ), TCI, >98.0 %) were used as received and passed through a column filled by basic alumina ((Carl Roth, aluminium oxide 90 active basic, 0.063-0.0200 mm)) to remove the inhibitor and stored in the fridge (0-5°C) before use.

1-iodooctane (copper as stabilizer, Sigma Aldrich, 98 %, bp 81 °C, 11 mbar), 1-iododecane (copper as stabilizer, Sigma Aldrich, 98 %, bp 132 °C, 20 mbar), *t*-butyl methylether (bp 78 °C) and 1-vinylimidazole (Sigma Aldrich, ≥99%, 51 °C under 3 mbar) were distilled prior to use for purification.

3,4-Epoxy cyclohexylmethyl-3',4'-epoxycyclohexane carboxylate (**13**, Sigma Aldrich) and bisphenol-A-diglycidylether (**15**) were available in the laboratory. 1,4-butanediol diglycidyl ether (**14**) was received as a gift from BASF and used as received.

Lithium bis(trifluoromethylsulfonyl)imide (IoLiTech), calcium chloride (CaCl₂, Carl Roth), magnesium sulfate (MgSO₄, Carl Roth), sodium bicarbonate (NaHCO₃, Carl Roth), sodium hydroxide (NaOH, Carl Roth) and potassium carbonate (K₂CO₃) were available at the lab.

Table 1: Structure of type I photoinitiators.

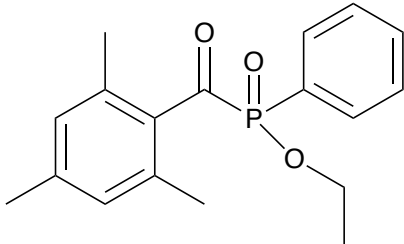
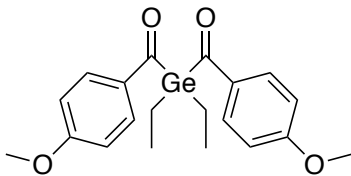
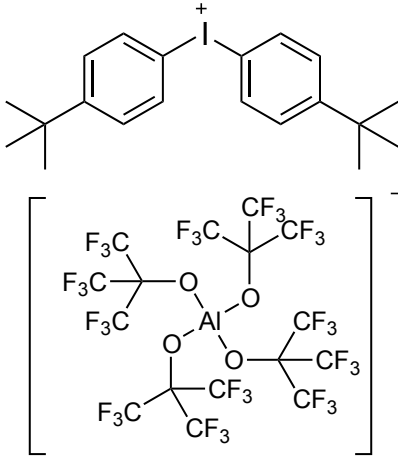
Photoinitiators	Chemical Structure
Ethyl (2,4,6-trimethylbenzoyl) phenylphosphinate (Irgacure® TPO- L)	
Di(4-methoxybenzoyl)diethylgermane Ivocerin®	

Table 2: Structure of onium salt.

Name ^a	Chemical Structure
Bis(<i>t</i> -butyl)-iodonium- tetrakis(perfluoro- <i>t</i> -butoxy)aluminate S 2617	

^aCommercial name from FEW Chemical GmbH.

3.2 Analytical Methods and Equipment

3.2.1 Nuclear Magnetic Resonance Spectroscopy (NMR)

The purity of the compounds was checked by nuclear magnetic resonance (NMR) spectroscopy. For this purpose, about 30 mg of the compound for a ^1H -NMR measurement and about 50 mg of the compound for a ^{13}C -NMR measurement were dissolved in 0.7 ml of deuterated solvent. Then NMR spectra were recorded with a Fourier 300 NMR spectrometer from Bruker. The measurement and data acquisition were carried out by the software "TopSpin 3.2" from Bruker. The software "MestReNova V8.1.1-11591" from Mestrelab Research S.L. was used for further data analysis.

3.2.2 Contact Angle Measurement (CA)

Wettability character of all cured films was investigated by measuring of the contact angle. The static contact angle measurements with sessile drop method was used to conduct the contact angle measurements with the OCA 15plus model contact angle meter from DataPhysics Instrument with a resolution of 0.1° in the measuring range of 1 - 180° . Performing of the experiments and evaluation of the drop shape to measure the contact angle was carried out by provided software drop shape analysis SCA20. A drop of solvent ($1\ \mu\text{L}$) was deposited on the films with a single electronic syringe unit. At least three contact angle tests were recorded for each film and solvent (distilled water, ethylene glycol, diiodomethane, and toluene) to obtain an average result, respectively.

3.2.3 Gel Permeation Chromatography (GPC)

A GPC Viscotek 270 max was used for investigation of (M_n) and dispersity (M_w/M_n) values of polymers. The device was equipped with a TGuard Col $10\times 4.6\ \text{mm}$ and two T6000 M General Mixed $3000\times 7.8\ \text{mm}$ columns. The column temperature was $30\ ^\circ\text{C}$. Tetrahydrofuran (THF) was used as eluent at a flow rate of $1\ \text{mL}\cdot\text{min}^{-1}$. A refractive index detector was applied for sample analysis. The system was calibrated by using 7 linear poly(methyl methacrylate) standards received from Shodex ($1850\ \text{g}\cdot\text{mol}^{-1}$; $6380\ \text{g}\cdot\text{mol}^{-1}$; $20100\ \text{g}\cdot\text{mol}^{-1}$; $73200\ \text{g}\cdot\text{mol}^{-1}$; $218000\ \text{g}\cdot\text{mol}^{-1}$; $608000\ \text{g}\cdot\text{mol}^{-1}$; and $1050000\ \text{g}\cdot\text{mol}^{-1}$). Omni SEC 4.6.2 was used to analyze the GPC data obtained.

3.2.4 Photo Differential Scanning Calorimetry (Photo-DSC)

Photopolymerization was carried out using photo-DSC device where a DSC TA Q2000 served as basis instrument. A UV LED emitting at $395\ \text{nm}$ set out as light source with a light intensity of $100\ \text{mW}\cdot\text{cm}^{-2}$ and $180\ \text{mW}\cdot\text{cm}^{-2}$ that was determined using an USB 4000

spectrometer from Ocean Optics [115-116]. A shutter system was synchronized with the Q2000 to turn on and turn off the light [115]. The sample (~5 mg) was put into the TA Tzero aluminum pan and placed opposite to the reference pan without lid. Photopolymerization was carried out under nitrogen atmosphere with 50 ml/min purge rate of the inert gas. The sample was heated up to desired temperature and held at that temperature for 8 minutes (min). Then, it was irradiated by constant radiation power for different irradiation times at desired temperature under nitrogen. The rate of polymerization (R_p in s^{-1}) was calculated from the raw data of the specific heat flow (dQ/dt in $J \cdot s^{-1} \cdot g^{-1}$) by multiplication with the molecular weight of the monomer (M in $g \cdot mol^{-1}$) and division through the molar polymerization enthalpy of the double bond (ΔH in $J \cdot g^{-1}$, $\Delta H = -84 \text{ kJ} \cdot mol^{-1}$ for the acrylate group [117], $\Delta H = -54.6 \text{ kJ} \cdot mol^{-1}$ for the methacrylate group [118], $\Delta H = -92 \text{ kJ} \cdot mol^{-1}$ for the vinyl group of the vinylimidazolium based ionic liquid monomers [64] and $\Delta H = -94.5 \text{ kJ} \cdot mol^{-1}$ for the epoxy group [119]) according to eq (3.1).

$$R_p = dQ/dt \cdot M \cdot 1/\Delta H \quad (3.1)$$

3.2.5 Differential Scanning Calorimetry (DSC)

Physical transition of the compounds was investigated by a DSC Q2000 from TA Instruments. The samples (4 -10 mg) were placed in an aluminium crucible. The second heating scan of each DSC curve was analyzed for determination of T_g for the monomers and polymers. Each sample was preheated to the temperature given in the method to eliminate any previous thermal history followed by quenching.

3.2.6 Dynamic Mechanical Analysis (DMA)

Dynamic Mechanical Analysis was performed on the films with DMA, TA Instruments, Q800 model operated in DMA Multi-Frequency-strain mode. The information of storage modulus (E'), loss modulus (E'') and the damping parameter ($\tan \delta$), as the ratio of the loss modulus to the storage modulus (E''/E'), can be obtained by application of a sinusoidal strain in this technique. The glass transition temperature of the films was determined by DMA using different techniques, 1) the onset point of sigmoidal change in the storage modulus (E') (Storage Modulus Extrapolated Onset) or tangent of storage modulus, 2) the peak maximum on the loss modulus (E'') versus temperature curve and 3) the peak maximum on the $\tan \delta$ versus temperature curve. The film was heated from -100 °C to 100 °C, 120 °C or 250 °C using 3 K/min heating rate with amplitude of 5 μm and oscillation frequency of 1Hz. The polymer films were removed from the glass substrate after curing and DMA measurement was performed.

3.2.7 Thermal Measurement by Thermal Camera

The temperature changes during irradiation of the sample on the glass substrate were recorded by using a thermal camera (testo 0563 0885 V7). The samples containing the monomers and the photoinitiators (Irgacure® TPO-L 1 wt %, Irgacure® TPO-L 3 wt %, Ivocerin® 1 wt %) were irradiated with the 395 nm light source for 10 min. The films were prepared on the glass substrate by using 120 μm spacer to maintain comparable thickness for all experiments. The glass substrate with deposited sample on it was purged with nitrogen in the plastic box equipped with a quartz glass window for 5 min before irradiation. The temperature generated during irradiation was recorded by a thermal camera (testo 0563 0885 V7).

3.2.8 Viscosity Measurement

Viscosity of the monomers, **11**, **12**, **13**, **14**, **15**, was measured at 60 °C by rotational rheometer (Modular Compact Rheometer MCR 302, Anton Paar) in the region of 0.1 s⁻¹ and 100 s⁻¹ shear rate. The rheometer was equipped with a cone plate (CP40-2: diameter: 39.974 mm, cone angle: 170 °). In an additional experiment, the viscosity of the liquid monomers of **11**, **13** and **14** was also evaluated at 23 °C.

3.2.9 Gel Content

The gel content of the cured films produced from difunctional monomers was determined by measuring the weight loss after 24 hours (h) of solvent extraction with chloroform at room temperature, according to the standard test method ASTM D2765–84.

3.3 Light Source UV-LED at 395 nm

UV LED which emits at 395 nm was used for the radical formation from photoinitiators. The intensity was measured with the fiber optic spectrometer USB4000 from Ocean Optics. UV LED at 395 nm was also used for the photodecomposition of the onium salt. For cationic polymerization of epoxide monomers, the intensity was first fixed to 100 mW·cm⁻² and then 180 mW·cm⁻² for additional experiments. Free radical polymerization was performed by constant light intensity of 100 mW·cm⁻².

4. Experimental Part

This chapter briefly discloses the experimental conditions used in this thesis. The conditions explained in this subchapter were previously published or submitted [64,112, 113, 114].

4.1 Sample Preparation

4.1.1 Photoinitiated Free Radical Polymerization

Commercially available monomers were removed from the inhibitor by passing through the column filled with basic aluminium oxide followed by distillation.

All samples were prepared in the brown vial. Since the 4-(4-methacryloyloxyphenyl)butan-2-one (**7**) is solid at room temperature, the samples of 4-(4-methacryloyloxyphenyl)butan-2-one (**7**) containing 1 % (w/w) of Irgacure® TPO-L, 3 % (w/w) of Irgacure® TPO-L and 1 % (w/w) of Ivocerin® were firstly immersed in a beaker half filled with warm water (at 40 °C) for 5 min to be melted. Then, they were well-mixed on the stirring plate for 30 min before the measurements.

The samples of liquid monomers, 1-octyl-3-vinylimidazolium bis(trifluoromethylsulfonyl)imide (**1a**), 1-decyl-3-vinylimidazolium bis(trifluoromethylsulfonyl)imide (**1b**), methyl 9-((meth)acryloyloxy)-10-hydroxyoctadecanoate / methyl 9-hydroxy-10-((meth)acryloyloxy)octadecanoate (**2, 3**), methyl 9-(1H-imidazol-1-yl)-10-(methacryloyloxy)octadecanoate / methyl 9-(methacryloyloxy)-10-(1H-imidazol-1-yl)octadecanoate (**4**), 1,6-hexanediol diacrylate (**5**), 1,6-hexanediol dimethacrylate (**6**), 2-phenoxyethyl methacrylate (**8**), phenyl methacrylate (**9**), ethane-1,2-diyl bis(9-methacryloyloxy-10-hydroxy octadecanoate) / ethane-1,2-diyl 9-hydroxy-10-methacryloyloxy-9'-methacryloyloxy10'-hydroxy octadecanoate / ethane-1,2-diyl bis(9-hydroxy-10-methacryloyloxy octadecanoate) (**10**) containing 1 % (w/w) of Irgacure® TPO-L, 3 % (w/w) of Irgacure® TPO-L and 1 % (w/w) of Ivocerin®, were directly mixed on the stirring plate for 30 min.

4.1.2 Photoinitiated Cationic Polymerization

1.48×10^{-5} mol onium salt (S2617) and 0.1 wt % sensitizer (ITX) relative to the total amount of the resulting mixture (500 mg) were well mixed with the monomers of 9,10-epoxystearic acid methyl ester (**11**), 3,4-epoxycyclohexylmethyl-3',4'-epoxycyclohexane carboxylate (**13**), 1,4-butanediol diglycidyl ether (**14**) in the brown vial. The solid epoxide monomers at room temperature, bis-(9,10-epoxystearic acid) 1,2-ethanediyl ester (**12**) and

bisphenol-A-diglycidylether (**15**), were first melted and then well mixed with the photoinitiating system before photopolymerization.

4.2 Film Preparation

The freshly prepared sample of the monomer ((4-(4-methacryloyloxyphenyl)-butan-2-one (**7**), 2-phenoxyethyl methacrylate (**8**), and phenyl methacrylate (**9**), respectively) containing 1 % (w/w) of Irgacure® TPO-L was deposited on a glass substrate, and a film was made on the substrate by using the 120 μm side of a four-way film applicator. After that, the glass plate was directly put in a plastic box equipped with a quartz glass window and purged with nitrogen for 5 min. Then, the film was immediately cured under the nitrogen atmosphere using a 395 nm light source at room temperature for the desired irradiation time.

The films made from epoxide monomers with a thickness of $\sim 50 \mu\text{m}$ were prepared by using two pieces of glass plate. The sample was deposited on the glass substrate and covered by additional glass plate completely. The substrate was placed on the heating plate set to 60 °C. The sample was irradiated by 395 nm light source for 20 min.

The films derived from the mixture of ethane-1,2-diyl bis(9-methacryloyloxy-10-hydroxy octadecanoate) / ethane-1,2-diyl 9-hydroxy-10-methacryloyloxy-9'-methacryloyloxy-10'-hydroxy octadecanoate / ethane-1,2-diyl bis(9-hydroxy-10-methacryloyloxy octadecanoate) (**10**) with a thickness of $\sim 50 \mu\text{m}$ were prepared by using two pieces of glass substrate. The sample was deposited on the glass substrate and covered by additional glass plate completely. The sample was irradiated by 395 nm light source for 10 min.

4.3 Photopolymerization Measurements

The sample ($\sim 5 \text{ mg}$) was weighed into the TA Tzero aluminum pan and photopolymerization was carried out under nitrogen atmosphere with 50 ml/min purge rate of the nitrogen. For free radical polymerization, irradiation power was set to $100 \text{ mW} \cdot \text{cm}^{-2}$ at 395 nm and the samples were generally irradiated for 10 min at 40 °C. Photo-DSC method temperature was set to 40 °C and temperature of the sample was isothermally equilibrated at 40 °C for 8 min.

The photopolymerizing mixtures of 1-octyl-3-vinylimidazolium bis(trifluoromethylsulfonyl)imide (**1a**), 1-decyl-3-vinylimidazolium bis(trifluoromethylsulfonyl)imide (**1b**), methyl 9-((meth)acryloyloxy)-10-hydroxyoctadecanoate / methyl 9-hydroxy-10-((meth)acryloyloxy)octadecanoate (**2**, **3**),

methyl 9-(1H-imidazol-1-yl)-10-(methacryloyloxy)octadecanoate / methyl 9-(methacryloyloxy)-10-(1H-imidazol-1-yl)octadecanoate (**4**), 1,6-hexanediol diacrylate (**5**), 1,6-hexanediol dimethacrylate (**6**), and ethane-1,2-diyl bis(9-methacryloyloxy-10-hydroxy octadecanoate) / ethane-1,2-diyl 9-hydroxy-10-methacryloyloxy-9'-methacryloyloxy-10'-hydroxy octadecanoate / ethane-1,2-diyl bis(9-hydroxy-10-methacryloyloxy octadecanoate) (**10**) containing 1 % (w/w) of Irgacure® TPO-L, 3 % (w/w) of Irgacure® TPO-L and 1 % (w/w) of Ivocerin® were irradiated at 40 °C for 10 min.

Moreover, temperature dependent irradiation experiments of 4-(4-methacryloyloxyphenyl)-butan-2-one (**7**) containing 1 % (w/w) of Irgacure® TPO-L and time dependent irradiation experiments of 4-(4-methacryloyloxyphenyl)-butan-2-one (**7**), 2-phenoxyethyl methacrylate (**8**) and phenyl methacrylate (**9**) containing 1 % (w/w) of Irgacure® TPO-L were performed by photo-DSC under nitrogen atmosphere, respectively.

For cationic polymerization, two different methods were carried out. Firstly, irradiation power was set to $100 \text{ mW} \cdot \text{cm}^{-2}$ at 395 nm and the samples were irradiated for 10 min at 60 °C. In an additional experiment, light intensity was increased to $180 \text{ mW} \cdot \text{cm}^{-2}$ at 395 nm and the fresh samples were irradiated for 20 min at 60 °C. Photo-DSC method temperature was set to 60 °C and temperature of the sample was isothermally equilibrated at 60 °C for 8 min.

4.3.1 Temperature Dependent Photo-DSC Measurements

For temperature dependent photo-DSC measurements of 4-(4-methacryloyloxyphenyl)-butan-2-one (**7**) containing 1 % (w/w) of Irgacure® TPO-L, the samples were irradiated at 40 °C, 55 °C, 70 °C, and 85 °C, respectively, for 10 min.

4.3.2 Time Dependent Photo-DSC Measurements

For time dependent measurements of 4-(4-methacryloyloxyphenyl)-butan-2-one (**7**) containing 1 % (w/w) of Irgacure® TPO-L, irradiation of the samples was carried out at 40 °C for 6 sec, 10 sec, 15 sec, 20 sec, 25 sec, 30 sec, and 10 min, respectively. Further time dependent photopolymerization of 4-(4-methacryloyloxyphenyl)-butan-2-one (**7**) containing 1 % (w/w) of Irgacure® TPO-L was investigated at 85 °C using an irradiation time of 6 sec, 20 sec, 25 sec, 30 sec and 10 min, respectively. The samples of the monomer 4-(4-methacryloyloxyphenyl)-butan-2-one (**7**) with 3 % (w/w) of Irgacure® TPO-L and 1 % (w/w) of Ivocerin®, respectively were irradiated at 40 °C only for 10 min.

Furthermore, time dependent photo-DSC measurements of 2-phenoxyethyl methacrylate (**8**) containing 1 % (w/w) of Irgacure® TPO-L were investigated at 40 °C for 6 sec, 20 sec,

25 sec, 40 sec, 55 sec, and 10 min, respectively. Moreover, time dependent photo-DSC measurements of phenyl methacrylate (**9**) containing 1 % (w/w) of Irgacure® TPO-L, were carried out at 40 °C for 6 sec, 20 sec, 40 sec, 50 sec, 90 sec and 10 min, respectively.

4.4 Thermal Polymerization

The mixture of 4-(4-methacryloyloxyphenyl)-butan-2-one (**7**) containing 1 % (w/w) of Irgacure® TPO-L was prepared in a Schlenk flask where a magnetic stirrer was previously placed. Then, the Schlenk flask was degassed by three Freeze-Pump-Thaw cycles. Then, the reaction mixture was heated up 85 °C and kept at this temperature for 3 h under dark. At the end of the reaction, the polymer was precipitated in methanol and dried under vacuum.

4.5 Synthetic Procedures

Procedures disclosed in this subchapter were previously submitted or published [64,112, 113, 114].

4.5.1 Synthesis of Ionic Liquids (**1a** and **1b**)

The ionic liquid monomers were synthesized in analogy to a procedure described in the literature [120]. 1-Iodoctane (0.5 mol) and 1-iododecane (0.5 mol), respectively were dropped to a stirred solution of 1-vinylimidazole (0.5 mol) dissolved in an equal amount on volume of *t*-butyl-methylether related to the total amount on reactants under nitrogen atmosphere at room temperature. The stirring process of the resulting solution was continued under inert atmosphere until the 1-vinylimidazole was fully converted as analyzed by ¹H-NMR spectroscopy. The raw product was washed with ethyl acetate 10 times followed by evaporation of ethyl acetate and drying under vacuum (10 mbar) at room temperature for 10 h. Yield was 55 % for 1-octyl-3-vinylimidazolium iodide and 67 % in case of 1-decyl-3-vinylimidazolium iodide. Anion exchange was carried out by separate dissolution of lithium bis(trifluoromethylsulfonyl)imide (LiNTf₂) and 1-octyl-3-vinylimidazolium iodide or 1-decyl-3-vinylimidazolium iodide in an equal amount of water relative to the weight of the reactants. Afterward, the LiNTf₂ water solution was slowly dropped to the imidazolium salt water solution during stirring at room temperature, and stirring was continued for 6 h. Dichloromethane (equal volume relative to the ionic liquid) was added to the two-phase mixture to reduce the viscosity of the ionic liquid phase. The organic phase was separated followed by washing with water until no halide was

detectable in the water phase after addition of a few drops of silver nitrate solution. Then, the organic phase was dried over magnesium sulfate followed by evaporation of the solvent under atmospheric pressure at 40 °C. The pressure was then decreased sequentially to 10 mbar. Finally, the ionic liquids were dried at room temperature under vacuum for 24 h resulting in 90 % yield of 1-octyl-3-vinylimidazolium bis(trifluoromethylsulfonyl)imide (**1a**) and 85 % yield of 1-decyl-3-vinylimidazolium bis(trifluoromethylsulfonyl)imide (**1b**) obtained by counter ion exchange. The ¹H-NMR spectra are depicted in Figure S01 and S02. The glass transition temperature was -73 °C for **1a** and -72 °C for **1b** as determined by DSC with the temperature range of - 140 °C to 50 °C using heating and cooling rates of 5 K/min.

¹H-NMR spectrum of the ionic liquid monomers taken at 300 MHz in CDCl₃.

N-octyl-*N'*-vinylimidazolium NTf₂ (**1a**): δ 9.34 (s, 1H), 7.71 (s, 1H), 7.50 (s, 1H), 7.20 (dd, 1H), 5.85 (dd, 1H), 5.43 (dd, 1H), 4.26 (t, 2H), 1.95-1.86 (m, 2H), 1.33 (d, 5H), 1.26 (s, 5H), 0.87 ppm (t, 3H) ppm.

N-decyl-*N'*-vinylimidazolium NTf₂ (**1b**): δ 9.53 (s, 1H), 7.73 (s, 1H), 7.51 (s, 1H), 7.24 (dd, 1H), 5.87 (dd, 1H), 5.43 (dd, 1H), 4.29 (t, 2H), 1.98-1.85 (m, 2H), 1.33 (d, 5H), 1.25 (s, 9H), 0.87 ppm (t, 3H) ppm.

4.5.2 Functionalization of Oleic Acid

Oleic acid, tech. % 90, was purified by the following steps before the synthesis of bis-(9,10-epoxystearic acid) 1,2-ethanediyl ester (**12**) and the isomer mixture consisting of ethane-1,2-diyl bis(9-methacryloyloxy-10-hydroxy octadecanoate), ethane-1,2-diyl 9-hydroxy-10-methacryloyloxy-9'-methacryloyloxy-10'-hydroxy octadecanoate, and ethane-1,2-diyl bis (9-hydroxy-10-methacryloyloxy octadecanoate) (**10**);

In a typical procedure, 75 g of oleic acid technical grade % 90, were mixed with 750 ml acetone, and the solution was cooled to -20 °C and kept at this temperature for 8-10 hours. The crystallized saturated fatty acids were separated followed by evaporation of the acetone from the remaining solution. The residue (67 % yield relative to the oleic acid used for purification) was diluted with fresh acetone (5 ml acetone / 1 g oleic acid) and cooled down to -40 °C. After cooling the solution at -40 °C and keeping it for 24 hours, the oleic acid crystals were isolated. The oleic acid was diluted with fresh acetone and crystallization was repeated at -40 °C several times for further purification of the oleic acid until the ¹H-NMR spectrum indicated a high purity of the oleic acid obtained. Yield on highly pure oleic acid that was free of both saturated fatty acids and higher unsaturated fatty acids was 70 % with respect to the material obtained after the first crystallization.

The oleic acid mix separated from saturated fatty acids only from commercial oleic acid (81% purity) by fractionalized crystallization was used for the synthesis of the isomer mixtures of methyl 9-((meth)acryloyloxy)-10-hydroxyoctadecanoate / methyl 9-hydroxy-10-((meth)acryloyloxy)octadecanoate (**2**, **3**) and methyl 9-(1H-imidazol-1-yl)-10-(methacryloyloxy)octadecanoate / methyl 9-(methacryloyloxy)-10-(1H-imidazol-1-yl)octadecanoate (**4**). Oleic acid (81 %, VWR) was purified by recrystallization from acetone at -20 °C as described in the literature [121]. In a first recrystallization step, saturated fatty acids were completely separated resulting in an oleic acid fraction that was free of saturated fatty acids. The oleic acid fraction is called oleic acid mix because oleic acid was the main constituent containing a small amount on higher unsaturated fatty acids and no saturated fatty acids.

4.5.2.1 Esterification of Oleic Acid with Methanol

Oleic acid mix (40 g) was dissolved in 20.3 ml methanol (rotidry, Carl Roth) followed by slowly addition of H₂SO₄ (1.5 ml) to this solution under stirring. The resulting mixture was heated up to 70 °C and kept at 70 °C for 18 h during stirring. Then, organic phase was separated followed by evaporation of the methanol excess. Furthermore, 750 ml saturated CaCl₂ solution were added to the residue followed by stirring the resulting mixture at 40 °C for 1 h. Then, the organic phase was separated, and washed with 100 ml deionized water each four times followed by stirring with 200 ml deionized water for 1 h. The resulting viscous liquid was extracted with 100 ml diethyl ether each three times. The organic phases were unified and dried over magnesium sulfate. After evaporation of diethyl ether, the remaining viscous liquid was dried under vacuum at 40 °C for 24 h resulting in methyl oleate mix in 85 % yield.

4.5.2.2 Epoxidation of Oleic Acid Methyl Ester

Formic acid (2.8 ml) was added to the methyl oleate mix (10 ml), and the suspension formed was cooled down to 0 °C. Then, 4.3 ml of 50 % hydrogen peroxide were carefully dropped to the solution at 0 °C during high speed stirring. The resulting solution was stirred at 0 °C for 1 h before the reaction mixture was allowed to heat up to room temperature in the presence of a cold water bath for 2 h followed by continuous stirring at room temperature in the absence of the water bath for further 3 h. Saturated NaHCO₃ solution was used to neutralize the light-yellow solution after the addition of 100 ml deionized water. Then, 100 ml ethyl acetate were added to the mixture. The organic phase

was separated and washed with 100 ml deionized water each two times. Finally, the organic phase was dried over magnesium sulfate followed by evaporation of ethyl acetate. The remaining viscous liquid was dried under vacuum (room temperature, 8 – 10 mbar) for 24 h, and 9,10-epoxy stearic acid methyl ester (**11**) was obtained in 88 % yield.

4.5.2.3 Functionalization of 9,10-Epoxy stearic Acid Methyl Ester by Ring Opening

Reaction of the Oxirane Group with (Meth)acrylic Acid (**2** and **3**)

For synthesis of methyl 9-(acryloyloxy)-10-hydroxyoctadecanoate / methyl 9-hydroxy-10-(acryloyloxy)octadecanoate mix (**2**), 9,10-epoxy stearic acid methyl ester mix (10 g), hydroquinone (20 mg) and DABCO (20 mg) were mixed, and stabilized acrylic acid (4,3 g) was carefully added to the mixture. The resulting solution was heated up to 95 °C during stirring and continuously stirred at this temperature for 20 h. After cooling the reaction mixture to room temperature, 100 ml diethyl ether were added to the mixture. Then, the organic phase was washed with 100 ml deionized water followed by neutralization with 1 M NaOH solution and further washing with deionized water. The organic phase was separated followed by drying over magnesium sulfate. After evaporation of diethyl ether, the remaining viscous liquid was dried under vacuum (8 mbar) at room temperature for 24 h resulting in 80 % yield on raw product. Purification of the raw product by column chromatography using a mixture of ethyl acetate:*n*-hexane mixture (2 : 3, v : v) as eluent resulted in 22 % yield of the two isomers (methyl 9-(acryloyloxy)-10-hydroxyoctadecanoate and methyl 9-hydroxy-10-(acryloyloxy)octadecanoate) as a mixture (**2**). The ¹H-NMR spectrum of **2** consisting of the two isomers, (methyl 9-(acryloyloxy)-10-hydroxyoctadecanoate and methyl 9-hydroxy-10-(acryloyloxy)octadecanoate), is depicted in Figure S03. The glass transition temperature of the monomer was -71 °C determined by DSC with the temperature range of -140 °C to 50 °C using heating and cooling rates of 5 K/min.

¹H-NMR spectrum of **2** (300 MHz, CDCl₃): δ 6.44 (dd, 1H), 6.20 – 6.11 (m, 1H), 5.86 (dd, 1H), 4.91 (td, 1H), 3.66 (d, 4H), 2.30 (t, 2H), 1.72 – 1.52 (m, 5H), 1.51-1.37 (m, 3H), 1.28 (d, 18H), 0.87 (t, 3H) ppm.

For synthesis of methyl 9-(methacryloyloxy)-10-hydroxyoctadecanoate / methyl 9-hydroxy-10-(methacryloyloxy)octadecanoate mix (**3**), 9,10- epoxy stearic acid methyl ester mix (10 g), hydroquinone (20 mg) and DABCO (20 mg) were mixed, and stabilized methacrylic acid (4,2 g) was carefully dropped into the mixture. The solution obtained was heated up to 95 °C during stirring and continuously stirred at this temperature for 20 h.

After cooling the reaction mixture to room temperature, 100 ml diethyl ether were added to the mixture followed by phase separation. Then, the organic phase was separated and washed with 100 ml deionized water followed by neutralization with 1 M NaOH solution and further washing with 100 ml deionized water before the organic phase was dried over magnesium sulfate. Finally, diethyl ether was evaporated, and the remaining viscous liquid was dried under vacuum (9 mbar) at room temperature for 24 h. Yield on raw product was 94 %. Purification of the raw product by column chromatography using silica as stationary phase and an ethyl acetate:*n*-hexane mixture (2 : 3, v : v) as eluent resulted in 40% yield of the two isomers (methyl 9-(methacryloyloxy)-10-hydroxyoctadecanoate and methyl 9-hydroxy-10-(methacryloyloxy)octadecanoate) as a mixture (**3**). The ¹H-NMR spectrum of the biobased methacrylate **3** consisting of the two isomers, (methyl 9-(methacryloyloxy)-10-hydroxyoctadecanoate and methyl 9-hydroxy-10-(methacryloyloxy)octadecanoate), is depicted in Figure S04. The glass transition temperature of the monomer was -73°C as determined by DSC with the temperature range of - 140 °C to 50 °C using heating and cooling rates of 5 K/min.

¹H-NMR spectrum of **3** (300 MHz, CDCl₃): δ 6.12 (t, 1H), 5.58 (t, 1H), 4.89 (td, 1H), 3.67 (s, 4H), 2.30 (t, 2H), 1.96 (s, 3H), 1.65 – 1.61 (m, 5H), 1.45 – 1.40 (m, 2H), 1.31 – 1.25 (d, 19H), 0.88 (t, 3H) ppm.

4.5.2.4 Synthesis of the Isomer Mixture Comprising Methyl 9-(1H-imidazol-1-yl)-10-(methacryloyloxy)octadecanoate and Methyl 9-(Methacryloyloxy)-10-(1H-imidazol-1-yl)octadecanoate (4)

Firstly, 9,10-epoxy stearic acid methyl ester mix (0.13 mole) and imidazole (0.88 mole) were dissolved in 80 ml 1,4-dioxane during stirring followed by heating the resulting solution to 95 °C and stirring for 24 h. Then, 1,4-dioxane was evaporated under vacuum (40°C, 107 mbar), and the dark brown residue was cooled down to room temperature before it was stirred with 500 ml deionized water for 2 h. Then, the organic phase was separated and washed with 200 ml deionized water each five times followed by addition of ethyl acetate (250 ml) and drying over magnesium sulfate. After that, evaporation of ethyl acetate under vacuum resulted in a yellow viscous product. Acetone (50 ml) was added to the yellow viscous residue followed by addition of 500 ml *n*-hexane for purification by crystallization, and the resulting mixture was cooled down to -20 °C for 24 h. The crystals obtained were filtrated after crystallization and washed with *n*-hexane. Further recrystallization was carried out by dissolution of the crystals obtained in a minimum

amount of acetone followed by addition of *n*-hexane and cooling down to -20 °C for 24 h. Filtration of the crystals, washing them with *n*-hexane and drying under vacuum at room temperature for 24 h resulted in methyl 9-hydroxy-10-(1H-imidazole-1-yl)octadecanoate / methyl 9-(1H-imidazol-1-yl)-10-hydroxy octadecanoate in 25% yield. In the second step, 3.42 mmol methyl 9-hydroxy-10-(1H-imidazole-1-yl)octadecanoate / methyl 9-(1H-imidazol-1-yl)-10-hydroxy octadecanoate and 0.05 mmol DMAP were dissolved in dichloromethane (15 ml) followed by addition of 0.38 ml triethylamine and 14.96 mmol methacrylic anhydride during stirring. The resulting solution was stirred at room temperature for 24 h. Then, 100 ml dichloromethane were added. The organic phase was washed with 200 ml deionized water each three times. Dichloromethane was evaporated, and the residue was stirred with 100 ml NaOH solution (8 g NaOH per 100 ml deionized water) at room temperature for 2 h followed by addition of 50 ml dichloromethane. The organic phase was separated and washed with 50 ml deionized water each two times. Then, the organic phase was dried over magnesium sulfate followed by evaporation of dichloromethane. The viscous liquid was dried under vacuum at room temperature for 24 h and the isomer mixture consisting of methyl 9-(1H-imidazol-1-yl)-10-(methacryloyloxy)octadecanoate and methyl 9-(methacryloyloxy)-10-(1H-imidazol-1-yl)octadecanoate (**4**) was obtained in 75 % yield. The ¹H-NMR spectrum of the biobased monomer (**4**), (methyl 9-(1H-imidazol-1-yl)-10-(methacryloyloxy)octadecanoate and methyl 9-(methacryloyloxy)-10-(1H-imidazol-1-yl)octadecanoate), is depicted in Figure S05. The glass transition temperature of the biobased monomer **4** was determined as 9 °C by DSC with the temperature range of - 60 °C to 80 °C using heating and cooling rates of 5 K/min. ¹H-NMR spectrum of **4** (300 MHz, CDCl₃): δ 7.49 (s, 1H), 7.08 (s, 1H), 6.96 (s, 1H), 6.12 (s, 1H), 5.62 (s, 1H), 5.22 (td, 1H), 4.06 (ddd, 1H), 3.66 (s, 3H), 2.28 (t, 2H), 1.97 (s, 3H), 1.75 (q, 2H), 1.57 (q, 2H), 1.39-1.31 (m, 2H), 1.23 (d, 20 H), 0.87 (t, 3H) ppm.

4.5.3 Synthesis of 4-(4-Methacryloyloxyphenyl)-butan-2-one (**7**)

4-(4-Hydroxyphenyl)butan-2-one (8.2 g) and triethylamine (5.8 g) were dissolved in dichloromethane (30 ml), and the solution was cooled down to 0 °C during stirring. Furthermore, a second solution made by dissolution of methacryloyl chloride (6.3 g) in 5 ml dichloromethane was slowly dropped to the first solution during stirring at 0 °C for 30 min. After two solutions were well mixed, the ice bath was removed, and the reaction mixture was heated up to room temperature. The resulting solution was stirred at room temperature for further 16 h followed by filtration of the precipitate. The latter was washed with 30 ml dichloromethane, and the organic phases were unified. The resulting organic

solution was washed with 30 ml HCl (0.5 M) at first, second with 20 ml K₂CO₃ solution (1 M), and finally twice with 10 ml deionized water each. After washing the organic phase with deionized water, it was dried over magnesium sulfate followed by evaporation of the solvent. The raw product of monomer **7** was obtained in 75% yield. The raw product was purified by column chromatography using a *n*-hexane: ethylacetate mixture (4:1, v: v) as eluent followed by recrystallization of **7** in *n*-hexane. Purified monomer **7** was obtained as white crystals (mp 29 °C) in 35% yield after drying under vacuum for 24 h. The ¹H-NMR spectrum of the monomer **7** is depicted in Figure S06. DSC analysis resulted in T_{cryst} = -7 °C and T_m = 29 °C. Method was set to temperature interval of -60 °C to 50 °C using heating and cooling rates of 5 K/min.

¹H-NMR spectrum of **7** (300 MHz, CDCl₃): δ 7.19 (d, 2H), 7.00 (d, 2H), 6.33 (s, 1H), 5.73 (t, 1H), 2.89 (t, 2H), 2.75(t, 2H), 2.13 (s, 3H), 2.05 (s, 3H) ppm.

4.5.4 Esterification of Oleic Acid with Ethylene Glycol

Purified oleic acid (40 g, 0.14 mole) and ethylene glycol (4,34 g, 0.07 mole) were added into 250 ml flask, which was equipped with a Reverse Dean Stark and a thermometer. Chloroform (100 ml) was added to the 250 ml flask and mixed until a well dissolved and colorless mixture was obtained. After that, 2.5 g *p*-toluenesulfonic acid were added to the flask under vigorous stirring, and the resulting mixture was heated up to 70 °C. The reaction was stirred at this temperature for 12 h. Then, the reaction mixture was cooled down, and mixed with saturated CaCl₂ solution (750 ml) at 40 °C for 1 h. After that, organic phase was washed with 100 ml deionized water each 4 times. The resulting colored viscous oil was stirred with 200 ml deionized water for 1 h. The solution was extracted with diethyl ether, and the organic phase was dried over magnesium sulfate. Diethyl ether was evaporated, and the raw product was obtained in 87.5 % yield. Then, the orange viscous liquid was diluted with ethyl acetate and passed through the column filled by basic alumina. After evaporation of ethyl acetate, the remaining viscous liquid was dried under reduced pressure for 24 h resulting in oleic acid 1,2-ethanediyl ester as yellow viscous oil in 70 % yield.

4.5.4.1 Epoxidation of Oleic Acid 1,2-Ethanediyl Ester

Formic acid (5.6 ml) was added to oleic acid 1,2-ethanediyl ester (17,4 g) followed by cooling down the solution to 0 °C. Then, 8.6 ml of % 50 hydrogen peroxide were carefully dropped during vigorous stirring into this solution at 0 °C. After that, the solution was further stirred at 0 °C for 1 h followed by slowly warming up the reaction mixture to room

temperature and continuous stirring at room temperature for 16 hours. Since the reaction was still highly exothermic, cold water bath was used to keep the reaction temperature at room temperature during stirring. After 16 h stirring process at room temperature, deionized water (100 ml) was added to the two phases consisting of a high amount of white solid and a low amount of liquid. The mixture was neutralized by 150 ml saturated sodium hydrogen carbonate solution. The resulting mixture was filtrated, and the precipitate was stirred with 100 ml water. The precipitate obtained by filtration was washed with deionized water several times until the pH of washing water was neutral. The isolated precipitate was dried under vacuum for 24 h followed by recrystallization in *n*-hexane and further drying under vacuum for 24 h. Finally, bis-(9,10-epoxystearic acid) 1,2-ethanediyl ester (**12**) was obtained in 72 % yield. The NMR spectra are depicted in Figure S07-a), and Figure S07-b).

¹H-NMR spectrum (300 MHz, CDCl₃) of **12**: δ 4.27 (s, 4H), 2.90 (s, 4H), 2.33 (t, 4H), 1.65-1.26 (m, 50), 0.88 (t, 6H) ppm.

¹³C-NMR spectrum (75 MHz, CDCl₃) of **12**: δ 173.55, 167.28, 167.25, 136.36, 125.58, 72.61, 62.01, 34.09, 33.70, 33.66, 31.87, 31.84, 30.69, 30.54, 29.58, 29.52, 29.43, 29.37, 29.33, 29.25, 29.21, 29.17, 20.09, 29.00, 25.64, 25.59, 25.41, 25.37, 24.83, 22.66, 18.46, 14.10 ppm.

4.5.4.2 Ring Opening Reaction of Bis-(9,10-epoxystearic acid) 1,2-Ethanediyl Ester

Bis-(9,10-epoxystearic acid) 1,2-ethanediyl ester (**12**) (16 mmol) was mixed with 20 mg hydroquinone and 20 mg 1,4-diazabicyclo(2.2.2)octane (DABCO). The solid mixture was heated up to 60 °C to be well mixed in the liquid state. After all reactants were well mixed in the liquid state, the heating of the flask was stopped. Then, stabilized methacrylic acid (49 mmol) was slowly dropped into the liquid mixture. The final solution was heated up to 95 °C during stirring and it was stirred at 95 °C for 24 h. Then, the mixture was cooled down to room temperature. After that, 100 ml diethyl ether were added at first followed by addition of 100 ml deionized water. The organic phase was separated and then neutralized by addition of 1 M sodium hydroxide solution. The resulting solution was washed with deionized water and dried over magnesium sulfate. After evaporation of the solvent and drying the residue under vacuum, the raw product of **10** was obtained in 92 % yield. Column chromatographic purification of this raw product using a diethyl ether, *n*-hexane mixture (vol:vol=2:1) as eluent resulted in 24 % yield of the three isomers (ethane-1,2-diyl bis(9-methacryloyloxy-10-hydroxy octadecanoate), ethane-1,2-diyl 9-hydroxy-10-methacryloyloxy-9'-methacryloyloxy-10'-hydroxy octadecanoate, and

ethane-1,2-diyl bis(9-hydroxy-10-methacryloyloxy octadecanoate)) as a mixture (**10**). The NMR spectra of the new biobased dimethacrylate consisting of the three isomers (ethane-1,2-diyl bis(9-methacryloyloxy-10-hydroxy octadecanoate), ethane-1,2-diyl 9-hydroxy-10-methacryloyloxy-9'-methacryloyloxy-10'-hydroxy octadecanoate, and ethane-1,2-diyl bis(9-hydroxy-10-methacryloyloxy octadecanoate)) are depicted in Figure S08-a) and Figure S08-b).

$^1\text{H-NMR}$ spectrum (300 MHz, CDCl_3) of **10**: δ 6.12 (s, 2H), 5.58 (s, 2H), 4.91-4.86 (m, 2H), 4.27 (s, 4H), 3.63 (s, 2H), 2.32 (t, 4H), 1.96 (s, 6H), 1.70-1.26 (m, 52), 0.88 (t, 6H) ppm.

$^{13}\text{C-NMR}$ spectrum (75 MHz, CDCl_3) of **10**: δ 173.55, 62.02, 57.24, 57.19, 34.08, 31.86, 29.55, 29.36, 29.22, 29.01, 27.84, 27.81, 26.61, 24.83, 22.67, 14.12 ppm.

5. Results and Discussion

Within the scope of this thesis, linear polymers and network systems were developed in line with principles of green chemistry and investigated using different methods. Photopolymerization technique was used to obtain these systems. Photokinetic study was carried out on the monomers synthesized via green approach. The results determined by kinetic investigation were compared to the systems based on traditional (meth)acrylates or epoxies. The monomers, which were used in this work, have been numerated and shown in Table 3 and Table 14.

Firstly, the biobased monomers (**2**, **3** and **4**) with one polymerizable group were derived from oleic acid mix which also contains lower amount of higher unsaturated fatty acids. Photoinitiated polymerization kinetic of biobased (meth)acrylates (**2,3** and **4**) and ionic liquids (**1a** and **1b**) was reported in comparison with the systems derived from commercial monomers (**5** and **6**) in the presence of 1 wt % for both photoinitiators, Irgacure® TPO-L and Ivocerin® and 3 wt % for Irgacure® TPO-L. Ionic liquid monomers (**1a** and **1b**) and methyl 9-(1H-imidazol-1-yl)-10-(methacryloyloxy)octadecanoate / methyl 9-(methacryloyloxy)-10-(1H-imidazol-1-yl)octadecanoate (**4**) exhibit quantitative conversion in case of higher concentration of Irgacure® TPO-L or Ivocerin® which is important for practical applications in coating. In addition to the influence of photoinitiator concentration or type on the efficiency of the system, monomer structure and functionality also have a significant effect on the polymerization kinetic.

Another monomer, 4-(4-methacryloyloxyphenyl)-butan-2-one (**7**) was synthesized, which can also be classified under green approach. It was aimed to reduce the effect of long aliphatic chain causing low T_g values for poly(methacrylates) modified from fatty acid esters, and to diversify the kinetic study by using the starting materials with different chemical structures. Monomer **7** shows significantly higher reactivity compared to the commercial systems prepared from **8** and **9** (Table 3). The major effect of monomer structure on the polymerization kinetic was discussed in detailed.

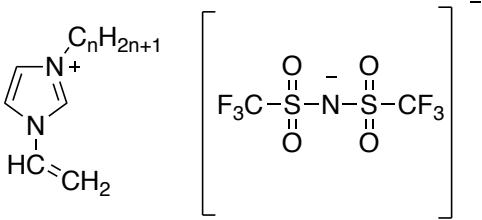
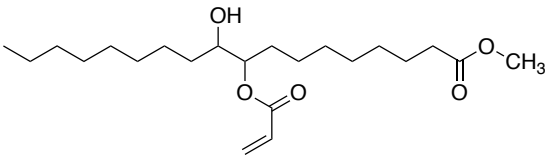
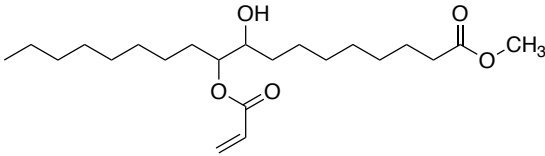
Crosslinked polymer, that can provide the surface resistance against different solvents, is another topic presented in this thesis. In order to create a biobased network system, the isomer mixture (**10**) consisting of ethane-1,2-diyl bis(9-methacryloyloxy-10-hydroxy octadecanoate), ethane-1,2-diyl 9-hydroxy-10-methacryloyloxy-9'-methacryloyloxy-10'-hydroxy octadecanoate, and ethane-1,2-diyl bis(9-hydroxy-10-methacryloyloxy octadecanoate (**10**) was synthesized which has not been previously reported in literature. Monomer **10** was copolymerized with monomer **4** and **7** in different stoichiometric ratios,

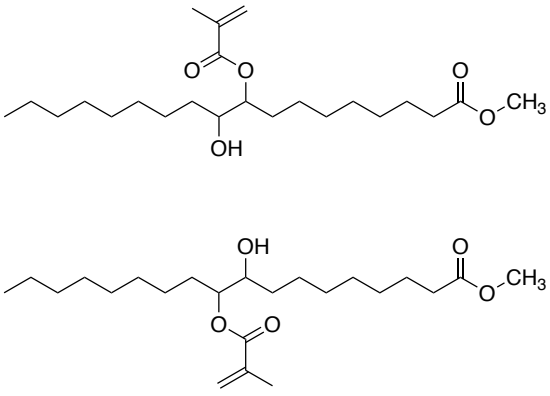
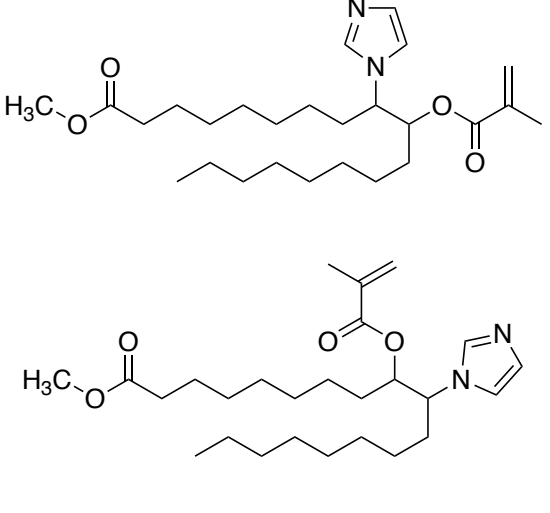
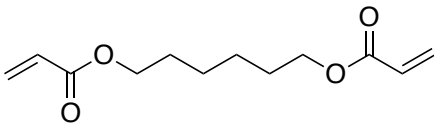
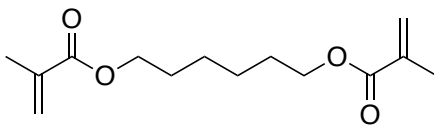
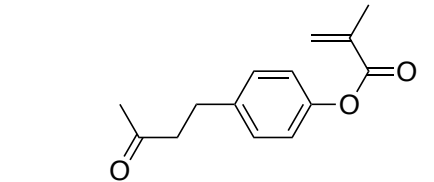
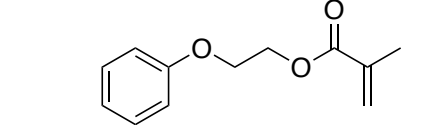
respectively to reduce the effect of long aliphatic chain and to increase the glass transition value. While the poly-**10** has the highest crosslink density, an increase in glass transition temperature, T_g , has been detected for copolymers derived from the mixture of monomer **10** and monomer **7** (1:9 mol:mol ratio).

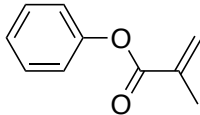
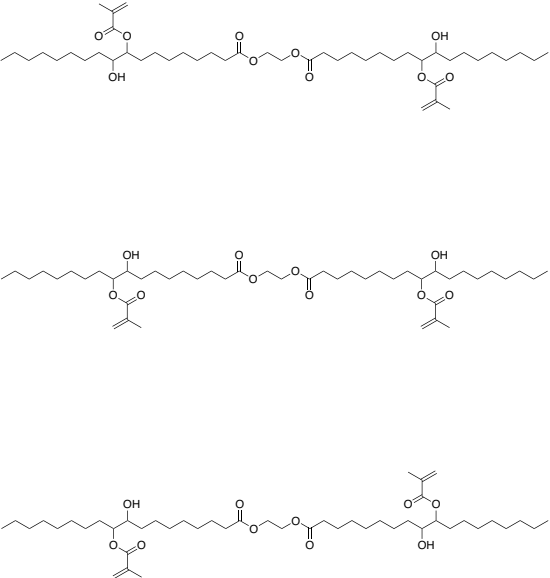
Another network system was manufactured from bis-(9,10-epoxystearic acid) 1,2-ethanediyl ester (**12**) via cationic photoinitiated polymerization in the presence of aluminate (S2617) and ITX as PIS. Photopolymerization kinetic was studied for 9,10-epoxystearic acid methyl ester (**11**) and bis-(9,10-epoxystearic acid) 1,2-ethanediyl ester (**12**) and the results of these biobased monomers were compared to those of commercial monomers such as 3,4-epoxycyclohexylmethyl-3',4'-epoxycyclohexane carboxylate (**13**), 1,4-butanediol diglycidyl ether (**14**), and diglycidylether of bisphenol-A (**15**). Mechanical properties of poly-**12** was improved by copolymerization of monomer **12** with monomer **15** in different mol ratios. Furthermore, evaluation of the mechanical properties, T_g , crosslink density, molecular weight between two crosslink points, and surface wettability of the polymer surfaces are presented in this work as well.

In the following subsections, each methodology is explained and kinetic details of the each system are evaluated.

Table 3: Structure of the monomers used in the following sections. Two isomers of **2**, **3**, and **4** and three isomers of **10** were drawn, respectively.

Monomers	Chemical Structure	No
N -octyl- and N -decyl N' -vinylimidazolium NTf ₂		1 (n=8 (1a), n=10 (1b))
Methyl 9-(acryloyloxy)-10-hydroxyoctadecanoate		2
Methyl 9-hydroxy-10-(acryloyloxy)octadecanoate		

<p>Methyl 9-(methacryloyloxy)-10-hydroxyoctadecanoate</p> <p>Methyl 9-hydroxy-10-(methacryloyloxy)octadecanoate</p>		<p>3</p>
<p>Methyl 9-(1H-imidazol-1yl)-10-(methacryloyloxy)octadecanoate</p> <p>Methyl 9-(methacryloyloxy)-10-(1H-imidazol-1yl)octadecanoate</p>		<p>4</p>
<p>1,6-Hexanediol diacrylate</p>		<p>5</p>
<p>1,6-Hexanediol dimethacrylate</p>		<p>6</p>
<p>4-(4-Methacryloyloxyphenyl)-butan-2-one</p>		<p>7</p>
<p>2-Phenoxyethyl methacrylate</p>		<p>8</p>

Phenyl methacrylate		9
Ethane-1,2-diyl bis(9-methacryloyloxy-10-hydroxy octadecanoate) Ethane-1,2-diyl 9-hydroxy-10-methacryloyloxy-9'-methacryloyloxy-10'-hydroxyoctadecanoate Ethane-1,2-diyl bis(9-hydroxy-10-methacryloyloxy octadecanoate)		10

5.1 Photoinitiated Polymerization of Monomers Modified from Oleic Acid Mix and Ionic Liquids

The biobased monomers, methyl 9-((meth)acryloyloxy)-10-hydroxyoctadecanoate / methyl 9-hydroxy-10-((meth)acryloyloxy)octadecanoate (**2** and **3**), and methyl 9-(1H-imidazol-1yl)-10-(methacryloyloxy)octadecanoate / methyl 9-(methacryloyloxy)-10-(1H-imidazol-1yl)octadecanoate (**4**), were synthesized from oleic acid mix comprising oleic acid as a main component and lower concentration of higher unsaturated fatty acid. The chemical structure of the monomers was displayed in Table 3.

Photoinitiated polymerization of biobased monomers (**2**, **3** and **4**) and ILs (**1a** and **1b**) was compared to the conventional 1,6-hexanediol di(meth)acrylate (**5** and **6**). The IL monomers of **1a** and **1b** were chosen due to their negligible vapour pressure and the presence of long alkyl chain in their chemical structure.

5.1.1 Comparison of Photopolymerization of Ionic Liquid Monomers (**1a**, **1b**), Methyl 9-(Acryloyloxy)-10-hydroxyoctadecanoate / Methyl 9-Hydroxy-10-(acryloyloxy)octadecanoate (**2**) with 1,6-Hexanediol Diacrylate (**5**)

Some results discussed in this subchapter were previously published [64].

Ionic liquid monomers (**1a** and **1b**), methyl 9-((meth)acryloyloxy)-10-hydroxyoctadecanoate / 9-hydroxy-10-((meth)acryloyloxy)octadecanoate (**2** and **3**) and methyl 9-(1H-imidazol-1yl)-10-(methacryloyloxy)octadecanoate / methyl 9-(methacryloyloxy)-10-(1H-imidazol-1yl)octadecanoate (**4**) are promising candidates for numerous applications such as coating by UV-curing. Irgacure® TPO-L and Ivocerin® were selected as photoinitiators for UV-curing experiments because of their high efficiency as already reported in the literature [60-64]. The photopolymerizing samples were prepared using 1 wt % for both photoinitiators, Irgacure® TPO-L and Ivocerin®. Additionally, the amount of Irgacure® TPO-L was increased from 1 wt % to 3 wt % in the photopolymerizing formulation due to the expectation of lower reactivity of Irgacure® TPO-L compared to the Ivocerin®. All synthesized monomers present the non-polar long alkyl chain in their structure. Besides, the hydroxy group of the monomer **2** and **3**, the imidazole group in the fatty acid methyl ester (**4**) and imidazolium moiety of the ionic liquids (**1a** and **1b**) form the polar part of the structures which are combined to the long alkyl chain.

The photoinitiated polymerization of **2**, **1a** and **1b** were performed at 40 °C for 10 min irradiation and the reactivity of these systems were investigated in comparison with the traditional diacrylate (**5**). The polymerization rate (R_p) was determined from the heat flux obtained as function of time (t) during photo-DSC measurements, eq (3.1). Molar polymerization enthalpy of vinylimidazolium based ionic liquids has not been previously reported in the literature. Thus, it was determined for the ionic liquid monomers by evaluation the value of the polymerization heat in the experiments showing quantitative conversion of the vinyl group confirmed by $^1\text{H-NMR}$ spectroscopy (see Figures S01 and S02). An average molar polymerization enthalpy for the ionic liquid monomers was determined - 92 kJ.mol⁻¹ upon the calculation which is relatively close to the molar polymerization value of vinyl acetate ($H_p = - 87.9$ kJ.mol⁻¹, [122,123]). The value ($\Delta H = - 92$ kJ.mol⁻¹), directly calculated for **1a** and **1b**, was used for further evaluation of conversion and R_p .

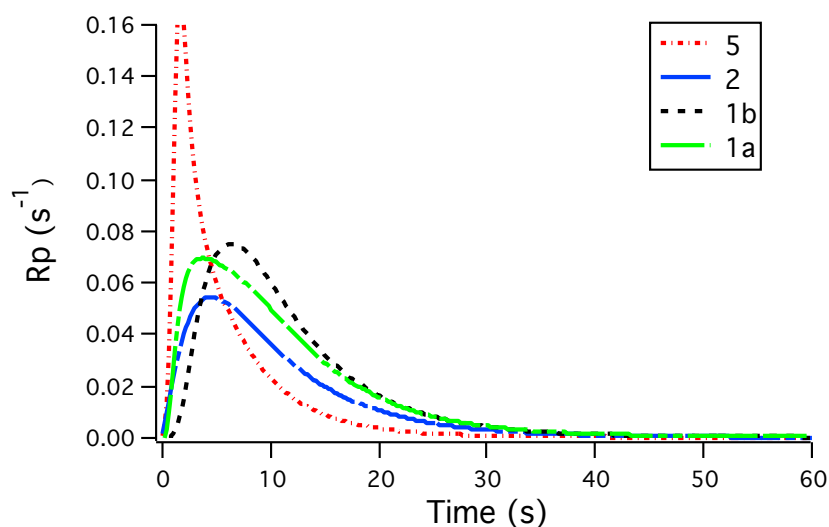


Figure 1: Polymerization rate (R_p (s^{-1})) as function of irradiation time (s) for photoinitiated polymerization of 1,6-hexanediol diacrylate (**5**), methyl 9-(acryloyloxy)-10-hydroxyoctadecanoate / methyl 9-hydroxy-10-(acryloyloxy)octadecanoate (**2**), *N*-octyl-*N*'-vinylimidazolium NTf2 (**1a**), and *N*-decyl-*N*'-vinylimidazolium NTf2 (**1b**) containing 1 wt % Irgacure® TPO-L. Irradiation was carried out at 40 °C for 10 min, adapted from [64].

Figure 1 shows the R_p curves obtained by Photo-DSC measurements of the ionic liquid monomers **1a** and **1b**, and biobased monomer **2** in comparison with the commercial diacrylate **5**.

Since the commercial diacrylate **5** comprises two polymerizable groups, it shows higher reactivity compared to the ionic liquid monomers (**1a** and **1b**) and biobased monomer **2** containing only one double bond. The monomer bearing more functional groups generally has higher reactivity [22]. In addition to this, monomer **2** has lower R_{p}^{max} value than ionic liquid monomers (**1a** and **1b**). Cationic and an anionic parts of the ionic liquid monomers and nanophase separation due to the long alkyl chain and the ionic group of the structure may cause the higher R_{p}^{max} value compared to the biobased acrylate **2**.

R_{p}^{max} and maximum time (t_{max}) to reach the R_{p}^{max} parameters were summarized in Table 4 to compare the reactivity of the monomers. It is clearly shown in Table 4 that ionic liquid monomers (**1a** and **1b**) and biobased monomer **2** have lower reactivity than commercial diacrylate **5** for all initiators and all initiator concentrations. Two functional groups in the chemical structure of the commercial monomer **5** may explain a higher reactivity [22].

Table 4: Maximum of the polymerization rate (R_p^{\max}), time (t_{\max}) to obtain the maximum of polymerization rate, and final conversion for photoinitiated polymerization of the ionic liquids **1a** and **1b**, methyl 9-((meth)acryloyloxy)-10-hydroxyoctadecanoate / methyl 9-hydroxy-10-((meth)acryloyloxy)octadecanoate **2** and **3**, methyl 9-(1H-imidazol-1yl)-10-(methacryloyloxy)octadecanoate / methyl 9-(methacryloyloxy)-10-(1H-imidazol-1yl)octadecanoate **4**, and the commercial di(meth)acrylates **5** and **6** containing either Irgacure® TPO-L (1 wt % and 3 wt %, respectively) and Ivocerin® (1 wt %) as photoinitiator for 10 min irradiation time at 40 °C, adapted from [64]).

Monomer	Initiator (wt %)	R_p^{\max} (s ⁻¹)	t_{\max} (s)	Final Conversion (%)
5	TPO-L 1 %	0,17	1,6	80
5	TPO-L 3 %	0,20	1,6	82
5	Ivocerin 1 %	0,19	1,6	83
1a	TPO-L 1 %	0,070	3,8	100
1a	TPO-L 3 %	0,079	3	100
1a	Ivocerin 1 %	0,071	2,6	100
1b	TPO-L 1 %	0,075	6,4	99
1b	TPO-L 3 %	0,091	3,8	100
1b	Ivocerin 1 %	0,093	3,4	100
2	TPO-L 1 %	0,055	4,6	73
2	TPO-L 3 %	0,057	3,6	71
2	Ivocerin 1 %	0,072	2,8	74
6	TPO-L 1 %	0,053	12,2	68
6	TPO-L 3 %	0,059	10,6	77
6	Ivocerin 1 %	0,066	11,4	82
3	TPO-L 1 %	0,023	10,6	90
3	TPO-L 3 %	0,031	8,6	95
3	Ivocerin 1 %	0,034	7,8	95
4	TPO-L 1 %	0,020	15	98
4	TPO-L 3 %	0,035	12,2	100
4	Ivocerin 1 %	0,020	10,4	100

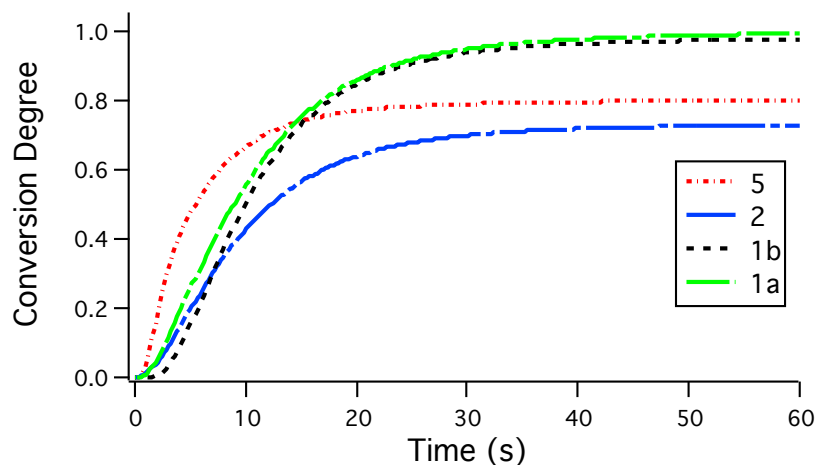


Figure 2: Conversion as function of irradiation time (s) for photoinitiated polymerization of 1,6-hexanediol diacrylate (**5**), methyl 9-(acryloyloxy)-10-hydroxyoctadecanoate / methyl 9-hydroxy-10-(acryloyloxy)octadecanoate (**2**), *N*-octyl-*N'*-vinylimidazolium NTf₂ (**1a**), and *N*-decyl-*N'*-vinylimidazolium NTf₂ (**1b**) containing 1 wt % Irgacure® TPO-L. Irradiation was carried out at 40 °C for 10 min adapted from [64].

The ionic liquid monomers **1a** and **1b** show quantitative conversion and it is independent on the type of initiator and initiator concentration. The full conversion was also confirmed by ¹H-NMR (Figure S01 and S02). The polymers made of **1a** and **1b** in the photo-DSC pan were completely dissolved in the deuterated solvent after 10 min irradiation process for ¹H-NMR measurement. The absence of the vinyl group in the spectra proves the quantitative conversion of the ionic liquid monomers after 10 min irradiation process (see Figures S01 and S02). Quantitative conversion of the monomer is quite important for practical applications. On the other hand, the final conversion of the acrylated monomers **2** and **5** is limited to about 70% or 80%, respectively. Interestingly, comparison of the R_p^{\max} values demonstrates the quite similar values for both photoinitiators. Even if, the Irgacure® TPO-L concentration is increased from 1% to 3%, the R_p^{\max} values of the acrylate monomers slightly increase.

5.1.2 Comparison of Photopolymerization of Methyl 9-(Methacryloyloxy)-10-hydroxyoctadecanoate / Methyl 9-Hydroxy-10-(methacryloyloxy)octadecanoate (**3**), Methyl 9-(1H-imidazol-1yl)-10-(methacryloyloxy)octadecanoate / Methyl 9-(Methacryloyloxy)-10-(1H-imidazol-1yl)octadecanoate (**4**) with 1,6-Hexanediol Dimethacrylate (**6**)

Some of the results explained in this subchapter were previously discussed [64].

The monomers bearing methacrylate group are also noteworthy as much as acrylated monomers because methacrylates are generally easy to handle due to their less reactivity

and less toxicity. Another case for acrylate monomers to be considered in addition to their higher toxicity and reactivity is that they can undergo Michael addition reaction in contrast to the methacrylates.

The biobased methacrylates (**3** and **4**) were polymerized by photoinitiated polymerization at 40 °C for 10 min irradiation. Kinetic investigation of these biobased systems were compared to the system made by photopolymerization of traditional 1,6-hexanediol dimethacrylate (**6**) in the presence of 3 wt % of Irgacure® TPO-L in addition to 1 wt % of both Irgacure® TPO-L and Ivocerin®. As previously discussed for biobased acrylate **2** and commercial diacrylate **5**, same trend in the reactivity was also observed for methacrylate monomers **3**, **4** and **6**. The biobased methacrylates **3** and **4** show lower reactivity in comparison with commercial methacrylate **6** comprising two double bonds as shown in Figure 3. Higher reactivity of the commercial dimethacrylate monomer **6** can be attributed to two functional groups in monomer structure [22]. Although the reactivity of the biobased methacrylates **3** and **4** is lower than commercial dimethacrylate **6**, they reach higher final conversion values after 10 min irradiation. The quantitative conversion is observed for biobased monomer **4** as it can be seen in Figure 4. In addition to this, while the final conversion of the biobased methacrylate **3** is about 90–95%, double bond conversion is limited to 70–80% for the crosslinking traditional monomer **6**, see Table 4. The biobased methacrylate **4** can be preferred for practical applications due to the full double conversion. Furthermore, three times higher concentration of TPO-L results in a slight increase in both $R_{p,max}$ and final conversion values (Table 4).

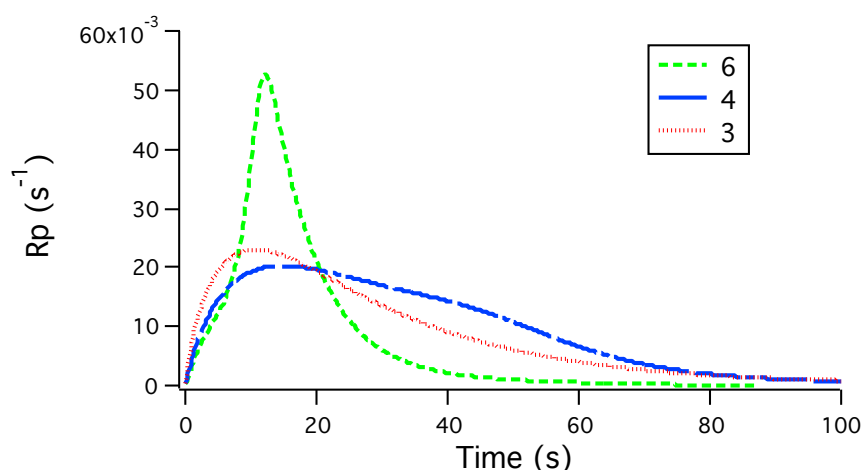


Figure 3: Polymerization rate (R_p (s^{-1})) as function of irradiation time (s) for photoinitiated polymerization of 1,6-hexanediol dimethacrylate (**6**), methyl 9-(1H-imidazol-1yl)-10-(methacryloyloxy)octadecanoate / methyl 9-(methacryloyloxy)-10-(1H-imidazol-1yl)octadecanoate (**4**), methyl 9-(methacryloyloxy)-10-hydroxyoctadecanoate / methyl 9-hydroxy-10-(methacryloyloxy)octadecanoate (**3**), containing 1 wt % Irgacure® TPO-L. Irradiation was carried out at 40 °C for 10 min, adapted from [64].

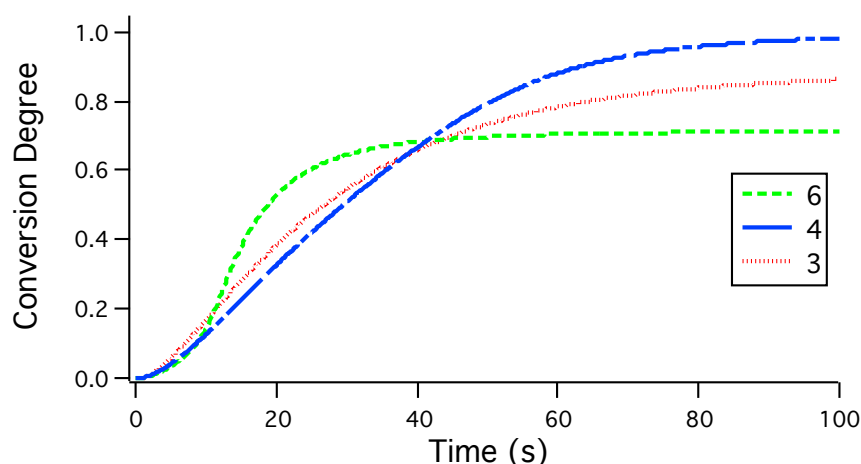


Figure 4: Conversion as function of irradiation time (s) for photoinitiated polymerization of 1,6-hexanediol dimethacrylate (**6**), methyl 9-(1H-imidazol-1yl)-10-(methacryloyloxy)octadecanoate / methyl 9-(methacryloyloxy)-10-(1H-imidazol-1yl)octadecanoate (**4**), methyl 9-(methacryloyloxy)-10-hydroxyoctadecanoate / methyl 9-hydroxy-10-(methacryloyloxy)octadecanoate (**3**) containing 1 wt % TPO-L. Irradiation was carried out at 40 °C for 10 min, adapted from [64].

Moreover, T_g of the polymers derived from monomers **2** and **4** is 19 °C which is lower than the polymerization temperature. It demonstrates that vitrification is not the case during polymerization reaction.

On the other hand, polymerization of commercial dimethacrylate **6** produces crosslinked network structure. Crosslinking reaction and vitrification may be a reason of the limited final conversion in case of monomer **6** (Figure 4, Table 4).

The ionic liquid monomers (**1a** and **1b**) and biobased methacrylate **4** are worthy materials for coating applications due to their quantitative conversion in the presence of Irgacure® TPO-L and Ivocerin® as photoinitiators. Despite the slightly higher efficiency was generally observed in case of 1 wt % Ivocerin compared to 1 wt % Irgacure® TPO-L, higher concentration of Irgacure® TPO-L (3 wt %) causes a similar performance for the photopolymerization processes as observed for 1 wt % Ivocerin. On the other hand, polymerization rate and conversion of the double bond are nearly independent on photoinitiator type and its concentrations in several experiments. It can be pointed out that monomer structure has a significant influence on polymerization kinetic. The ionic liquid monomers (**1a** and **1b**) with quantitative conversion and biobased monomers **3** and **4** with greater than 90 % or quantitative conversion can be interesting candidates for different applications such as anti-microbial surfaces and coating manufacturing for protection of the surfaces against weather. In addition, the (meth)acrylates **2**, **3**, and **4** functionalized from oleic acid mix may reduce the carbon footprint of coated surfaces.

5.2 Comparison of Photopolymerization Kinetic of Monomers Bearing Methacrylate and Phenyl Groups (7, 8 and 9)

Some results discussed in this subchapter were previously published [112].

The monomers modified from fatty acid methyl esters (**2,3** and **4**) or ionic liquids (**1a** and **1b**) have potential for practical applications because of their high conversion values. However, the polymers comprising long aliphatic chain show low glass transition temperature. Therefore, synthesis of the another monomer bearing different pendant group is beneficial not only to vary final material properties but also to examine the influence of monomer structure in terms of polymerization kinetic. Accordingly, 4-(4-methacryloyloxyphenyl)-butan-2-one (**7**) was synthesized and investigated by photoinitiated polymerization.

Photopolymerization of the 4-(4-methacryloyloxyphenyl)-butan-2-one (**7**) monomer was carried out using 1 wt % of both Irgacure® TPO-L and Ivocerin® as well as 3 wt % of Irgacure® TPO-L for different temperatures and different irradiation times as described in 4.3.1 and 4.3.2. Since both Norrish type I photoinitiators exhibit comparable performance in the photopolymerization kinetic of (meth)acrylated fatty acid methyl esters or ILs, same photoinitiators were applied for photopolymerization of new 4-(4-methacryloyloxyphenyl)-butan-2-one. The polymerization kinetic was reported for 4-(4-methacryloyloxyphenyl)-butan-2-one (**7**) in comparison with commercial 2-phenoxyethyl methacrylate (**8**) and phenyl methacrylate (**9**) in the presence of 1 wt % of Irgacure® TPO-L. The commercial methacrylates **8** and **9** were chosen for the comparison of photopolymerization kinetic due to the similarity in their molecular structure based on the presence of aromatic group.

GPC and DSC measurements were performed to complement the discussion of the kinetic study and material properties. Thermal polymerization of **7** containing 1 wt % of Irgacure® TPO-L was also carried out separately in order to discuss about possible thermal process during photoinitiated polymerization of **7** at elevated temperature.

5.2.1 Photoinitiated Polymerization of 4-(4-Methacryloyloxyphenyl)-butan-2-one (7) at 40°C

Photopolymerization of monomer **7** was performed in the presence of Ivocerin® (1 wt %) and Irgacure® TPO-L (1 wt % and 3 wt %, respectively) using photo-DSC. It is clearly seen in Figure 5 that polymerization rate rises rapidly up to the R_p^{\max} . Unexpectedly, a slight shoulder was observed in the polymerization rate as function of time graphs of 4-(4-methacryloyloxyphenyl)-butan-2-one (**7**) for all cases. Moreover, the shoulder is more

distinct when 1 wt % Irgacure[®] TPO-L is applied for photopolymerization. Polymerization rate decreases rapidly after reaching up to its maximum value in all experiments. Quantitative conversion is observed for both photoinitiators and concentrations as shown in Figure 6 and Table 5. The irradiation time to reach full conversion or maximum polymerization rate is shorter in case of higher Irgacure[®] TPO-L (3 wt %) concentration or Ivocerin[®] (1 wt %), while the polymerization occurs slightly slower in the presence of 1 wt % Irgacure[®] TPO-L. The phenomenon that the shoulder is more pronounced for the system comprising 1 wt % Irgacure[®] TPO-L may be related to its slower polymerization rate and lower reactivity than (3 wt %) Irgacure[®] TPO-L or (1 wt %) Ivocerin[®]. Therefore, 1 wt % Irgacure[®] TPO-L was selected as a model system to investigate the occurrence of shoulder in the graph.

More detailed investigation was performed to make a deeper explanation about pronounced shoulder in the polymerization rate versus time curve when 1 wt % Irgacure[®] TPO-L was used for photopolymerization experiments. Therefore, additional time dependent measurements at 40 °C and temperature dependent measurements (55 °C , 70 °C and 85 °C) for 10 min irradiation were carried out in the presence of 1 wt % Irgacure[®] TPO-L, respectively. Afterwards, photopolymers were analyzed separately by GPC, DSC and ¹H-NMR for further investigation. All results were summarized in Table 7 and Table 8.

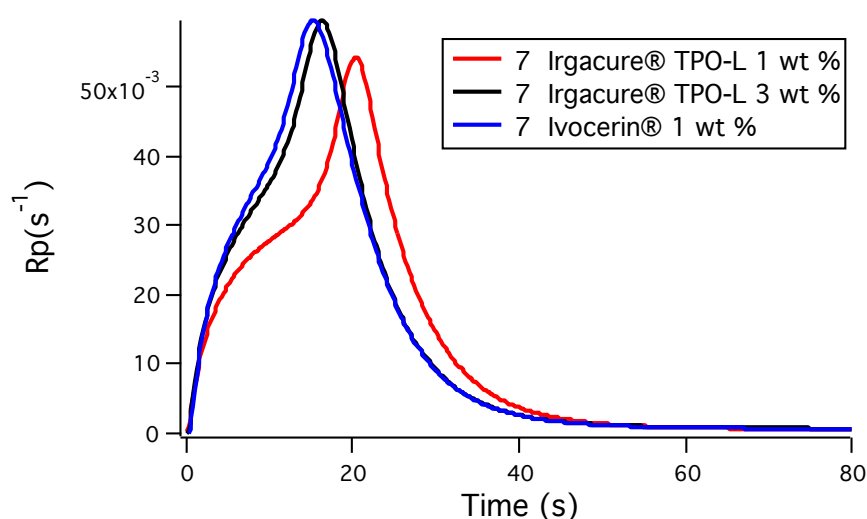


Figure 5: Polymerization rate (R_p (s^{-1})) as function of irradiation time (s) for photoinitiated polymerization of 4-(4-methacryloyloxyphenyl)-butan-2-one (**7**) containing Irgacure[®] TPO-L (1 wt % and 3 wt %, respectively) or Ivocerin[®] (1 wt %) at 40 °C for 10 min, adapted from [112].

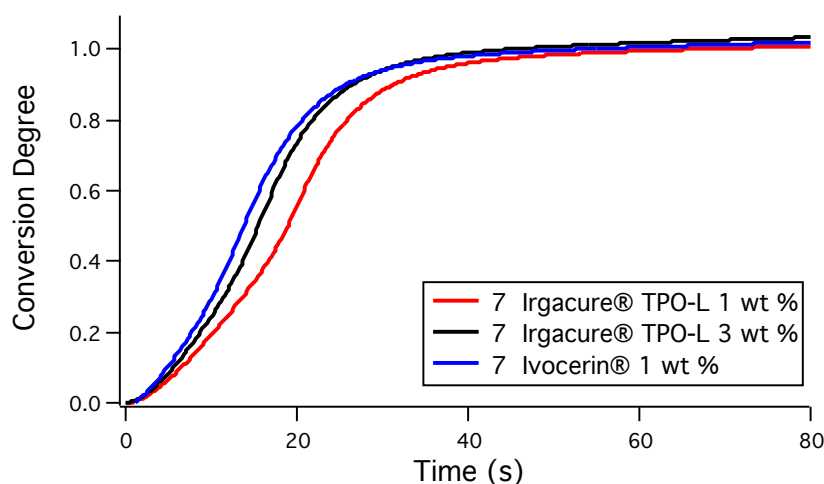


Figure 6: Conversion as function of irradiation time (s) for photoinitiated polymerization of 4-(4-methacryloyloxyphenyl)-butan-2-one (**7**) containing Irgacure® TPO-L (1 wt % and 3 wt %, respectively) or Ivocerin® (1 wt %) at 40 °C for 10 min, adapted from [112].

Table 5: Maximum polymerization rate (R_p^{\max}), time (t_{\max}) to obtain the maximum polymerization rate and final conversion for photoinitiated polymerization of 4-(4-methacryloyloxyphenyl)-butan-2-one (**7**) in the presence of Irgacure® TPO-L (1 wt % and 3 wt %, respectively) or Ivocerin® (1 wt %), and 2-phenoxyethyl methacrylate (**8**) as well as phenyl methacrylate (**9**) containing each TPO-L (1 wt %) for 10 min irradiation time at 40 °C, adapted from [112].

Monomer	Initiator (wt %)	R_p^{\max} (s ⁻¹)	t_{\max} (s)	Final Conversion (%)
7	TPO-L 1 %	0,05	23	100
7	TPO-L 3 %	0,06	16	100
7	Ivocerin 1 %	0,06	15	100
8	TPO-L 1 %	0,02	46	100
9	TPO-L 1 %	0,01	86	81

Conversion data calculated from photo-DSC measurements are slightly lower than the data collected by ¹H-NMR analysis for the samples irradiated at a shorter time (Table 7). However, both methods show an increase in double bond conversion when the samples are subjected to a longer irradiation time. Moreover, final conversion values determined by Photo-DSC and ¹H-NMR are quite similar for the sample irradiated for 10 min.

There is a significant increase in the values of dispersity (\bar{M}_w/\bar{M}_n) and weight average molecular weight (M_w) of the polymers irradiated for 25 s in comparison with those determined for the photopolymer irradiated for 15 s or less as seen in Table 7. The number average molecular

weight, M_n , also relates to the exposure time but the effect of the irradiation period is greater on M_w values compared to M_n (Table 7). In addition to the photopolymers obtained by Photo-DSC measurements, the mixture containing 1 wt % Irgacure[®] TPO-L was also cured on the glass substrate for 6s and 10 min irradiation at room temperature, respectively in order to obtain greater amount of purified polymer for further analysis. Heat generation during the irradiation process of the sample on the glass substrate was detected by thermal camera. The temperature increase due to the light source was determined in the absence of sample on the glass substrate (blank) as well and it was measured 40 °C. Temperature slightly increases (45 °C to 53 °C) during polymerization of the sample compared to an increase in the temperature measured for blank (40 °C) (Figure 7, Table 6). This experiment shows that there is a slight difference between photopolymerization at Photo-DSC and the photopolymerization on the glass substrate.

DSC analysis was also performed to get further information about the photopolymers obtained after different irradiation times (Table 8 and Table 9). The glass transition temperature (T_g), recrystallization temperature ($T_{recryst}$), and melting temperature (T_m) of the photopolymerizing mixtures of **7** irradiated for 6 s and 10 s were determined by DSC, and they show semicrystallinity up to 10 s irradiation. There was still high amount of unreacted monomer **7** and low amount of photopolymer in the reaction medium after 6 s or 10 s irradiation. It may result in a detection of T_g , $T_{recryst}$ and T_m on DSC curve (Figure 8).

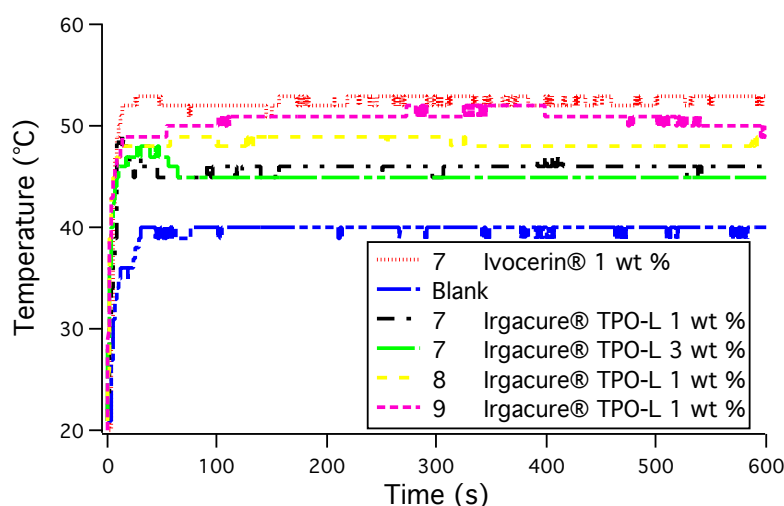


Figure 7: Temperature measured during irradiation of a pure glass substrate (blank) and glass substrates coated with monomer (**7**, **8**, or **9**) containing photoinitiator (Irgacure[®] TPO-L 1 wt % or 3 wt % or Ivocerin[®] 1wt%) with light of 395 nm for 10 min. The films were prepared on a glass substrate using the 120 μm side of a four-way film applicator to maintain comparable thickness for all films. The films on glass substrates were purged with nitrogen in a plastic box equipped with a quartz glass window before irradiation for 5 min. Then, irradiation was carried out in the nitrogen atmosphere using a 395 nm light source for 10 min, and the temperature changes were recorded during irradiation using a thermal camera (testo 0563 0885 V7), adapted from [112].

Table 6: Temperature measured after irradiation of a pure glass substrate (blank) and glass substrates coated with monomer (**7**, **8**, or **9**) containing photoinitiator (1 wt % or 3 wt % Irgacure® TPO-L or 1 wt % Ivocerin®) with light of 395 nm after 10 min of irradiation, adapted from [112].

Monomer	Initiator (wt %)	Generated Temperature (°C) during irradiation
Blank (Glass substrate without monomer-initiator mixture)	-	40
7	TPO-L 1%	46
7	TPO-L 3 %	45
7	Ivocerin 1 %	53
8	TPO-L 1%	49
9	TPO-L 1%	51

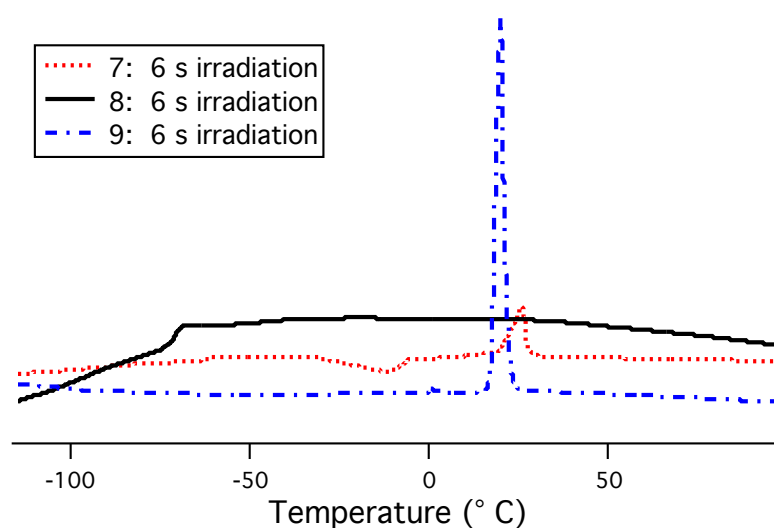


Figure 8: DSC curves of photopolymerizing mixtures containing 1 wt % Irgacure® TPO-L and monomer **7** ($T_g = -62$ °C; $T_{\text{recryst}} = -12$ °C; $T_m = 26$ °C), **8** ($T_g = -71$ °C), or **9** ($T_m = 21$ °C) after 6 s irradiation at 40°C in the photo-DSC, adapted from [112].

The amount of photopolymer made from **7** increases as a result of an extension of the irradiation time from 10 s to 15 s which results in a higher glass transition temperature. Additionally, crystallization is not observed for the photopolymerizing mixture obtained after 15 s irradiation, shown in Figure 9 and Table 9.

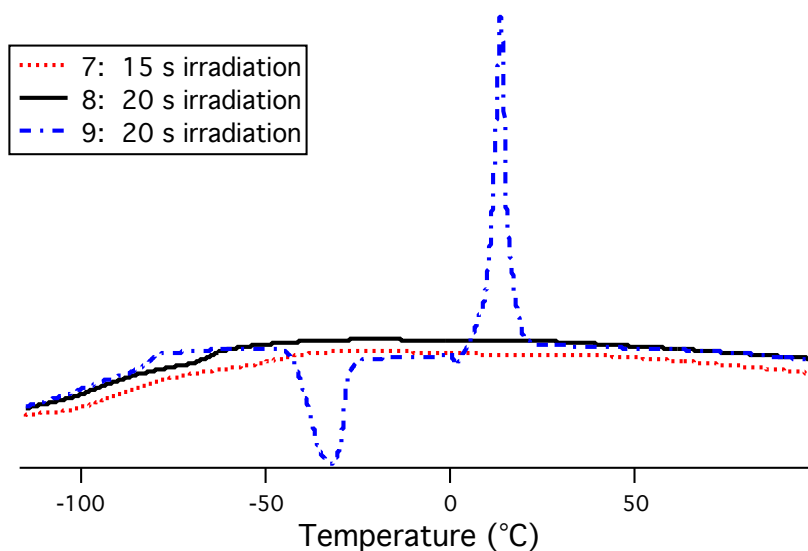


Figure 9: DSC curves of photopolymerizing mixtures containing monomer and 1 wt % Irgacure® TPO-L (monomer **7**: $T_g = -44$ °C; **8**: $T_g = -65$ °C, and **9**: $T_g = -81$ °C; $T_{\text{recryst}} = -33$ °C; $T_m = 13$ °C) after 15 s (**7**) or 20 s (**8** and **9**, respectively) irradiation at 40 °C in the photo-DSC, adapted from [112].

There is a great increase in T_g of more than 80 K determined during irradiation of **7** within the time frame between 15 s and 25 s. T_g of the photopolymer mixture irradiated for 25 s reaches 40 °C (Table 9) which is an indication of vitrification after 25 s irradiation because T_g of the sample rises to the photopolymerization temperature. This irradiation time frame also corresponds to a noticeable increase in both M_w and dispersity (\mathcal{D}) (Table 7). It was previously reported that M_w of the photopolymer increases during free radical polymerization in correlation with the final conversion of the double bond [124-126]. As the conversion degree reaches higher values, the viscosity of the polymerization medium increases and the mobility of the polymer radicals are hindered. The polymerizing system is in the glassy state.

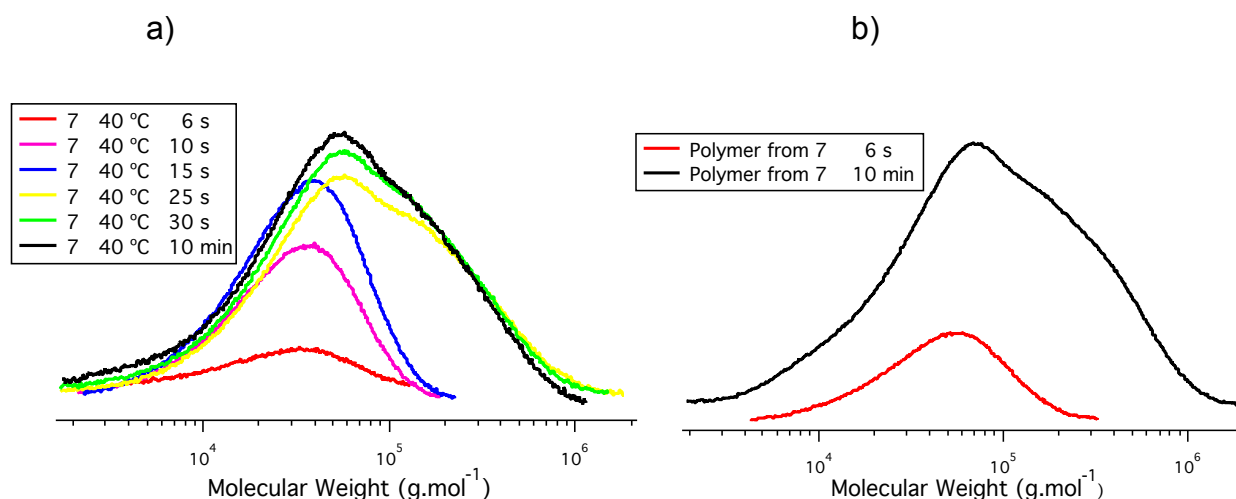


Figure 10: An overlay of GPC chromatograms (RI detector) of photopolymers obtained by photoinitiated polymerization of 4-(4-methacryloyloxyphenyl)-butan-2-one (**7**) containing 1 wt % Irgacure® TPO-L; a) in the photo-DSC pan at 40 °C after irradiation for 6 s, 10 s, 15 s, 25 s, 30 s, and 10 min; b) after irradiation on a glass substrate outside of the photo-DSC at room temperature for 6 s and 10 min, respectively to isolate higher amount on purified polymer, adapted from [112].

Table 7: Monomer conversion obtained from both photo-DSC and $^1\text{H-NMR}$ measurements, number average molecular weight (M_n), weight average molecular weight (M_w), and dispersity (\mathcal{D}) of the polymer obtained during photoinitiated polymerization of **7**, **8**, and **9** using 1 wt % Irgacure® TPO-L at a given temperature (T) after selected irradiation time (t), adapted from [112].

Monomer	T (°C)	t (s)	Conversion Photo-DSC (%)	Conversion $^1\text{H-NMR}$ (%)	M_n (kg/mol)	M_w (kg/mol)	\mathcal{D}
7	40	6	9	18	29	46	1.6
7	40	10	12	32	24	43	1.8
7	40	15	22	44	26	49	1.9
7	40	20	44	58	NA	NA	NA
7	40	25	70	88	48	161	3.3
7	40	30	85	90	46	146	3.1
7	40	600	100	94	34	130	3.9
7	55	600	100	98	38	126	3.3
7	70	600	100	100	40	123	3.0
7	85	6	9	32	36 and 1,110	60.3 and 2,509	1.7 and 2.3
7	85	20	53	96	48 and 2,792	118 and 4,271	2.4 and 1.5

Monomer	T (°C)	t (s)	Conversion Photo-DSC (%)	Conversion ¹ H-NMR (%)	M _n (kg/mol)	M _w (kg/mol)	Đ
7	85	25	73	100	50 and 2,699	123 and 3,991	2.4 and 1.5
7	85	30	76	100	44 and 2,596	118 and 3,962	2.7 and 1.5
7	85	600	100	100	48 and 3,104	122 and 5,000	2.5 and 1.6
8	40	6	3	9	14	23	1.7
8	40	20	22	31	13	24	1.9
8	40	25	30	41	14	27	2.0
8	40	40	54	69	19	67	3.6
8	40	55	88	100	26	180	6.8
8	40	600	100	100	25	182	7.2
9	40	6	1	2	8	12	1.5
9	40	20	10	18	8	13	1.7
9	40	40	22,5	32	8	15	1.8
9	40	50	29	40	8	16	2.0
9	40	90	56	78	16	113	7.1
9	40	600	81	80	14	90	6.4

*NA: Not Analyzed

Table 8: Glass transition temperature (T_g), number average molecular weight (M_n), weight average molecular weight (M_w), and dispersity (Đ) of purified polymers obtained either by photoinitiated polymerization of **7**, **8**, and **9** using 1 wt % Irgacure® TPO-L at a given temperature (T) after selected irradiation time (t) on a glass substrate^{a)} or thermal initiated polymerization in the presence of the photoinitiator at 85 °C in the absence of light^{b)} adapted from [112].

Monomer	T (°C)	t (s)	T _g (°C)	M _n (kg/mol)	M _w (kg/mol)	Đ
7	46 ^{a)}	6	52	35	60	1.7
7	46 ^{a)}	600	65	45	418	3.6
7	85 ^{b)} without light	3 h	NA	523	2000	3.8

Monomer	T (°C)	t (s)	T _g (°C)	M _n (kg/mol)	M _w (kg/mol)	Đ
8	49 ^{a)}	600	52	30	291	9.6
9	51 ^{a)}	600	135	19	103	5.3

*NA: Not Analyzed

*The glass transition temperature of the photopolymers made of **7**, **8**, and **9** was investigated in a temperature interval: -120 C to 100 C using heating and cooling rates of 10 K/min.

Table 9: Polymerization temperature (T), irradiation time (t), glass transition temperature (T_g), recrystallization temperature during heating (T_{recryst}), melting temperature (T_m), enthalpy of recrystallization ($\Delta H_{recryst}$), enthalpy of melting (ΔH_m) obtained during photoinitiated polymerization of **7**, **8**, and **9** using 1 wt % Irgacure® TPO-L at a given temperature (T) after selected irradiation time (t), adapted from [112].

Monomer	T (°C)	t (s)	T _g (°C)	T _{recryst} (°C)	T _m (°C)	$\Delta H_{recryst}$ (J/g)	ΔH_m (J/g)
7	40	6	-62	-12	26	34	39
7	40	10	-56	-5	25	13	18
7	40	15	-44	-	-	-	-
7	40	25	40	-	-	-	-
7	40	30	42	-	-	-	-
7	40	600	45	-	-	-	-
7	85	6	-57	2	24	7	10
7	85	20	50	-	-	-	-
7	85	600	55	-	-	-	-
8	40	6	-71	-	-	-	-
8	40	20	-65	-	-	-	-
8	40	40	-30	-	-	-	-
8	40	600	42	-	-	-	-
9	40	6	-	Crystallization during cooling	21	-	87
9	40	20	-81	-33	13	46	68

Monomer	T (°C)	t (s)	T _g (°C)	T _{recryst} (°C)	T _m (°C)	ΔH _{recryst} (J/g)	ΔH _m (J/g)
9	40	40	-	Crystallization during cooling	12	-	1
9	40	90	45	-	-	-	-
9	40	600	52	-	-	-	-

Table 10: Polymerization temperature (T), maximum of the polymerization rate (R_p^{\max}), time (t_{\max}) to obtain the maximum of the polymerization rate, and final monomer conversion (%) for photoinitiated polymerization of 4-(4-methacryloyloxyphenyl)-butan-2-one (**7**), 2-phenoxyethyl methacrylate (**8**), and phenyl methacrylate (**9**) containing 1 wt % Irgacure[®] TPO-L each after 10 min irradiation at various temperatures, adapted from [112].

Monomer	T (°C)	R_p^{\max} (s ⁻¹)	t_{\max} (s)	Final conversion photo-DSC (%)	Final conversion ¹ H-NMR (%)
7	40	0,05	23	100	94
7	55	0,05	23	100	98
7	70	0,06	22	100	100
7	85	0,06	21	100	100
8	40	0,03	46	100	100
9	40	0,01	86	81	80

5.2.2 Photoinitiated Polymerization of 4-(4-Methacryloyloxyphenyl)-butan-2-one (**7**) at Elevated Temperature

Photopolymerization temperature was gradually increased from 40 °C to 55 °C, 70 °C and 85 °C in order to avoid the vitrification effect of the polymerizing formulation containing **7**. Vitrification does not take place when the photopolymerization of monomer **7** is carried out at a temperature of 70 °C or 85 °C above T_g of the photopolymer ($T_g = 65$ °C, Table 8). Although R_p^{\max} does not significantly change as a result of stepwise temperature increase for the irradiation process, polymerization of **7** occurs slightly faster at 85 °C (Table 10). Double bond conversion of **7** reaches over 90 % when the polymerization is performed at 40 °C for 10 min light exposure. Additionally, quantitative conversion is observed when the polymerization temperature is increased to 70 °C or 85 °C (Table 10). A T_g of 65 °C for the purified polymer **7** (Table 8) shows that when the mixture of **7** is polymerized at 70 °C

which is slightly over the glass transition temperature, the vitrification effect is eliminated. This may be a reason of the full conversion of **7** observed at 70 °C or 85 °C while the double bond conversion is 94% or 98% at 40 °C or 55 °C. Photoinitiated polymerization was also studied as a function of time at 85 °C. This experiment made it possible to examine the thermal decomposition of the photoinitiator. Conversion scales up with the irradiation time which corresponds to the result observed at photopolymerization temperature of 40 °C. Therefore, it can indicate that photopolymerization temperature may not effect the photoinitiator decomposition by light exposure leading to production of initiating radicals. However, polymerization temperature causes a significant effect on the molecular weight of the photopolymer (Table 7). A second fraction with the higher molecular weight was observed for the photopolymer obtained at reaction temperature of 85 °C (Figure 11). This higher molecular weight fraction was observed even for the photopolymer obtained after 6 s irradiation at 85 °C. The second fraction representing the polymer with higher molecular weight does not appear on the GPC chromatogram of the photopolymers irradiated at 40 °C. It may be resulted by additional thermal process occurred during irradiation at 85 °C. Another experiment was performed to clarify the additional thermal process during photopolymerization of **7** at 85 °C and the same sample of **7** containing 1 wt % Irgacure[®] TPO-L was polymerized at 85 °C for 3 h in the absence of light. GPC result of that polymer isolated after thermal polymerization at 85 °C shows a higher molecular weight polymer with a broad molecular weight distribution. The lower molecular weight polymer fraction, which is characteristic for photopolymers, was not seen in the GPC chromatogram of the polymer obtained by thermally induced polymerization. The two molecular weight fractions may indicate that extra thermal process takes place during the photopolymerization of monomer **7** at 85 °C. The intensity of the lower molecular weight fraction increases by irradiation time although the intensity of the higher molecular weight fraction keeps nearly constant. Regardless of the short or longer irradiation time (6s or 10 min), the second fraction, which appears as a shoulder of the low molecular weight polymer with approximately constant intensity, was observed in all GPC results of the photopolymer obtained at 85 °C. Even if the photopolymer structure is dominant in the GPC chromatogram, the other higher molecular weight fraction can not be neglected and shows the extra thermal process during the irradiation process at 85 °C. The additional DSC experiment of the same mixture of the monomer **7** containing 1 wt % Irgacure[®] TPO-L indicates that exothermal process starts at around 80 °C. It supports the results previously mentioned.

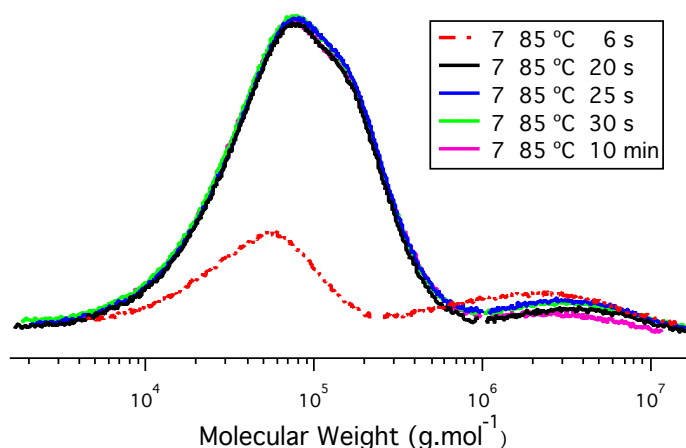


Figure 11: An overlay of GPC chromatograms (RI detector) of photopolymers obtained by photoinitiated polymerization of 4-(4-methacryloyloxyphenyl)-butan-2-one (**7**) containing 1 wt % Irgacure® TPO-L after an irradiation time at 85 °C for 6 s, 20 s, 25 s, 30 s, and 10 min, adapted from [112].

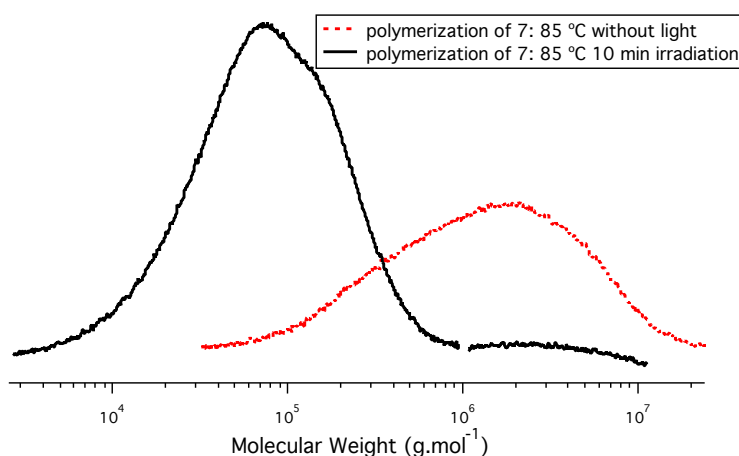


Figure 12: An overlay of GPC chromatograms (RI detector) of polymers obtained by photoinitiated polymerization of 4-(4-methacryloyloxyphenyl)-butan-2-one (**7**) containing 1 wt % Irgacure® TPO-L after irradiation at 85 °C for 10 min (black line) compared with a polymer received by thermal polymerization in the presence of the photoinitiator at 85 °C in the absence of light for 3 hours (red line), adapted from [112].

Since it can be interesting to compare the monomer **7** comprising an aromatic group to the commercial monomers bearing an aromatic group as well, 2-phenoxyethyl methacrylate (**8**) and phenyl methacrylate (**9**) were selected for further kinetic investigations.

5.2.3 Comparison of 4-(4-Methacryloyloxyphenyl)-butan-2-one (**7**) with Further Methacrylates Comprising a Phenyl Moiety

4-(4-Methacryloyloxyphenyl)-butan-2-one (**7**), 2-phenoxyethyl methacrylate (**8**) and phenyl methacrylate (**9**) have a phenyl group in their chemical structure. The methacrylate group is directly attached to phenyl group in case of monomer **7** and **9**. Therefore, phenyl methacrylate (**9**) can be an alternative model monomer for comparison of monomer **7**. Furthermore, the influence of 3-oxobutyl moiety presented in monomer **7** on the polymerization kinetic can be examined by comparison with **9**. On the other hand, the methacrylate group is not directly bonded to aromatic group since the ethoxy substituent is presented between methacrylate group and phenyl ring in the structure of monomer **8**. It may provide an additional information about how the position of the phenyl ring effects the double bond reactivity. In addition to this, the difference in physical properties of the monomers **7-9** is a direct result of the various substitution in the structure. The monomers **7** ($T_{\text{crys}} = -7\text{ }^{\circ}\text{C}$ during cooling, $T_{\text{m}}=29\text{ }^{\circ}\text{C}$) and **9** ($T_{\text{crys}} = -45\text{ }^{\circ}\text{C}$ during cooling, $T_{\text{m}}=21\text{ }^{\circ}\text{C}$) show crystallization whereas monomer **8** ($T_{\text{g}} = -73\text{ }^{\circ}\text{C}$) shows glass forming behaviour. It indicates that directly bonded methacrylate group to the phenyl ring results in a crystal formation and the presence of ethoxy group as a separator between methacrylate and phenyl ring causes amorphous behaviour of the monomer **8**.

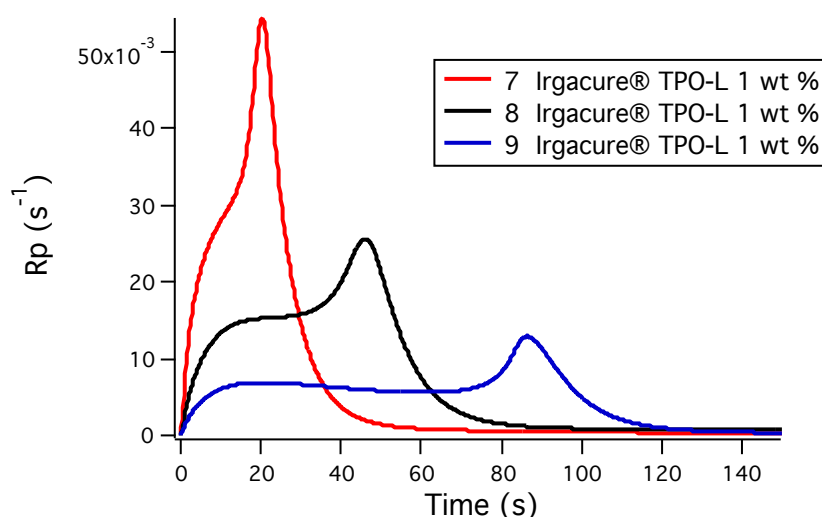


Figure 13: Polymerization rate (R_p (s^{-1})) as function of irradiation time (s) for photoinitiated polymerization of 4-(4-methacryloyloxyphenyl)-butan-2-one (**7**), 2-phenoxyethyl methacrylate (**8**) and phenyl methacrylate (**9**) containing 1 wt % Irgacure[®] TPO-L at 40 °C for 10 min, adapted from [112].

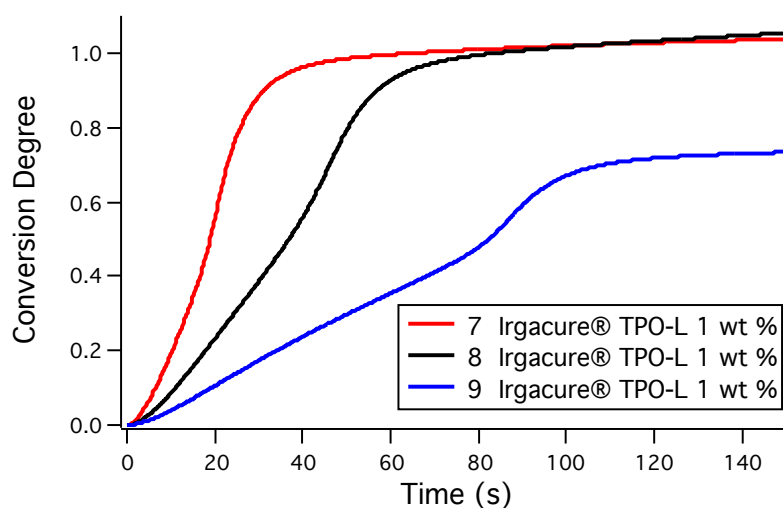


Figure 14: Conversion as function of irradiation time (s) for photoinitiated polymerization of 4-(4-methacryloyloxyphenyl)-butan-2-one (**7**), 2-phenoxyethyl methacrylate (**8**) and phenyl methacrylate (**9**) containing 1 wt % Irgacure[®] TPO-L at 40 °C for 10 min, adapted from [112].

Photopolymerization kinetic of the monomer **7-9** is also dependent on the substitution pattern. R_p value increases during the first 10 s irradiation for all monomers. However, polymerization rate of **8** and **9** stays constant after about 15 s irradiation, which indicates the ideal polymerization kinetic. After the period when polymerization rate remains constant, R_p shows a further increase until it reaches the R_p^{\max} (Figure 13). This period is longer in case of monomer **9** which may be caused by lower reactivity of **9** in comparison with monomer **8**. According to the plot of the polymerization rate as function of the irradiation time, reactivity of the monomers increases in the order $\mathbf{9} < \mathbf{8} < \mathbf{7}$ and t_{\max} values decreases in the order $\mathbf{9} > \mathbf{8} > \mathbf{7}$. The substitution of aromatic group by 3-oxobutyl at *p*-position in regard to methacrylate group may result an increase in the reactivity of the monomer **7**.

As it can be clearly seen in Figure 14, conversion is quantitative for monomer **7** and **8** after less than 150 s irradiation although it is 81 % for monomer **9** after 10 min irradiation. Final conversion was also confirmed by ¹H-NMR and the results obtained after 10 min irradiation correspond each other. To get further information about photoinitiated polymerization of **7-9**, time dependent measurements were performed for commercial **8** and **9** at 40 °C as well. GPC analysis were carried out to determine the molecular weight and molecular weight distribution of the photopolymers obtained after various irradiation time, which are shown in Table 8. Furthermore, the glass transition temperature values of the photopolymerizing mixture and purified polymer were also detected. The T_g is higher for purified photopolymers obtained from **7** and **9** than that of **8**. The aromatic group is

directly bonded to the polymethacrylate segment made of **7** and **9** which makes the structure more rigid. On the other hand, the ethylene group creates a distance between the phenyl ring and the segment of the polymethacrylate chain in case of photopolymer derived from **8** which makes it more flexible and mobile. In addition to this, the bulky 3-oxobutyl substituent at the phenyl group in the structure of **7** leads to the lower T_g for the photopolymer obtained from **7** in comparison with the photopolymer manufactured from **9**. As demonstrated in Table 7, the number average molecular weight (M_n) of **8** is relatively same before an irradiation time of 40 s. It slightly rises until irradiation process is completed. Contrarily to the slight variation on the M_n with radiation, M_w of **8** continuously increases with the irradiation time of 40 s or longer. The stronger effect of the irradiation period on the M_w compared to the M_n leads to a greater dispersity and higher glass transition temperature of the polymer derived from **8** during the photopolymerization process (Table 8). The glass transition temperature of the photopolymer **8** irradiated for 40 s is $-30\text{ }^\circ\text{C}$ which is quite low than the polymerization temperature of $40\text{ }^\circ\text{C}$ (Table 9). This might be a reason that polymerization rate of **8** stays constant for a longer polymerization time compared to **7**. After 10 min irradiation, T_g reaches $42\text{ }^\circ\text{C}$ which is near the polymerization temperature of $40\text{ }^\circ\text{C}$. GPC result of the isolated and purified polymer of **8** from the glass substrate shows higher M_n and M_w as well as broader dispersity (Table 8 and Table 9). It also has higher T_g value which is $52\text{ }^\circ\text{C}$. Full monomer conversion was achieved for **8** even if the reactivity of **8** is lower than monomer **7**.

The monomer **9** can be a typical model for comparison with **7** since phenyl group is directly bonded to the methacrylate group in both monomer structures. The only difference between **7** and **9** is that phenyl group has the 3-oxobutyl substituent at para position in case of monomer **7**. Both monomers exhibit crystallisation and the crystals of **7** and **9** melts below the polymerization temperature. Though, the melting point of photopolymerizing mixture of **9** decreases during the first 40 s irradiation of the photopolymerization process, it shows semicrystallinity with the T_g of $-81\text{ }^\circ\text{C}$ after 20 s irradiation (Table 9). However, the glass transition temperature of the photopolymerizing mixture rises to $45\text{ }^\circ\text{C}$ with the longer irradiation time of 90 s. It is slightly higher than the polymerization temperature. This time frame corresponds the area where the polymerization rate increases and approaches its maximum as well as a significant increase in the conversion is observed. The reason of the great increase in both R_p and conversion after about 100 s irradiation may be explained by glass transition temperature of the polymerizing mixture of **9** near the polymerization temperature after about 100 s irradiation. In addition to this, the similar values of T_g of **9** and polymerization temperature

after about 100 s irradiation may also be a reason of the limited conversion around 80 % for monomer **9**. The purified photopolymer obtained from **9** has significantly higher glass transition temperature compared to that of photopolymerizing mixture of **9** irradiated for 10 min (Table 8). The limited final conversion of **9** indicates that there is still unreacted monomer in the polymerizing mixture which can act as a diluent and cause the significant reduction in the T_g of the photopolymerizing mixture. There is also a considerable difference on the weight average molecular weight and dispersity of the photopolymer derived from **9** after 90 s irradiation process (Table 7). Characterization of the degree of polymerization (X_n) of the purified photopolymers obtained from **7** ($X_n = 194$), **8** ($X_n = 146$), and **9** ($X_n = 117$), displays that the largest macromolecules were acquired by photoinitiated polymerization of **7**. The difference in the chemical structure of **7** and **9**, hydrogen at the *p*-position of the phenyl ester in case of **9** and the 3-oxobutyl moiety at the aromatic group in case of **7**. It can be concluded that 3-oxobutyl substituent presented in the structure of monomer **7** might be in charge of the higher reactivity and faster photopolymerization.

5.3 Design of New Polymeric Networks Based on Green Methacrylates

Some results discussed in this subchapter were submitted to publish [113].

Linear polymers are soluble in the solvents which provides the opportunity for further analysis by GPC or NMR. On the other hand, crosslinked polymers form a network by a kind of interconnection of the polymer chains. It provides the strength and stability to the material. Crosslinked polymers are also not soluble in any solvents. It is possible to generate a surface showing a good solvent resistance. In addition to the linear polymers, crosslinked materials were also produced and analyzed in this thesis.

New biobased dimethacrylate consisting of the three isomers, ethane-1,2-diyl bis(9-methacryloyloxy-10-hydroxy octadecanoate), ethane-1,2-diyl 9-hydroxy-10-methacryloyloxy-9'-methacryloyloxy-10'-hydroxy octadecanoate, and ethane-1,2-diyl bis(9-hydroxy-10-methacryloyloxy octadecanoate) (**10**), was synthesized in three steps as described under the headline of 4.5.4. Even though the yield of the raw product **10** was 92 % in the third step, it significantly decreased to 24 % after purification by column chromatography. Three possible isomer structures of the monomer **10** may form after ring opening reaction of epoxy group with methacrylic acid. However, possible isomer structures of monomer **10** can not be separated by NMR spectroscopy due to the similarity in the surrounding. DSC analysis of the monomer **10** shows that it has a low glass transition temperature at $-50\text{ }^\circ\text{C}$.

Photokinetic investigation of biobased dimethacrylate **10** was studied in the presence of the photoinitiators, 1 % (w/w) of Irgacure® TPO-L, 3 % (w/w) of Irgacure® TPO-L, and 1 % (w/w) of Ivocerin®. Furthermore, it has been aimed to make a variation on the final material properties by introduction of the comonomer to the polymer network structure. For this purpose, copolymerization of biobased dimethacrylate **10** with 4-(4-methacryloyloxyphenyl)-butan-2-one (**7**), which has been recently reported as a green and highly reactive monomer [112,127], has been carried out in different stoichiometric ratios in order to vary thermal and mechanical properties. In addition to this, monomer **10** has also been copolymerized with biobased monomer **4** derived from oleic acid. Thermal and mechanical analysis of the crosslinked films have been investigated. Discussion is supported by analysis of the reactivity of the sustainable starting materials towards the photoinitiated free radical polymerization and by investigation of the relation between final material properties and the starting material structure as well. Surface wettability of the cured films was tested using solvents with different polarity. Crosslink density and molecular weight between two crosslink points (M_c) were also determined according to the rubber elasticity theory.

5.3.1 Photoinitiated Homopolymerization of the Biobased Dimethacrylate (**10**)

Photoinitiated polymerization of newly developed monomer **10** was investigated in the presence of photoinitiators, 1 % (w/w) Irgacure® TPO-L, 3 % (w/w) Irgacure® TPO-L and 1 % (w/w) Ivocerin®. It can be clearly seen in Figure 15 and Figure 16, the polymerizing mixture of monomer **10** containing Ivocerin® exhibits higher reactivity compared to the sample comprising same amount of Irgacure® TPO-L. R_p^{\max} value shows a rise as a result of an increase in the photoinitiator concentration from 1 wt % to 3 wt % in case of TPO-L. On the other hand, the presence of 3 wt % Irgacure® TPO-L or 1 wt % Ivocerin® in the photopolymerizing formulation results in a similar final double bond conversion of 66 % after 10 min irradiation (Figure 16, Table 11). Additionally, polymerization occurs faster in case of higher photoinitiator concentration. It can be said according to Figures 15-16 that, even if there is no significant difference between efficiency of the systems, the formulation containing higher amount of Irgacure® TPO-L or Ivocerin® has a slightly higher reactivity and final conversion in comparison with the system comprising lower Irgacure® TPO-L concentration.

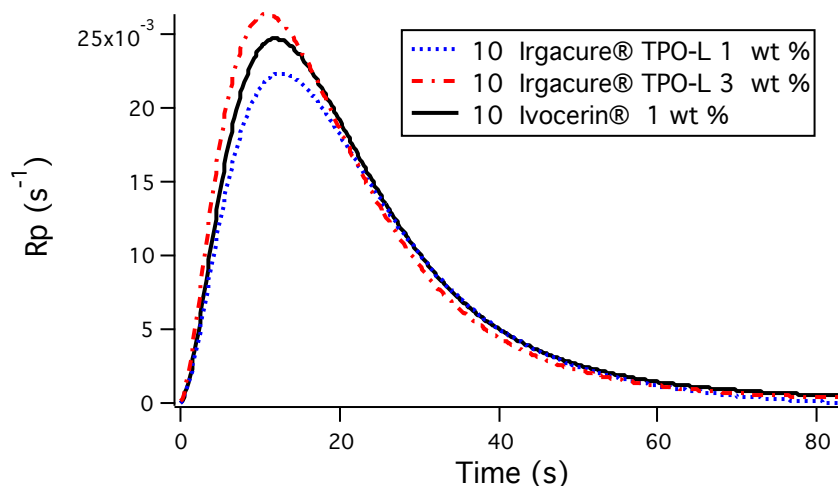


Figure 15: Polymerization rate (R_p (s^{-1})) as function of irradiation time (s) for photoinitiated polymerization of ethane-1,2-diyl bis(9-methacryloyloxy-10-hydroxy octadecanoate) / ethane-1,2-diyl 9-hydroxy-10-methacryloyloxy-9'-methacryloyloxy-10'-hydroxy octadecanoate / ethane-1,2-diyl bis(9-hydroxy-10-methacryloyloxy octadecanoate) (**10**) containing Irgacure® TPO-L (1 wt % and 3 wt %, respectively) or Ivocerin® (1 wt %) at 40 °C for 10 min, adapted from [113].

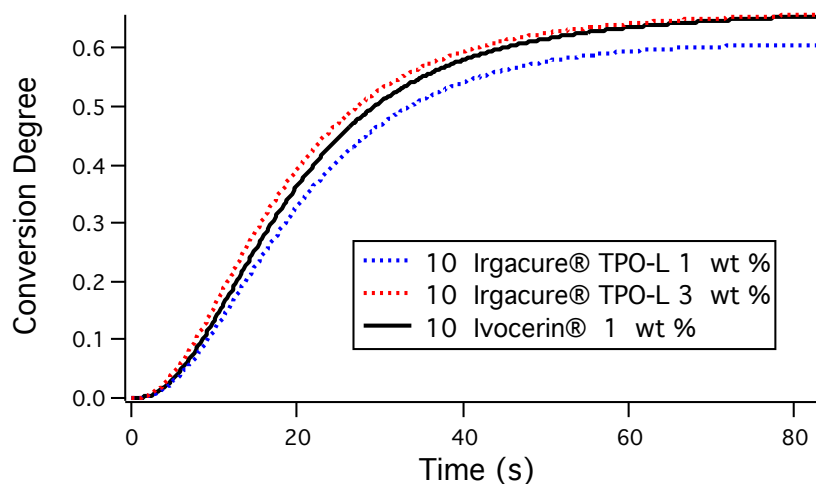


Figure 16: Conversion as function of irradiation time (s) for photoinitiated polymerization of ethane-1,2-diyl bis(9-methacryloyloxy-10-hydroxy octadecanoate) / ethane-1,2-diyl 9-hydroxy-10-methacryloyloxy-9'-methacryloyloxy-10'-hydroxy octadecanoate / ethane-1,2-diyl bis(9-hydroxy-10-methacryloyloxy octadecanoate) (**10**) containing Irgacure® TPO-L (1 wt % and 3 wt %, respectively) or Ivocerin® (1 wt %) at 40 °C for 10 min, adapted from [113].

Table 11: Maximum of the polymerization rate (R_p^{\max}), time (t_{\max}) to obtain the maximum of the polymerization rate, and final conversion for photoinitiated polymerization of the ethane-1,2-diyl bis(9-methacryloyloxy-10-hydroxy octadecanoate) / ethane-1,2-diyl 9-hydroxy-10-methacryloyloxy-9'-methacryloyloxy-10'-hydroxy octadecanoate / ethane-1,2-diyl bis(9-hydroxy-10-methacryloyloxy octadecanoate) (**10**), 4-(4-methacryloyloxyphenyl)-butan-2-one (**7**), methyl 9-(1H-imidazol-1yl)-10-(methacryloyloxy)octadecanoate / methyl 9-(methacryloyloxy)-10-(1H-imidazol-1yl)octadecanoate (**4**), as well as the mixtures of **10** and **7** (molar ratio= 1:1 and 1:9, respectively) as well as **10** and **4** (molar ratio= 1:9) using either Irgacure® TPO-L (1 wt % and 3 wt %, respectively) or Ivocerin® (1 wt%) as photoinitiator and 10 min irradiation time at 40°C, adapted from [113].

Monomer	Initiator (wt %)	R_p^{\max} (s ⁻¹)	t_{\max} (s)	Final Conversion (%)
10	TPO-L 1 %	0,022	13	61
10	TPO-L 3 %	0,026	11	66
10	Ivocerin 1 %	0,025	12	66
7	TPO-L 1 %	0,05	23	100
7	TPO-L 3 %	0,06	16	100
7	Ivocerin 1 %	0,06	15	100
10:7 (1:1, mol:mol)	TPO-L 1 %	0,038	11	82
10:7 (1:1, mol:mol)	TPO-L 3 %	0,039	11	83
10:7 (1:1, mol:mol)	Ivocerin 1 %	0,042	10	84
10:7 (1:9, mol:mol)	TPO-L 1 %	0,046	15	85
10:7 (1:9, mol:mol)	TPO-L 3 %	0,048	12	90
10:7 (1:9, mol:mol)	Ivocerin 1 %	0,051	12	90
4	TPO-L 1 %	0,020	15	98
4	TPO-L 3 %	0,035	12	100
4	Ivocerin 1 %	0,020	10	100
10:4 (1:9, mol:mol)	TPO-L 1 %	0,023	12	70
10:4 (1:9, mol:mol)	TPO-L 3 %	0,030	10	78
10:4 (1:9, mol:mol)	Ivocerin 1 %	0,029	9	77

Homopolymerization of monomer **10** has a limited final double bond conversion of 66 % in the presence of 3 wt % Irgacure® TPO-L or 1 wt % Ivocerin® (Table 11). Contrarily, methacrylates **7** and **4** show quantitative conversion, respectively (Table 11). As homopolymer **10** has a glass transition temperature well below photopolymerization

temperature (Table 12), vitrification is not the reason of limited conversion. However, restriction on the mobility of growing polymer chain observed in the crosslinking reactions due to the network formation may limit the final double bond conversion in case of dimethacrylate **10** [110,128]. In addition to the homopolymerization of **10**, monomer **10** was copolymerized with the comonomer containing a rigid aromatic structure in order to increase the glass transition temperature. An increase in the glass transition temperature can make the material more preferred and suitable for possible coating application.

5.3.2 Photoinitiated Copolymerization of the Biobased Dimethacrylate (**10**) with Methacrylate **7** and **4**, Respectively

It was decided to perform copolymerization of monomer **10** with a comonomer which has a potential to provide more rigidity to the resulting polymer network and to increase the low glass transition temperature of poly-**10** for possible coating applications. In accordance with this purpose, monomer **7**, comprising a phenyl ring, and biobased monomer **4**, bearing an imidazolium ring, were selected as a comonomer in the photoinitiated copolymerization experiments.

Polymerization kinetic of monomer **7** was previously investigated and reported that it is a highly reactive monomer [112] and it can be classified as a green material [127]. As already depicted in Table 8, purified poly-**7** has a glass transition temperature of 65 °C. Firstly, the copolymerizing mixtures were prepared from a 1:1 mol:mol ratio of monomer **10** and **7** in the presence of 1 % or 3 % (w/w) Irgacure® TPO-L and 1 % (w/w) Ivocerin®, respectively for photoinitiated copolymerization experiments and investigated by Photo-DSC. Higher concentration of Irgacure® TPO-L or usage of Ivocerin® instead of Irgacure® TPO-L does not cause a significant difference on the performance of the systems. All systems show quite similar reactivity and final double conversion (82%, 83%, 84%) as shown in Figure 17 and 18. Kinetic data summarized in Table 11 show that addition of highly reactive comonomer **7** in the photopolymerizing mixture results a rise in both R_p^{\max} and final conversion after 10 min exposure at 40 °C. The copolymerizing system is much more reactive compared to the homopolymerizing formulation of monomer **10**. The R_p^{\max} and final conversion reached the higher values for copolymerization of the mixture containing stoichiometric ratio from both monomers in comparison with homopolymerization of monomer **10**. Even if the copolymerizing system of **10:7** (1:1 mol:mol) did not reach the values obtained for homopolymerization of **7**, system efficiency increased approximately 25 % as a result of incorporation of comonomer **7**.

However, glass transition temperature of the final material produced from the mixture containing equal amount on monomer **10** and **7** is still low according to the DSC measurement or analysis of storage or loss modulus versus temperature curves (Table 12). Polymer chains are still pretty flexible and move around easily causing a low glass transition temperature.

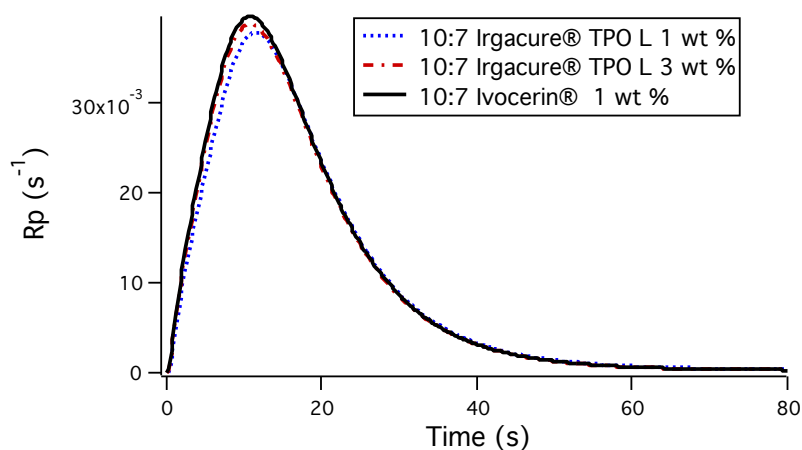


Figure 17: Polymerization rate (R_p (s^{-1})) as function of irradiation time (s) for photoinitiated copolymerization of ethane-1,2-diyl bis(9-methacryloyloxy-10-hydroxy octadecanoate) / ethane-1,2-diyl 9-hydroxy-10-methacryloyloxy-9'-methacryloyloxy-10'-hydroxy octadecanoate / ethane-1,2-diyl bis(9-hydroxy-10-methacryloyloxy octadecanoate) (**10**) and 4-(4-methacryloyloxyphenyl)-butan-2-one (**7**) (1:1, mol:mol) containing Irgacure® TPO-L (1 wt % and 3 wt %, respectively) or Ivocerin® (1 wt %) at 40 °C for 10 min, adapted from [113].

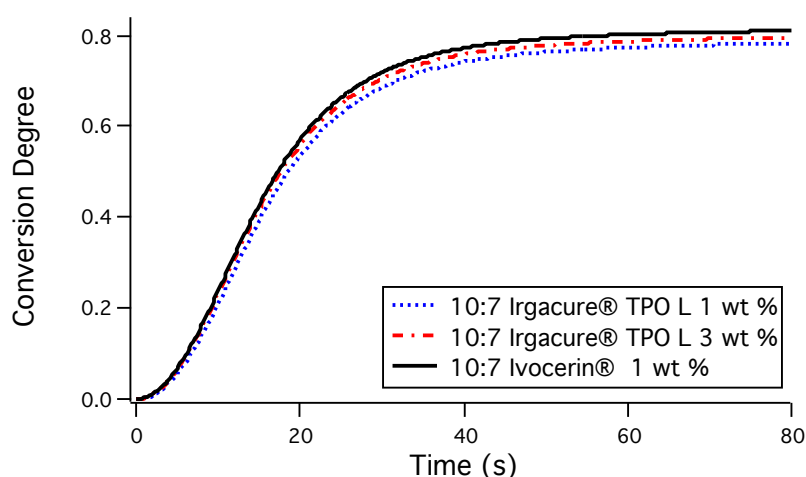


Figure 18: Conversion as function of irradiation time (s) for photoinitiated copolymerization of the ethane-1,2-diyl bis(9-methacryloyloxy-10-hydroxy octadecanoate) / ethane-1,2-diyl 9-hydroxy-10-methacryloyloxy-9'-methacryloyloxy-10'-hydroxy octadecanoate / ethane-1,2-diyl bis(9-hydroxy-10-methacryloyloxy octadecanoate) (**10**) and 4-(4-methacryloyloxyphenyl)-butan-2-one (**7**) (1:1, mol:mol) containing Irgacure® TPO-L (1 wt % and 3 wt %, respectively) or Ivocerin® (1 wt %) at 40 °C for 10 min, adapted from [113].

To dominate the influence of 4-(4-methacryloyloxyphenyl)-butan-2-one (**7**) distribution on the polymer network, the concentration of comonomer **7** was increased from 1 mol to 9 mol. The glass transition values were determined above room temperature for the copolymers, which were derived from the mixture containing an excess amount of monomer **7**. The results determined by DSC and DMA demonstrate that excess amount of monomer **7** relative to monomer **10** causes an expected rise on the T_g value of the copolymers (**10:7**, 1:9 mol:mol) (Table 12). Moreover, maximum polymerization rate increased and final conversion reached around 85-90 % when the higher amount on monomer **7** was applied for copolymer synthesis. While the sample containing 1 wt % of Irgacure® TPO-L exhibits slightly lower reactivity, the photopolymerizing formulation containing 3 wt% of Irgacure® TPO-L or 1 wt% of Ivocerin® shows similar reactivity and same final double bond conversion of 90%. Three times higher photoinitiator concentration leads to a small change on the efficiency of the system as shown in Figure 19, Figure 20 and Table 11. Polymerization occurs slightly faster in the presence of 3 wt % Irgacure® TPO-L or 1 wt% Ivocerin® which was also reported for the photokinetic analysis of homopolymerization **7**.

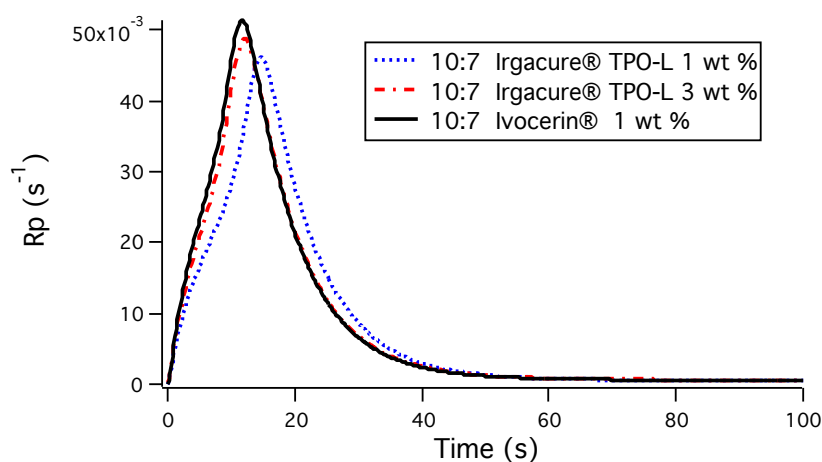


Figure 19: Polymerization rate (R_p (s^{-1})) as function of irradiation time (s) for photoinitiated copolymerization of ethane-1,2-diyl bis(9-methacryloyloxy-10-hydroxy octadecanoate) / ethane-1,2-diyl 9-hydroxy-10-methacryloyloxy-9'-methacryloyloxy-10'-hydroxy octadecanoate / ethane-1,2-diyl bis(9-hydroxy-10-methacryloyloxy octadecanoate) (**10**) and 4-(4-methacryloyloxyphenyl)-butan-2-one (**7**) (1:9, mol:mol) containing Irgacure® TPO-L (1 wt % and 3 wt %, respectively) or Ivocerin® (1 wt %) at 40 °C for 10 min, adapted from [113].

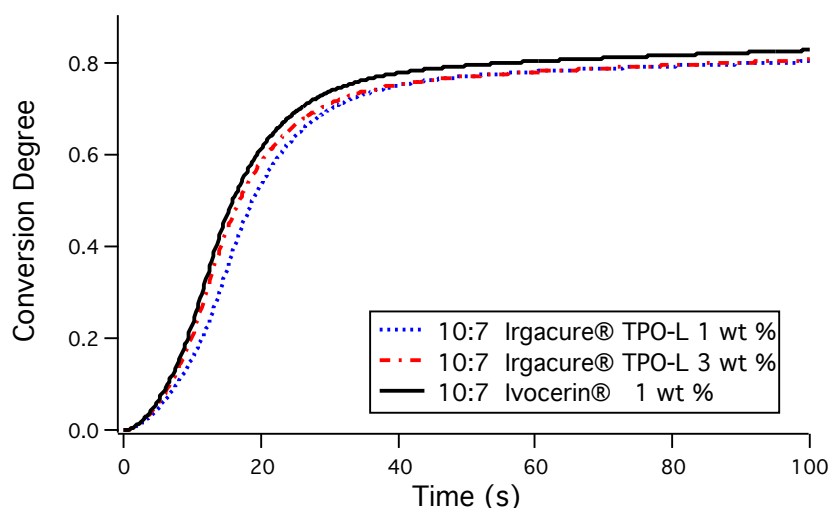


Figure 20: Conversion as function of irradiation time (s) for photoinitiated copolymerization of ethane-1,2-diyl bis(9-methacryloyloxy-10-hydroxy octadecanoate) / ethane-1,2-diyl 9-hydroxy-10-methacryloyloxy-9'-methacryloyloxy-10'-hydroxy octadecanoate / ethane-1,2-diyl bis(9-hydroxy-10-methacryloyloxy octadecanoate) (**10**) and 4-(4-methacryloyloxyphenyl)-butan-2-one (**7**) (1:9, mol:mol) containing Irgacure® TPO-L (1 wt % and 3 wt %, respectively) or Ivocerin® (1 wt %) at 40 °C for 10 min, adapted from [113].

The new biobased dimethacrylate (**10**) was also copolymerized with another biobased monomer of methyl 9-(1H-imidazol-1-yl)-10-(methacryloyloxy)octadecanoate / methyl 9-(methacryloyloxy)-10-(1H-imidazol-1-yl)octadecanoate (**4**) in order to expand the study about the effect of monomer structure on final material properties and design of network system because polymer properties are directly dependent upon the chemical structure of the starting materials. Although monomer **4** is not as reactive as monomer **7**, it shows quantitative conversion after 10 min irradiation as disclosed in Table 11. Biobased monomer **4** has a long alkyl chain carrying an imidazole ring in the monomer structure as already shown in Table 3. Despite the imidazole ring may provide structural rigidity, the structure is still dominated by long alkyl chain which can be described as a flexible spacer. Copolymerization kinetic of the **10:4** mixture (molar ratio **10:4** = 1:9) shows that the presence of excess amount of comonomer **4** in the photopolymerizing sample does not make a significant change on both R_p^{\max} and t_{\max} compared to the values obtained from homopolymerization of monomer **10** (Figure 21 and Figure 22, Table 11) because R_p^{\max} and t_{\max} data are quite similar for monomer **10** and **7**. Therefore, it is also expected to observe similarities in the data for copolymer system of **10:4**.

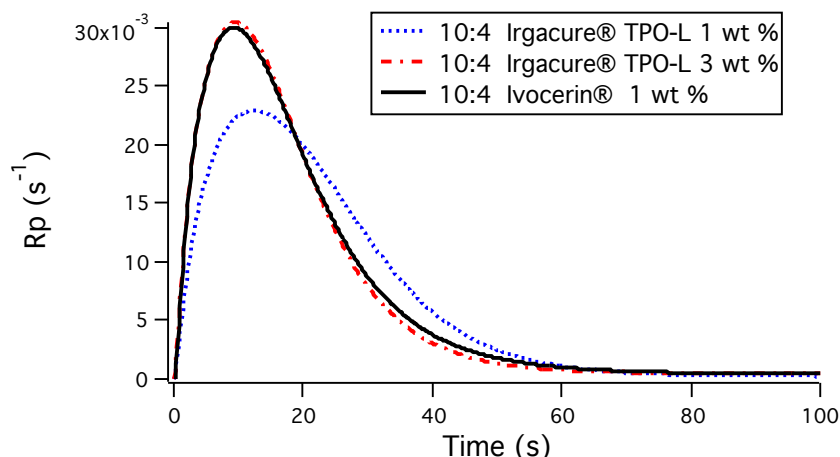


Figure 21: Polymerization rate (R_p (s^{-1})) as function of irradiation time (s) for photoinitiated copolymerization of ethane-1,2-diyl bis(9-methacryloyloxy-10-hydroxy octadecanoate) / ethane-1,2-diyl 9-hydroxy-10-methacryloyloxy-9'-methacryloyloxy-10'-hydroxy octadecanoate / ethane-1,2-diyl bis(9-hydroxy-10-methacryloyloxy octadecanoate) (**10**) and methyl 9-(1H-imidazol-1-yl)-10-(methacryloyloxy)octadecanoate / methyl 9-(methacryloyloxy)-10-(1H-imidazol-1-yl)octadecanoate (**4**) (1:9, mol:mol) containing Irgacure® TPO-L (1 wt % and 3 wt %, respectively) or Ivocerin® (1 wt %) at 40 °C for 10 min, adapted from [113].

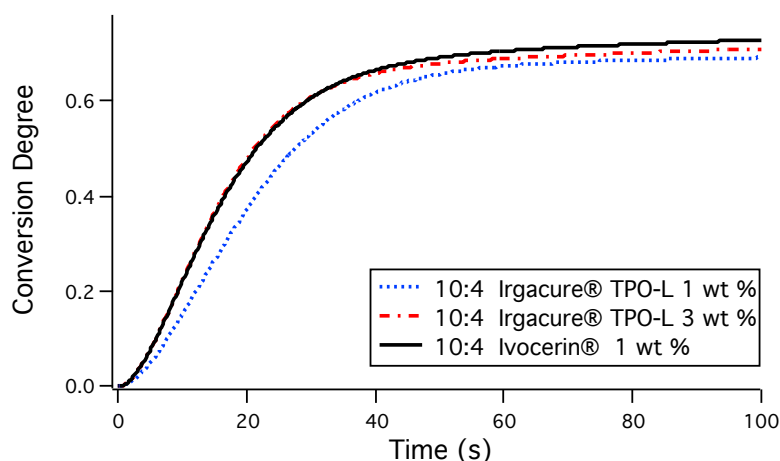


Figure 22: Conversion as function of irradiation time (s) for photoinitiated copolymerization of the ethane-1,2-diyl bis(9-methacryloyloxy-10-hydroxy octadecanoate) / ethane-1,2-diyl 9-hydroxy-10-methacryloyloxy-9'-methacryloyloxy-10'-hydroxy octadecanoate / ethane-1,2-diyl bis(9-hydroxy-10-methacryloyloxy octadecanoate) (**10**) and methyl 9-(1H-imidazol-1-yl)-10-(methacryloyloxy)octadecanoate / methyl 9-(methacryloyloxy)-10-(1H-imidazol-1-yl)octadecanoate (**4**) (1:9, mol:mol) containing Irgacure® TPO-L (1 wt % and 3 wt %, respectively) or Ivocerin® (1 wt %) at 40 °C for 10 min, adapted from [113].

Final double bond conversion reaches the higher values (70-78%) by addition of monomer **4** which exhibits quantitative conversion in the homopolymerization experiments (Table 11).

On the other hand, glass transition temperature of the resulting material did not shift to higher values after copolymerization of **10** with **4** in consideration of the results obtained from DSC measurement or analysis of the storage or loss modulus (Table 12). The presence of long alkyl chain in the monomer **4** structure provides extra flexibility to the polymer chains and results a low glass transition temperature. To get a deeper insight of the final material properties, the films were prepared from the homopolymer and copolymer mixtures and investigated by DSC and DMA techniques. Furthermore, sol gel analysis of the resulting polymers was done as well.

5.3.3 Crosslinked Films Derived by Photoinitiated Homopolymerization of the Biobased Dimethacrylate (10) and Copolymerization with Methacrylate 7 and 4, Respectively

Some results discussed in this subchapter were submitted to publish [113].

The homopolymerizing mixtures of monomer **10**, copolymerizing mixtures of **10:7** (mol ratio= 1:1 and 1:9) and **10:4** (mol ratio= 1:9) were cured on the glass substrate, respectively, by 395 nm light source. The gel content of the crosslinked polymers was determined between 86 % and 99 % (Table 12). Lower gel content was calculated for the copolymers derived from the mixture **10:4** (mol ratio= 1:9) and **10:7** (mol ratio= 1:9) as a result of a reduction in the mean functionality of the system. Furthermore, glass transition temperatures for the polymers were analyzed using both techniques, DSC and DMA. It was possible to remove free-standing films from the glass substrate for all samples except for co-(**10-7**) (1:9, mol:mol) containing Ivocerin®. Both techniques confirm that the poly-**10**, co-(**10-7**) obtained from a stoichiometric ratio of the monomers, (Figure S09, S10) and co-(**10-4**) derived from monomer **4** excess (Figure S12), possess low glass transition temperatures when both storage modulus and loss modulus were analyzed to identify the T_g values (Table 12) for DMA analysis. Monomer **10** has a long alkyl chain substituted by methacrylate groups. Long aliphatic structure of the material enables the flexible rotation to the polymer network and causes a low glass transition temperature. On the other hand, both DSC and DMA techniques indicate that excess amount on monomer **7** in the copolymerizing mixture leads to a polymer with a higher glass transition value (Figure S11, Table 12) due to the effect of more rigid aromatic **7** structural segments in co-(**10-7**) comprising the methacrylate group directly bound to the phenyl ring. Glass transition temperatures obtained by DSC technique are lower than those analyzed by DMA due to the frequency effect [129]. Furthermore, the T_g values identified from $\tan \delta$ are between 44 °C and 72 °C (Table 12). Interestingly, while an intense peak of $\tan \delta$ centered at higher

temperature in case of co-(**10-4**), an additional broad shoulder was appeared at lower temperature region (Figure S12). $\tan \delta$ curve gives the first maximum in transition region, and second maximum in the rubbery region, then gradually decreases. A shoulder on the damping curve may be caused by heterogeneous network formation which was previously reported in the literature [27,130-131]. Broad $\tan \delta$ can be attributed to non-homogeneity of the crosslinked network [131-132]. In addition, the comparison of the loss modulus curves of the poly-**10**, co-(**10-7**) and co-(**10-4**) presented in Figure 23 displays that the graphs maximise in the low temperature region for poly-**10**, co-(**10-4**) and co-(**10-7**) (mol ratio=1:1). On the other hand, the peak in the loss modulus of co-(**10-7**) (mol ratio=1:9) is appeared at higher temperature region. It was found that the incorporation of excess amount of **7** into the network formation results in observing a shift in T_g towards higher temperature region. It shows that the presence of aromatic group in the monomer **7** provides the rigidity to the polymer network and results an increase in the glass transition value.

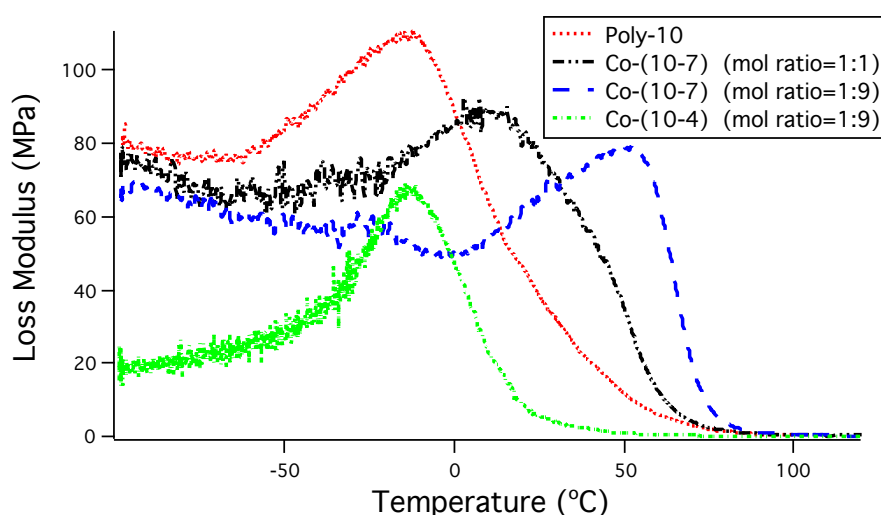


Figure 23: Overlay of loss modulus (MPa) as function of temperature (°C) measured by DMA on homopolymer (poly-**10**) and copolymer (co-(**10-7**)) (stoichiometric ratio of the monomers and molar ratio=1:9) an co-(**10-4**) (molar ratio=1:9) films, adapted from [113].

Moreover, crosslink density (ν) of the networks and molecular weight between two junctions (M_c) were investigated using the following equations (5.1) and (5.2);

$$\nu = \frac{E'}{3RT} \quad (5.1)$$

$$M_c = \frac{\rho_{material}}{\nu} \quad (5.2)$$

The equation 5.1 was evaluated using rubber elasticity theory where E' is the storage modulus in the rubbery plateau, R is the ideal gas constant ($8.314 \text{ J}\cdot\text{mol}^{-1}\text{K}^{-1}$), T is the absolute temperature in K when the all polymers reach the rubbery plateau. Additionally, the molecular weight of the segments between two crosslink points was determined using equation 5.2 where (ρ_{material}) is the material density. The results calculated were summed up in Table 13. As expected, homopolymer of **10** has the highest crosslink density as a result of two polymerizable functional groups in its structure. On the other hand, crosslink density dramatically decreases for the copolymers resulted by copolymerization with monomer **7** and **4**, respectively, bearing only one methacrylate group. The lowest value is calculated in case of co-(**10-7**) prepared from the mixture containing excess amount of monomer **7**. The monomer **7** comprises only one methacrylate group which leads to a reduction in the average functionality of the polymerizing mixture. Therefore, lower crosslink density was obtained in the presence of higher concentration of monomer **7** in the mixture. When the effect of photoinitiator has been considered, the results show that three times higher concentration of Irgacure® TPO-L or usage of Ivocerin® instead of 1 wt % Irgacure® TPO-L leads to a higher crosslink density for the resulting material. M_c data calculated exhibit opposite tendency than crosslink density. It may explain higher conversion values obtained for copolymers because higher M_c value relates to higher mobility of the segments during chain growth. Poly-**10** has the lowest molecular weight segments and co-(**10-7**) containing excess amount of **7** has higher M_c data which results in a loosely crosslink network (Table 13). It can be concluded that although polymerization kinetic is nearly independent on the photoinitiator concentration or type, crosslink density and M_c values are highly dependent on photoinitiator concentration or type .

Table 12: Glass transition temperatures of the homopolymer (poly-**10**), and copolymers (co-**10-7**) (1:1, mol:mol), co-(**10-7**) (1:9, mol:mol) and co-(**10-4**) (1:9, mol:mol) films, adapted from [113].

Polymer	Initiator (wt%)	Tg DSC (°C)	Tg Storage Modulus (°C)	Tg Loss Modulus (°C)	Tg Tan δ (°C)	Gel Content (%)
Poly-10	TPO-L 1 %	-28	-24	-20	44	97
Poly-10	TPO-L 3 %	-27	-25	-15	44	99
Poly-10	Ivocerin 1 %	-30	-29	-17	45	98
Co-(10-7) (1:1, mol:mol)	TPO-L 1 %	-27	-11	-6	50	98

Polymer	Initiator (wt%)	Tg DSC (°C)	Tg Storage Modulus (°C)	Tg Loss Modulus (°C)	Tg Tan δ (°C)	Gel Content (%)
Co-(10-7) (1:1, mol:mol)	TPO-L 3 %	-29	-5	7	57	99
Co-(10-7) (1:1, mol:mol)	Ivocerin 1 %	-28	-12	2	50	99
Co-(10-7) (1:9, mol:mol)	TPO-L 1 %	36	7	54	70	91
Co-(10-7) (1:9, mol:mol)	TPO-L 3 %	37	9	52	72	91
Co-(10-7) (1:9, mol:mol)	Ivocerin 1 %	41	-	-	-	92
Co-(10-4) (1:9, mol:mol)	TPO-L 1 %	-26	-28	-25	3 59	88
Co-(10-4) (1:9, mol:mol)	TPO-L 3 %	-27	-22	-17	8 59	86
Co-(10-4) (1:9, mol:mol)	Ivocerin 1 %	-33	-26	-19	6 57	89

*DSC method was set to temperature interval: -120°C to 100°C using heating and cooling rate of 10 K/min for isolated poly-10.

*DSC method was set to temperature interval: -120°C to 100°C using heating and cooling rate of 10 K/min for isolated co-(10:7) (mol ratio=1:1).

*DSC method was set to temperature interval: -120°C to 150°C using heating and cooling rate of 10 K/min for isolated co-(10:7) (mol ratio=1:9).

*DSC method was set to temperature interval: -120°C to 150°C using heating and cooling rate of 10 K/min for isolated co-(10:4) (mol ratio=1:1).

Table 13: Density of the crosslinked films, temperature used for calculation of the crosslink density (T_{rubbery}) using both the real part of the elastic modulus (E') and density of the films, crosslinks density, and molecular weight between crosslink points (M_c) for poly-**10**, co-(**10-7**) (1:1, mol:mol), co-(**10-7**) (1:9, mol:mol) and co-(**10-4**) (1:9, mol:mol) films, adapted from [113].

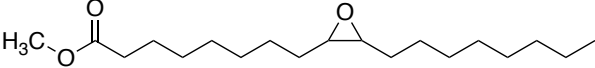
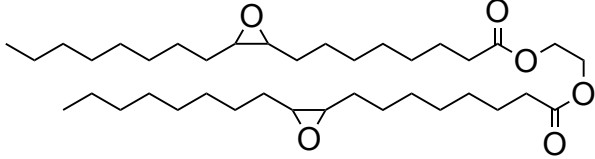
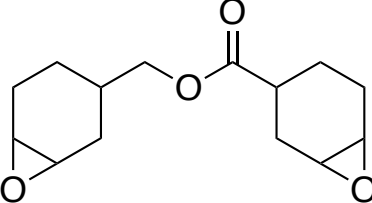
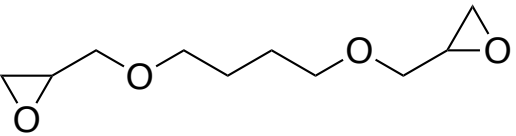
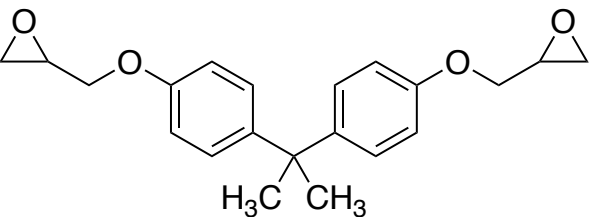
Polymer	Initiator (wt%)	Density (g/cm ³)	T_{rubbery} (K)	Crosslink Density (mol/m ³)	M_c (g/mol)
Poly- 10	TPO-L 1 %	1.10	362	1202	915
Poly- 10	TPO-L 3 %	1.03	363	1865	556
Poly- 10	Ivocerin 1 %	0.92	363	1520	605
Co-(10-7) (1:1, mol:mol)	TPO-L 1 %	1.19	368	110	10818
Co-(10-7) (1:1, mol:mol)	TPO-L 3 %	0.96	375	316	3127
Co-(10-7) (1:1, mol:mol)	Ivocerin 1 %	1.11	368	290	3447
Co-(10-7) (1:9, mol:mol)	TPO-L 1 %	1.12	383	46	24309
Co-(10-7) (1:9, mol:mol)	TPO-L 3 %	1.09	385	88	12386
Co-(10-4) (1:9, mol:mol)	TPO-L 1 %	1.17	372	41	28536
Co-(10-4) (1:9, mol:mol)	TPO-L 3 %	1.09	372	111	9820
Co-(10-4) (1:9, mol:mol)	Ivocerin 1 %	1.13	370	117	9658

5.4 Photoinitiated Cationic Polymerization of Biobased Epoxides in Comparison with Commercial Epoxides

Biobased epoxies, functionalized from the vegetable oils with epoxy groups, are also promising candidates for cationic photoinitiated polymerization. These materials have a wide application areas such as adhesives, coating or electronic applications. They exhibit good adhesion to the different surfaces. Epoxy resins generally show low shrinkage and high strength [133-134]. On the other hand, cationic photoinitiated polymerization has many advantages compared to the free radical technique such as dark curing, insensitivity to the atmospheric oxygen. In addition to the systems produced by free radical mechanism, biobased epoxies (**11** and **12**) have been photopolymerized via cationic route and deeply investigated in this part of the thesis.

Synthesis of biobased 9,10-epoxystearic acid methyl ester (**11**) and bis-(9,10-epoxystearic acid) 1,2-ethanediyl ester (**12**) has been explained and photokinetic study of these biobased epoxies has been carried out in comparison with commercial epoxies such as 3,4-epoxycyclohexylmethyl-3',4'-epoxycyclohexane carboxylate (**13**), 1,4-butanediol diglycidylether (**14**), and bisphenol-A diglycidylether (**15**) using bis-(*t*-butyl)-iodonium-tetrakis(perfluoro-*t*-butoxy)aluminate (S2617, Table 2) in the presence of isopropylthioxanthone (ITX) as sensitizer to initiate cationic polymerization. Additionally, mechanical properties, wettability of the crosslinked films as well as glass transition temperature have been investigated. Some results discussed in this subchapter were published [114].

Table 14: Structure of the monomers used in this section, adapted from [114].

Monomers	Chemical Structure	No
9,10-Epoxystearic acid methyl ester		11
Bis-(9,10-epoxystearic acid) 1,2-ethanediyl ester		12
3,4-Epoxycyclohexylmethyl-3',4'-epoxycyclohexane carboxylate		13
1,4-Butanediol diglycidyl ether		14
Bisphenol-A-diglycidylether		15

Since two biobased epoxide compounds (**11** and **12**), that were derived from purified oleic acid, are much more pure than the substances such as epoxidized vernonia, castor, linseed or soybean oils, which contain naturally occurring mixture of different compounds, it is more appropriate and easy to compare them with the commercial epoxides used in this work regarding to the kinetic study. All compounds have definite structure and high purity for comparison of the photokinetic study.

Transitions of all epoxide monomers were determined by DSC and data were collected in Table 15. The crosslinked polymers were isolated by extraction with chloroform for 24 h and dried under reduced pressure for DSC measurements. While epoxides derived from oleic acid show only melting during heating scan, all commercial epoxides exhibit glass transition at low temperature region. Since the biobased difunctional epoxide monomer **12** and aromatic monomer **15** are solid at room temperature, photopolymerization study is needed to be performed at elevated temperature where both monomers are liquid. Viscosity of the monomers, that may affect the photopolymerization kinetic during the application of thin film, was also examined at both 60 °C and 23 °C and data were collected in Table 15. According to the results, aromatic monomer **15** and cycloaliphatic monomer **13** exhibit nearly shear rate independent viscosity (Figure S13). In contrast to monomer **13** and **15**, biobased mono- and di-functional epoxides of **11** and **12**, as well as aliphatic monomer **14** have intensely shear rate dependent viscosity (Figure S13). The region where the viscosity is independent on the shear rate starts at 1.5 s⁻¹ for monomer **11**, **12** and **14** at 23 °C or 3 s⁻¹ for monomer **11** and **12** at 60 °C (Figure S13).

Table 15: Melting temperature (T_m , °C) and glass transition temperature (T_g , °C) obtained by DSC measurements of 9,10-epoxystearic acid methyl ester (**11**), bis-(9,10-epoxystearic acid) 1,2-ethanediyl ester (**12**), 3',4'-epoxycyclohexylmethyl-3',4'-epoxycyclohexane carboxylate (**13**), 1,4-butanediol diglycidyl ether (**14**) and bisphenol-A-diglycidylether (**15**) as well as the mixtures of **12:15** (molar ratio of **12:15** = 1:1, 1:5 and 1:9) and additionally viscosity (η , mPa.s) of the monomers and monomer mixtures (molar ratio of **12:15** = 1:1, 1:5 and 1:9) at 60 °C at a given shear rate ($\dot{\gamma}$, 1/s) where the viscosity becomes independent on the shear rate or if the viscosity is independent on the shear rate at all (*) and viscosity (η , mPa.s) at 23 °C for liquid monomers at room temperature, adapted from [114].

Monomer	η (mPa.s) (60°C)	$\dot{\gamma}$ (1/s) (60°C)	η (mPa.s) (23°C)	$\dot{\gamma}$ (1/s) (23°C)	T_m (°C)	T_g (°C)
11	6.2	>3	19.1	>1.5	10 and 15	-
12	5.6	>3	solid	-	50 and 60	-
13	46.2	*	425.1	>1.5	-	-57
14	5.9	>1.5	19.3	>1.5	-18	-56

Monomer	η (mPa.s) (60°C)	$\dot{\gamma}$ (1/s) (60°C)	η (mPa.s) (23°C)	$\dot{\gamma}$ (1/s) (23°C)	T _m (°C)	T _g (°C)
15	229.7	>1.5	solid	-	44	-15
12:15 (Mol ratio=1:1)	43.5	>1.5	solid	-	45 and 56	-23
12:15 (Mol ratio=1:5)	101	>1.5	solid	-	41 and 53	-25
12:15 (Mol ratio=1:9)	141.3	>1.5	solid	-	39 and 51	-36

*The method was set to a temperature interval: from -40°C to 90°C using heating and cooling rates of 5 K/min for **11** and **12**. A temperature interval: from -78 °C to 60 °C using heating and cooling rates of 5 K/min was set for **13**, **14** and a temperature interval: from -78 °C to 70 °C using heating and cooling rates of 5 K/min was used for **15**.

5.4.1 Photoinitiated Polymerization of 9,10-Epoxy Stearates **11** and **12** in Comparison with the Commercial Cycloaliphatic Diepoxide **13** and Aliphatic Diepoxide **14**

Photoinitiated polymerization was carried out at both light intensities of 100 mW.cm⁻² and 180 mW.cm⁻². Since higher light intensity results a higher maximum polymerization rate and conversion values, 180 mW.cm⁻² was chosen for comparison study of the epoxides.

Photopolymerizing mixture prepared from epoxide **14** exhibits the highest reactivity for both light intensities. Furthermore, the system derived from cycloaliphatic epoxide **13** shows lower reactivity than epoxy stearates **11** and **12** after 20 min irradiation, Table 16, Figure 24. Higher viscosity of monomer **13** in comparison with the aliphatic epoxides may limit the final epoxy group conversion. The mobility of the growing chains is restricted, and the diffusion process is limited due to the higher viscosity of **13**. Moreover, the epoxycyclohexane groups in monomer **13** show less flexibility than the epoxy functional groups directly bound to the alkylene moiety. Less flexible nature of epoxycyclohexane structures could be an another possible explanation for less reactivity of **13**. It was previously reported in the literature that lower reactivity of **13** was associated with the cycloaliphatic structure [135]. On the other hand, biobased monomer **11** containing only one functional group exhibits 78 % final conversion after 20 min irradiation at 180 mW.cm⁻² which is higher than that of the other formulations, Table 16, Figure 25. While the difunctional epoxide systems form a network structure, monofunctional monomer **11** produces a linear polymer, which may be a reason of higher final conversion. Epoxy group conversion of biobased monomer **12** or commercial monomer **14** reaches over 60 %. Final epoxy group conversion of the monomers increases in the order **13**<**12**<**14**.

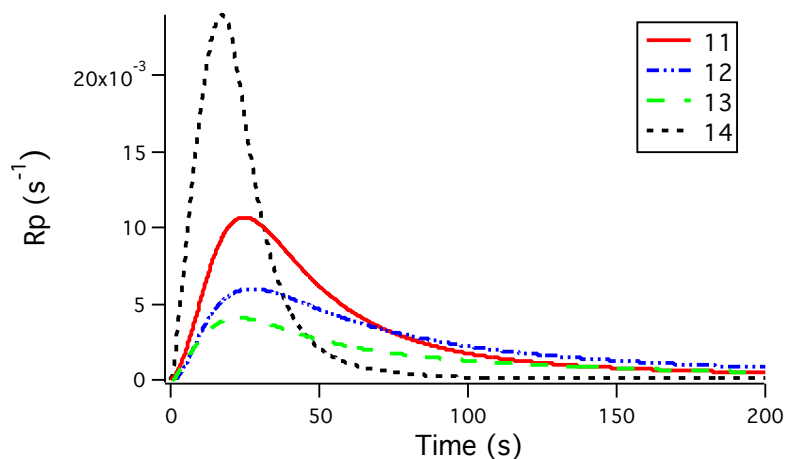


Figure 24: Polymerization rate (R_p (s^{-1})) as function of irradiation time (s) for photoinitiated polymerization of 9,10-epoxystearic acid methyl ester (**11**), bis-(9,10-epoxystearic acid) 1,2-ethanediyl ester (**12**), 3',4'-epoxycyclohexylmethyl-3',4'-epoxycyclohexane carboxylate (**13**) and 1,4-butanediol diglycidyl ether (**14**) containing ITX and S2617 by constant radiation power of $180 \text{ mW}\cdot\text{cm}^{-2}$ for 20 min irradiation at 60°C , adapted from [114].

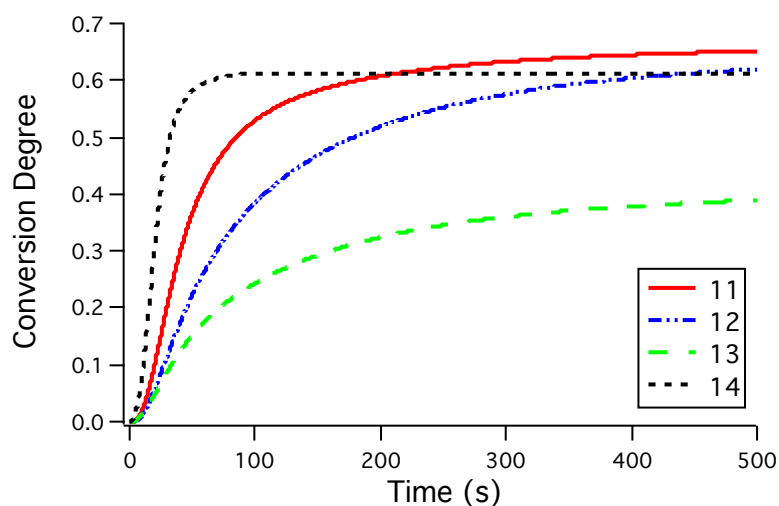


Figure 25: Conversion as function of irradiation time (s) for photoinitiated polymerization of 9,10-epoxystearic acid methyl ester (**11**), bis-(9,10-epoxystearic acid) 1,2-ethanediyl ester (**12**), 3',4'-epoxycyclohexylmethyl-3',4'-epoxycyclohexane carboxylate (**13**) and 1,4-butanediol diglycidyl ether (**14**) containing ITX and S2617 by constant radiation power of $180 \text{ mW}\cdot\text{cm}^{-2}$ for 20 min irradiation at 60°C , adapted from [114].

Table 16: Maximum of the polymerization rate (R_p^{\max}), time (t_{\max}) to obtain the maximum of the polymerization rate, and final conversion for photoinitiated polymerization of 9,10-epoxystearic acid methyl ester (**11**), bis-(9,10-epoxystearic acid) 1,2-ethanediyl ester (**12**), and 3',4'-epoxycyclohexylmethyl_3',4'-epoxycyclohexane carboxylate (**13**) and 1,4-butanediol diglycidyl ether (**14**) using ITX and S2617 and 20 min irradiation time at 60°C, adapted from [114].

Monomer	Intensity (mW.cm ⁻²)	R_p^{\max} (s ⁻¹)	t_{\max} (s)	Final Conversion (%)
11	180	0,011	24	78
12	180	0,006	28	64
13	180	0,004	23	41
14	180	0,024	22	69
11	100	0,008	33	62
12	100	0,002	53	38
13	100	0,002	30	37
14	100	0,019	17	61

DSC measurements of the isolated polymers were performed and data were summarized in Table 17. Low glass transition temperature of the homopolymers made from **11**, **12** and **14** can be explained with the aliphatic chain present in their structure, which provides higher flexibility and the mobility to the network [136]. Contrarily, poly-**13** has a glass transition temperature of 55 °C which is almost the same as the polymerization temperature. It might be an another reason for limited conversion of monomer **13** (Table 17, Figure 25).

The monomer **11** bearing only one functional group forms a viscous liquid polymer after photopolymerization reaction. Formation of the viscous polymer with low molecular weight after direct cationic or free radical polymerization of the vegetable oils was already reported in literature [137,138]. GPC analysis of the linear polymer made by cationic photopolymerization of **11** demonstrates that the number average molecular weight (M_n) is quite low which is 2.047 g.mol⁻¹ (Figure S15). The low molecular weight of poly-**11** indicates oligomer structure with a dispersity of 2.1.

Table 17: Glass transition temperature (T_g , °C) and gel content of the polymers derived from 9,10-epoxystearic acid methyl ester (**11**), 9,10-epoxystearic acid 1,2-ethane diyl ester (**12**), and 3',4'-epoxycyclohexylmethyl-3',4'-epoxycyclohexane carboxylate (**13**), 1,4-butanediol diglycidyl ether (**14**) and bisphenol-A-diglycidylether (**15**), adapted from [114].

Polymer	T_g (°C)	Gel Content
11	-38	-
12	-22	92
13	55	89
14	-12	95
15	70	99

*A temperature interval: from -120°C to 100°C using heating and cooling rate of 10 K/min was selected for the poly-**11**, poly-**12** and poly-**14**. Furthermore, a temperature interval: from -75°C to 200°C using heating and cooling rate of 10 K/min was chosen for the poly-**13**. The method was set to a temperature interval from -75°C to 150°C using heating and cooling rate of 10 K/min for the poly- **15**.

*The poly-**11** is not crosslinked polymer.

Gel content of the crosslinked films made of **12**, **13** and **14** was analyzed (Table 17). While the crosslinked polymers of **12** and **14** give over 90 % gel content, the polymer derived from **13** shows 89 % gel content.

Additionally, dynamic mechanical analysis was performed to analyze mechanical properties of the poly-**13** over a wide temperature range. It was possible to remove the film of **13** from the glass substrate for DMA analysis because of higher glass transition temperature. Two maximums were appeared on the loss modulus versus temperature graph of poly-**13** as shown in Figure S16, Table 19, which can be attributed to the non-homogeneous network structure comprising two phases. High amount of unreacted monomer **13** due to the limited conversion around 41 % may cause the occurrence of the first maximum at low temperature region of the loss modulus curve (Figure S16) because glass transition temperature of the epoxide **13** was previously reported as -60 °C [139] and also determined as -57 °C by DSC measurement as summarized in Table 15. Moreover, the second maxima appeared at the higher temperature region of the loss modulus (150 °C) can be associated with polymer network produced from monomer **13** which corresponds to 89 % of the film obtained by the sol gel analysis. Tan δ versus temperature graph exhibits one broad peak at low temperature range (-50 °C and -60 °C) and one narrow peak at 162 °C which also corresponds the result obtained from the loss modulus.

5.4.2 Photoinitiated Copolymerization of Bis-(9,10-epoxystearic acid) 1,2-Ethanediyyl Ester (12) with Bisphenol-A-diglycidylether (15)

Aromatic diglycidyl ether (15) is a good candidate to enhance the thermo-mechanical properties of the resulting material. As already disclosed in literature, incorporation of aromatic 15 into the polymeric network provides better thermal and mechanical properties [118, 140-143]. In literature, the mixture of monomer 15 and epoxidized vegetable oil is generally cured thermally with anhydride [140-141,143-144] or amine [142,145] and resulting material shows improved hardness. In this study, aromatic diglycidyl ether 15 is preferred as a comonomer to increase the T_g of crosslinked polymer made from biobased diepoxide 12. For this reason, concentration of aromatic 15 in the polymerizing mixture was diversified (1:1, 1:5 and 1:9, mol:mol) to get a deeper information about the effect of 15 on both final material properties such as contact angle, thermal or mechanical behaviour and polymerization kinetic.

Analysis of polymerization kinetic demonstrates that presence of equal or higher amount of monomer 15 in the formulation causes a greater reactivity, which leads to higher R_p^{\max} values as well as faster polymerization compared to the homopolymerization of biobased 12 (Figure 26). Although, the monomer 15 is highly reactive, it has a limited final conversion of 51 %. Vitrification at low irradiation period might be a reason for the limited final conversion of 15 in comparison with copolymerization reactions. As depicted in Table 15, pure monomer 15 has significantly higher viscosity at 60 °C which causes a decrease in diffusion process (Figure S14). Addition of biobased monomer 12 to the copolymerizing mixture results in an increase in the final conversion, especially in case of 1:5 and 1:9 mol:mol formulations (Figure 27). Incorporation of monomer 12 into the copolymerizing samples presents a higher mobility due to the more flexible structure which leads to the higher conversion values. It also causes a variation on the glass transition temperature of the resulting materials.

The DSC analysis shows that addition of aromatic monomer 15 to the copolymerizing mixtures generates crosslinked polymers with significantly higher glass transition temperature. It can be clearly concluded that, T_g values of the copolymers rise up as a result of an increase in monomer 15 concentration in the mixture. The material derived from the mixture containing the highest amount on monomer 15 (mol ratio=1:9) exhibits the greatest T_g value (68 °C) in all copolymer systems, which is slightly lower than T_g of poly-15 (70 °C) and significantly higher than T_g of poly-12 (-22 °C). While a stable film of poly-12 was not possible to obtain for DMA analysis, copolymers of 12:15 were removed easily from the glass substrate for further analysis by DMA. In principal, T_g values differ

depending on the method used for identification [146]. Higher glass transition value analyzed by DMA may be attributed to the frequency effect, which was previously discussed in the literature [129]. All data were summarized in Table 19.

The $\tan \delta$ versus temperature graph of poly-**15** exhibits a β relaxation at low temperature region and then, it maximises at higher temperature which is the indication for T_g of the material (Figure S17). A β relaxation is also detected on the DMA analysis of the copolymers made from the mixture of two monomers **12:15** with 1:1, 1:5 and 1:9 mol:mol (Figure S18, S19, S20). A β relaxation was already reported for the epoxy network systems in the literature [146-147]. When the interaction of poly-(ethyleneimide) with epoxy resin of aromatic **15** was studied, a β relaxation was also discussed for polyethyleneimine crosslinked diglycidyl ether of bisphenol-A [149]. Even if the relaxation peak has the low intensity in comparison with the peak identifying the T_g , it has been detected for the cross-linked poly-**15** as well as copolymers of **12:15**. Furthermore, onset and endset points on the storage modulus have been specified and temperature difference (ΔT) has been evaluated from these values. The greater temperature difference from endset and onset point of the storage modulus (ΔT) was calculated for copolymers of **12:15** compared to poly-**12** indicating non-homogeneous network formation originated by the difference in monomer structures. Although both techniques give different T_g values, it can be clearly seen in Table 19 that glass transition region shifts to higher temperatures as a result of higher distribution of aromatic **15** in the network structure. As we expected, low glass transition value of poly-**12** increases due to the presence of the aromatic groups in the chain segments by copolymerization with **15** because bulky groups present in polymer chain restrict the flexibility of the segments and increase the chain stiffness in contrast the effect of long alkyl chain. Gel content analysis of the polymer networks shows high gel content values which are over 95 % (Table 19). The lowest gel content was calculated for poly-**13** which can be related with the limited final conversion.

Table 18: Maximum of the polymerization rate (R_p^{\max}), time (t_{\max}) to obtain the maximum of the polymerization rate, and final conversion for photoinitiated polymerization of **15**, **12:15** (1:1, mol:mol), **12:15** (1:5, mol:mol) and **12:15** (1:9, mol:mol) using ITX and aluminate and 20 min irradiation time at 60 °C, adapted from [114].

Monomer 12 (mol)	Monomer 15 (mol)	R_p^{\max} (s ⁻¹)	t_{\max} (s)	Final Conversion (%)
-	1	0,033	7,0	51
1	1	0,012	8,4	56
1	5	0,017	8,0	80
1	9	0,019	7,8	85

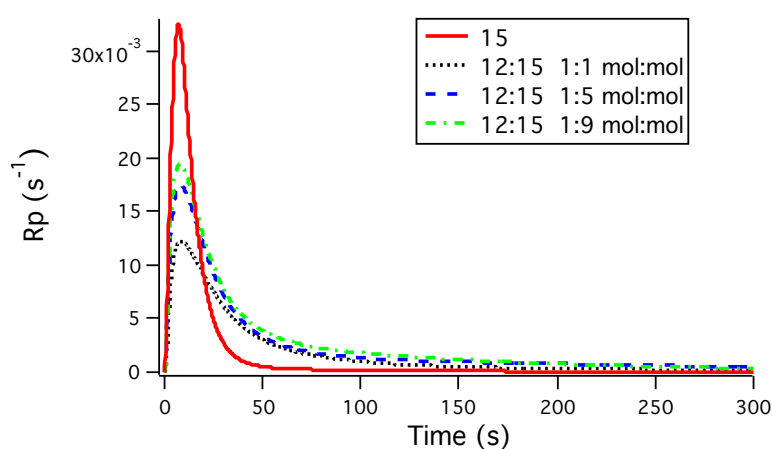


Figure 26: Polymerization rate (R_p (s⁻¹)) as function of irradiation time (s) for photoinitiated polymerization of **15**, **12:15** (1:1, mol:mol), **12:15** (1:5, mol:mol) and **12:15** (1:9, mol:mol) containing ITX and S2617 by constant radiation power of 180 mW.cm⁻² for 20 min irradiation at 60 °C, adapted from [114].

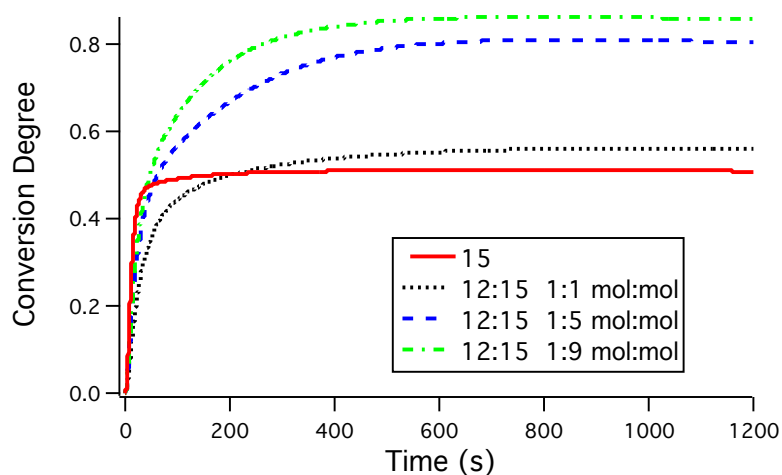


Figure 27: Conversion as function of irradiation time (s) for photoinitiated polymerization of **15**, **12:15** (1:1, mol:mol), **12:15** (1:5, mol:mol) and **12:15** (1:9, mol:mol) containing ITX and S2617 by constant radiation power of 180 mW.cm⁻² for 20 min irradiation at 60 °C, adapted from [114].

Table 19: Glass transition temperature and secondary relaxation* (e. g. β relaxation) of the isolated polymers made of the samples of **15**, **12:15** (1:1, mol:mol), **12:15** (1:5, mol:mol) and **12:15** (1:9, mol:mol) containing ITX and S2617. *secondary relaxation in the $\tan \delta$ curve and loss modulus curve, respectively may be attributed to non-reacted monomer (in case of poly-**13**) or β relaxation (in case of poly-**15** and poly-(**12-15**)), adapted from [114].

Polymer	T _g DSC (°C)	T _g E' (Onset) (°C)	T _g E' (Endset Point) (°C)	T _g Loss Modulus (°C)	T _g Tan δ (°C)	ΔT (K)	Gel Cont ent (%)
Poly-15	70	163 (T _g) -84 (β relaxation)	187 (T _g) -30 (β relaxation)	164 (T _g) -68 (β relaxation)	185 (T _g) -58 (β relaxation)	24	99
Co- (12-15) 1:9 mol:mol	68	75 (T _g) -87 (β relaxation)	148 (T _g) -29 (β relaxation)	127 (T _g) -91 (β relaxation)	140 (T _g) -80 (β relaxation)	73	99
Co- (12-15) 1:5 mol:mol	31	40 (T _g) -86 (β relaxation)	124 (T _g) -33 (β relaxation)	105 (T _g) -71 (β relaxation)	119 (T _g) -53 (β relaxation)	84	98
Co- (12-15) 1:1 mol:mol	11	14 (T _g)	55 (T _g)	39 (T _g)	55 (T _g)	41	97
Poly-12	-22	n. d.	n. d.	n. d.	n. d.	n.d.	92
Poly-13	55	133 (T _g) -100 (β relaxation or remaining monomer)	166 (T _g) -28 (β relaxation or remaining monomer)	150 (T _g) -65 (β relaxation or remaining monomer)	161 (T _g) -55 (β relaxation or remaining monomer)	33	89

* ΔT =from endset and onset point

Moreover, crosslink density (ν) and molecular weight between two junctions (M_c) of the polymer networks were investigated using the equations (5.1) and (5.2);

The data depicted in Table 20 demonstrate that co-(**12-15**) derived from the mixture of 1:5 mol:mol ratio has the highest crosslink density of 2976 mol/m³ followed by poly-**15** with 2327 mol/m³ crosslink density. The crosslink density of the polymer prepared from

aromatic **15** and triethylenetetramine was previously reported as 2320 mol/m³ which is similar the value obtained for poly-**15** in this study [142]. Crosslink density for the polymer network manufactured from aromatic **15** and triethylenetetramine reduced as a result of incorporation of epoxidized soybean oil into the network system [142].

The evaluation of M_c data (Table 20) discloses that molecular weight of the segment between two crosslink points is greater than the molecular weight of the one monomer segment meaning occurrence of the chain extension reaction by ring opening polymerization in addition to the crosslinking reaction for both poly-**15** and co-(**12-15**) with highest crosslink density. The network of co-(**12-15**) formed as a result of curing the mixture of 1:5 mol:mol exhibits nearly ideal polymer network due to the quite similar value to the theoretically calculated M_c value of 387 g/mol. On the other hand, calculation of the greatest M_c data for the poly-**13** network obtained from the lowest molecular weight monomer may imply that the monomer **13** with bulky substituents may lead to a greater degree of chain extension comparative to the crosslink reaction.

Table 20: Crosslink density of the isolated polymers made from **15,13**, and **12:15** mixtures (molar ratio **12:15** = 1:1; 1:5; 1:9), respectively using ITX and S2617 for photoinitiated polymerization, adapted from [114].

Polymer	Monomer Ratio 12:15 mol:mol	T (°C) applied for E'_{rubbery} plateau	E'_{rubbery} plateau (MPa)	Density (g/cm ³)	Crosslink Density (mol/m ³)	M_c (g/mol)
Poly-15	homopolymer	230	29.19	1.167	2327	501
Co-(12-15)	1:9	200	11.83	1.103	1003	1100
Co-(12-15)	1:5	180	33.63	1.036	2976	348
Co-(12-15)	1:1	120	13.68	1.096	1396	785
Poly-13	homopolymer	210	6.56	1.168	545	2144

5.5 Surface-Wetting Characterization for Crosslinked Polymers by Contact Angle Measurement

The surface properties can be varied in regard to monomer structure. Contact angle measurement is a versatile and useful technique for surface characterization. Sessile drop method, which is widely preferred and simple, was used for the contact angle measurements. It is an efficient tool to determine the hydrophobic/ hydrophilic or wetting character of the surfaces which is a crucial parameter especially for production of water resistance or corrosion resistance surface in coating application. Wetting study of the

surfaces derived from difunctional monomer **10** or **12** was performed by dropping of the solvents with different polarity such as distilled water, ethylene glycol, toluene and diiodomethane and data were collected in Table 21. However, it was not possible to obtain a droplet in case of toluene for the films derived from methacrylates.

Table 21: Contact angles for distilled water, ethylene glycol and diiodomethane measured on the crosslinked films of poly-**10**, co-(**10-7**) (1:1, mol:mol), co-(**10-7**) (1:9, mol:mol), co-(**10-4**) (1:9, mol:mol), poly-**12**, poly-**13**, poly-**14**, poly-**15**, co-(**12-15**) (1:1, mol:mol), co-(**12-15**) (1:5, mol:mol) and co-(**12-15**) (1:9, mol:mol) made by photoinitiated polymerization. Toluene is also used as an additional solvent for the films modified from epoxies(**12,13,14,15**), adapted from [113, 114].

Polymer	Initiator	Distilled Water	Ethylene Glycol	Diiodomethane	Toluene
Poly- 10	TPO-L 1 %	84.3°±0.5	62.0°±0.1	56.2°±2.0	-
Poly- 10	TPO-L 3 %	84.5°±0.5	63.0°±0.1	52.6°±0.4	-
Poly- 10	Ivocerin 1 %	85.1°±0.2	64.0°±0.1	49.6°±0.2	-
Co-(10-7) (1:1, mol:mol)	TPO-L 1 %	81.2°±0.5	56.2°±1.0	45.4°±0.2	-
Co-(10-7) (1:1, mol:mol)	TPO-L 3 %	81.9°±0.3	56.9°±0.6	44.5°±0.8	-
Co-(10-7) (1:1, mol:mol)	Ivocerin 1 %	83.9°±0.6	58.9°±0.4	46.1°±0.9	-
Co-(10-7) (1:9, mol:mol)	TPO-L 1 %	76.3°±0.1	51.4°±0.3	38.3°±0.1	-
Co-(10-7) (1:9, mol:mol)	TPO-L 3 %	75.5°±0.4	51.0°±0.2	38.9°±0.3	-
Co-(10-7) (1:9, mol:mol)	Ivocerin 1 %	76.1°±0.2	54.8°±0.3	43.3°±0.6	-
Co-(10-4) (1:9, mol:mol)	TPO-L 1 %	88.2°±0.1	68.7°±0.4	55.7°±0.3	-
Co-(10-4) (1:9, mol:mol)	TPO-L 3 %	87.8°±0.1	68.6°±0.2	54.8°±0.4	-

Polymer	Initiator	Distilled Water	Ethylene Glycol	Diiodomethane	Toluene
Co-(10-4) (1:9, mol:mol)	Ivocerin 1 %	88.5°±0.3	67.1°±0.2	49.6°±1.0	-
Poly-12	S2617	97.9°±1.5	74.1°±0.6	68.0°±1.0	15.9°±0.7
Poly-13	S2617	84.0°±1.0	25.6°±0.5	44.0°±1.2	8.9°±1.5
Poly-14	S2617	71.5°±0.2	66.9°±0.3	55.1°±0.8	11.2°±1.1
Poly-15	S2617	84.4°	52.3°±0.1	59.0°±0.6	18.2°±0.5
Co-(12-15) (1:1, mol:mol)	S2617	88.7°±0.2	55.4°±0.6	65.6°±0.4	12.6°±0.4
Co-(12-15) (1:5, mol:mol)	S2617	87°±0.3	55.1°±0.4	57.5°±0.1	9.6°±0.3
Co-(12-15) (1:9, mol:mol)	S2617	86.5°±0.5	53.0°±0.4	59.0°±0.3	9.8°±0.3

The linear homopolymer of monomer **11** can not be involved in comparison study because it is well soluble in organic solvents such as chloroform or tetrahydrofuran and solid surface can not be obtained after curing process. When distilled water was used as a solvent for the measurements, all films give higher CA values. Contact angle higher than 90° usually implies that wetting of the surface is unfavourable. It is expected to collect high CA values because of the distribution of the long alkyl chain in the network structure. The surface derived from biobased epoxide **12** gives the highest CA value with water and exhibits hydrophobic character (>90°) which is important for coating applications (Table 21). On the other hand, CA values of the water droplet on the film of poly-**13** and poly-**14** were determined 84.0° and 71.5°. Slightly higher CA of the poly-**13** surface may be associated with greater hydrophobic character of poly-**13** due to the higher content on aliphatic parts. Contact angle values decrease for ethylene glycol, diiodomethane and toluene in comparison with distilled water. It demonstrates that organic solvents spread over a larger area on the surfaces in comparison with water and it is crucial for coating application. On the other hand, the values significantly differ for poly-**12**, poly-**13** and poly-**14**. The films of epoxies show the lowest CA values in case of toluene. Distilled water gives the highest CA values for co-(**12-15**) as observed for homopolymers. The results of contact angle measurements for distilled water and ethylene glycol show a slight increase

in case of co-(**12-15**) in comparison with poly-**15** because of the influence of long aliphatic chain presented by **12**.

Moreover, contact angle obtained from the droplet of the different solvents on the coated surfaces made from methacrylates increases in the order diiodomethane<ethylene glycol<distilled water. It can be clearly seen that copolymers of **10** and **7** exhibit lower contact angle and hence more hydrophilic character than poly-**10** due to the less apolar character of **7**. With an excess amount of **7**, the surfaces of co-(**10-7**) become more hydrophilic. In contrast to this, incorporation of excess amount on **4** into the copolymer network causes an increase in contact angle and hence makes the surface more hydrophobic in comparison with poly-**10** surface. It is found that the CA is around 88° for co-(**10-4**) indicating the slight hydrophilicity of co-(**10-4**).

Surface free energy of the films were evaluated by using the solvents with different polarity. The equation (5.3) was used for calculation as defined in the literature [150,151].

$$\frac{\sigma_1}{2 \cdot \sqrt{\sigma_1^d}} \cdot (1 + \cos \theta) = \sqrt{\sigma_s^p} \cdot \sqrt{\frac{\sigma_l^p}{\sigma_l^d}} + \sqrt{\sigma_s^d} \quad (5.3)$$

In addition to the surface free energy (σ_s), dispersion (σ_s^d) and polar component of the surface free energy of epoxy films (σ_s^p) were calculated by using the surface tension components of the test solvents used in this study. (Water (surface tension $\sigma_l = 72.8$ mN/m, dispersion part $\sigma_l^d = 21.8$ mN/m and polar part $\sigma_l^p = 51.0$ mN/m), diiodomethane (surface tension $\sigma_l = 50.8$ mN/m, dispersion part $\sigma_l^d = 50.8$ mN/m and polar part $\sigma_l^p = 0.0$ mN/m), ethylene glycole (surface tension $\sigma_l = 47.7$ mN/m, dispersion part $\sigma_l^d = 30.9$ mN/m and polar part $\sigma_l^p = 16.8$ mN/m), and toluene (surface tension $\sigma_l = 28.4$ mN/m, dispersion part $\sigma_l^d = 26.1$ mN/m and polar part $\sigma_l^p = 2.3$ mN/m) [149,150]. The data determined were collected in Table 22.

Table 22: Surface free energy (σ_s), polar (σ_s^p) and dispersion (σ_s^d) components of the surface free energy for the films of poly-**10**, co-(**10-7**) (1:1, mol:mol), co-(**10-7**) (1:9, mol:mol), co-(**10-4**) (1:9, mol:mol), poly-**12**, poly-**13**, poly-**14**, poly-**15**, co-(**12-15**) (1:1, mol:mol), co-(**12-15**) (1:5, mol:mol) and co-(**12-15**) (1:9, mol:mol) made by photoinitiated polymerization, adapted from [113, 114].

Film	Initiator	σ_s (mN/m)	σ_s^p (mN/m)	σ_s^d (mN/m)
Poly-10	TPO-L 1 %	31.6	4.8	26.9
Poly-10	TPO-L 3 %	32.0	4.8	27.2
Poly-10	Ivocerin 1 %	32.2	4.7	27.5
Co-(10-7) (1:1, mol:mol)	TPO-L 1 %	36.2	5.1	31.1
Co-(10-7) (1:1, mol:mol)	TPO-L 3 %	36.0	4.9	31.2
Co-(10-7) (1:1, mol:mol)	Ivocerin 1 %	34.8	4.4	30.4
Co-(10-7) (1:9, mol:mol)	TPO-L 1 %	41.9	6.9	34.9
Co-(10-7) (1:9, mol:mol)	TPO-L 3 %	39.9	6.7	33.2
Co-(10-7) (1:9, mol:mol)	Ivocerin 1 %	38.0	7.0	31.0
Co-(10-4) (1:9, mol:mol)	TPO-L 1 %	29.0	4.3	24.7
Co-(10-4) (1:9, mol:mol)	TPO-L 3 %	29.4	4.4	24.9
Co-(10-4) (1:9, mol:mol)	Ivocerin 1 %	30.1	4.2	26.0
Poly-12	S2617	25.4	1.3	24.2
Poly-13	S2617	38.0	3.9	34.2
Poly-14	S2617	33.2	10.1	23.1
Poly-15	S2617	31.4	4.9	26.5
Co(12-15) (1:9, mol:mol)	S2617	31.4	4.0	27.4
Co(12-15) (1:5, mol:mol)	S2617	31.4	3.6	27.7
Co(12-15) (1:1, mol:mol)	S2617	29.3	3.9	25.5

Similar results previously reported for other crosslinked epoxides in the literature [152,153] agree that networks of aliphatic epoxies have a small distribution of the polar component

(σ_s^p) to the surface free energy (σ_s). The film with the lowest surface free energy and polar part of the surface free energy was derived from biobased monomer **12**. It is a result of the main distribution of long alkyl chain substituted by two functional groups into the polymer network. The result shows that the surface produced from biobased difunctional epoxide (**12**) may have a potential for water-resistance or anti-corrosion coating application but low glass transition temperature of poly-**12** is not preferred for coating industry. For this reason, biobased monomer **12** has been copolymerized with bisphenol-A-diglycidylether (**15**).

According to the surface free energy data summed up in Table 22, surface free energy (σ_s) and contribution of the polar components of the surface free energy (σ_s^p) are lower in case of poly-**10** and co-(**10-4**) in comparison with the films derived from the mixture of **10:7** due to the dominant apolar structural elements existing on the coated surfaces. On the other hand, involvement of excess amount on comonomer **7** with more polar structure compared to the comonomer **4** results an increase in both surface free energy (σ_s) and polar components of the surface free energy (σ_s^p), as expected. Despite distribution of the comonomer **7** on the surfaces after photoinitiated copolymerization with **10** leads to lower contact angle values and higher surface free energy, the glass transition values successfully shifted to the higher temperature region. The experiments performed for modification of the polymer network show that the final material properties can be easily diversified by variation on the monomer structures.

According to the contact angle measurements and surface free energy calculations, the poly-**12** exhibits hydrophobic surface reflecting poor wetting and low surface free energy. On the other hand, lower contact angle in case of poly-**10** indicates a more hydrophilic surface and higher surface energy than poly-**12** because the distribution of polar hydroxyl groups on the surface causes a droplet with a smaller contact angle and better wetting.

In all cases, the droplet of water gives the highest contact angle in comparison with the CA values obtained from other solvents. It can be said that organic solvents have a tendency to spread better on the surfaces which is crucial for film preparation.

6. Conclusion

Photo-curing has become a well established technology in the field of coating applications. This process presents many advantages over thermal polymerization such as fast curing, low energy consumption, VOC free formulations and mild reaction conditions which suit some basis requirements of the green chemistry. Interest in photochemical processes has growth rapidly in the field of synthetic polymer chemistry. It offers an alternative to design of tailor-made polymers. Free radical polymerization is widely used in the industrial application of photochemical strategies such as thin film application, stereolithography, dental fillings, adhesives, nanocomposites or polymer gels. Utilization of typical free radical polymerization mechanism in UV-radiation technology involves the combination of the mono- or multi-functional (meth)acrylates and suitable photoinitiator for light source. The wide choice of the monomer options with the high reactivity makes the radical mechanism preferred for UV-radiation technology in industrial applications. The (meth)acrylate-based polymer networks obtained by UV-curing exhibit special chemical and mechanical properties which makes them commercially favoured. On the other hand, cationic photopolymerization process has remarkable benefits compared to the typical free radical polymerization technique. One main advantage is that carbo-cationic chain is not inhibited by atmospheric oxygen and the growing chain exhibits stability during the polymerization. Therefore, inert atmosphere is not needed during the irradiation process. The other unique phenomenon is that the active acidic species generated from initiator have a relatively long life-time. This feature as known as dark curing means that cationic polymerization may proceed after the irradiation is stopped. Both techniques have their unique advantages. In principal, photoinitiated processes offer environmental friendly reaction conditions which makes it desirable for wide range of applications. Additionally, it is fast and preferable way to design of polymers in regards of modification on the structure and variation on the material properties.

In principal, the photopolymerization requires well defined reaction conditions. In addition to the photoinitiating system and monomer, light source is the another requirement which needs to be well matched with the nature of the initiator. UV-light is commonly employed in the curing processes. It has been characterized by the benefits of relatively monochromatic light option, non-ozone release, compact size and long-life time. In this work, highly reactive Type I photoinitiators of Ivocerin® from acyl germane derivative and Irgacure® TPO-L from phosphine oxide family have been used for free radical polymerization processes. For cationic photoinitiated polymerization, PIS has been

employed where formation of initiating radicals or cations occurs upon an electron transfer between excited sensitizer and initiator. For this system, newly developed aluminate (S2617) has been combined with a sensitizer (ITX) which facilitates to eliminate harmful effect of hexafluorophosphates.

Another crucial component for the efficiency of photopolymerizing system is monomer to combine with defined reaction conditions in terms of PIS and light source. Even if the wide range of commercially monomers are available, derivation of the biobased polymerizable structure is quite important for photoinitiated processes known as environmental friendly. Although the technique suits requirements of the green chemistry with solvent-free formulation, low energy consumption and mild reaction conditions, usage of renewable materials for sample preparation allows the system to be more nature friendly. For this purpose, vegetable oils are good candidates to synthesize biobased monomers for polymerizable formulations. However, naturally occurring double bonds in their structure are not adequately reactive. Therefore, modification of the available functional groups in the vegetable oils gives an opportunity to synthesize biobased monomers for possible polymerization processes. Furthermore, structural functionality can also be governed by modification steps which has an impact on both reactivity of the system and final material properties. For this purpose, oleic acid was used as a sustainable starting material for synthesis of monomers with different functional groups.

Firstly, (meth)acrylates (**2,3** and **4**) consisting of two isomers, methyl 9-((meth)acryloyloxy)-10-hydroxyoctadecanoate / methyl 9-hydroxy-10-((meth)acryloyloxy)octadecanoate (**2** and **3**) and methyl 9-(1H-imidazol-1-yl)-10-(methacryloyloxy)octadecanoate / methyl 9-(methacryloyloxy)-10-(1H-imidazol-1-yl)octadecanoate (**4**) were derived from the oleic acid mix containing additionally low concentration of higher unsaturated fatty acids. Moreover, *N*-octyl-*N'*-vinylimidazolium bis(trifluoromethylsulfonyl)imide and *N*-decyl-*N'*-vinylimidazolium (**1a** and **1b**) were synthesized because ILs were considered to be suitable for the comparison study with the biobased monomers (**2,3** and **4**) due to the presence of long alkyl chain in their structure. Additionally, both monomer types have green approach because (meth)acrylated fatty acid methyl esters (**2,3** and **4**) were modified from vegetable oil, and ILs (**1a** and **1b**) have non-volatile character. Furthermore, traditional monomers 1,6-hexanediol di(meth)acrylate (**5**, **6**) were also included in the photokinetic investigation and the photopolymerization was carried out in the presence of (1 wt % or % 3 wt %) Irgacure® TPO-L and (1 wt %) Ivocerin®, respectively. Maximum polymerization rate of the systems slightly differs depending on the photoinitiator type, Irgacure® TPO-L or Ivocerin®. The formulation

containing 1 wt % Ivocerin® has slightly higher efficiency in comparison with the same amount of Irgacure® TPO-L for many systems. Another point leading to a positive effect on the polymerization process, is an increase in the Irgacure® TPO-L concentration. On the other hand, the results obtained from the kinetic study display that ionic liquid monomers (**1a**, **1b**) and biobased methacrylate **4** have full double bond conversion after 10 min irradiation in case of Irgacure® TPO-L or Ivocerin®. Quantitative conversion makes them potential alternatives for coating applications. Another result that needs to be highlighted is that the systems of the biobased monomers and ILs generate heat in longer irradiation period. However, heat release during the polymerization processes of the commercial monomers occurs in a shorter time. Transportation of heat in a longer curing time may make the biobased (meth)acrylates (**2**, **3**, **4**) and ionic liquid monomers (**1a**, **1b**) preferable for photopolymerizing systems instead of the commercial monomers (**5**, **6**). Higher amount of heat release during polymerization can be conducted to the crosslinking in case of monomers **5** and **6**. The results show that photoinitiator type or concentration is not only parameter that differs the photopolymerization kinetic, but also monomer structure has a significant impact on the efficiency of the system.

The photocurable monomers, derived from fatty acids having a long alkyl chain, are promising candidates for photopolymerization processes. They have a green approach as well as high conversion degree. However, the materials obtained from these monomers generally show low T_g values due to the flexible nature of the structure. Therefore, 4-(4-methacryloyloxyphenyl)-butan-2-one (**7**) was synthesized because it was supposed to bring rigidity to the polymer thanks to the aromatic ring in the structure. Photokinetic investigation of newly developed monomer **7** in comparison with traditional monomers, 2-phenoxyethyl methacrylate (**8**) and phenyl methacrylate (**9**), shows that the combination of high reactivity with quantitative conversion in case of monomer **7** makes it a promising candidate for replacement with the traditional monomers of **8** and **9**. Due to the soluble nature of the photopolymers, it was possible to make a deeper investigation about the chemical reactivity and comparison study for the photopolymers. According to the GPC result, the photopolymer of **7** has a high molecular weight and an additional second fraction with the higher molecular weight is appeared on the chromatogram when polymerization is carried out at 85 °C. It is associated with the additional thermal process during photopolymerization at 85 °C. Moreover, DSC analysis shows that poly(methacrylate) with higher glass transition temperature of 65 °C was successfully obtained. Although monomers **7**, **8** and **9** have similarities in their structures, they show significantly different efficiency during the photopolymerization which may be attributed to

the position of the substituents at the phenyl ring. The experiments prove that monomer structure plays a key role on the polymerization kinetic.

In addition to the linear systems derived from biobased monomers, ILs or commercial monomers, designing crosslinked polymers and investigation of the material properties are other topics discussed in this thesis. Therefore, new biobased monomers, ethane-1,2-diyl bis(9-methacryloyloxy-10-hydroxy octadecanoate) / ethane-1,2-diyl 9-hydroxy-10-methacryloyloxy-9'-methacryloyloxy10'-hydroxy octadecanoate / ethane-1,2-diyl bis(9-hydroxy-10-methacryloyloxy octadecanoate) (**10**) and bis-(9,10-epoxystearic acid) 1,2-ethanediyl ester (**12**) were synthesized by functionalization of the carboxylic acid and the internal double bond, respectively, found in purified oleic acid.

Photokinetic investigation of biobased monomer **10** and the mixtures of **10** and **7** as well as **10** and **4** shows that it is possible to generate a network in a short irradiation time. It can be concluded that not only final conversion but also rate of polymerization increased by incorporation of comonomer **7** into the photopolymerization mixture of monomer **10** because monomer **7** has quantitative conversion in homopolymerization experiments. Both techniques, DSC and DMA, demonstrate that low glass transition temperature of the poly-**10** successfully increased by copolymerization with excess amount on monomer **7** because of the more rigid nature and copolymers co-(**10-7**) (1:9, mol:mol) show glass transition above room temperature. Additional copolymerization experiments of the monomer **10** with monomer **4** have been carried out for alteration of the final materials and analysis the effect of imidazole ring on the material properties. However, when DSC and storage or loss modulus are analyzed, co-(**10-4**) has a low glass transition temperature due to the high content on highly flexible aliphatic structural parts. On the other hand, $\tan \delta$ versus temperature curve of co-(**10-4**) displays that a shoulder was appeared at low temperature region in addition to the intense broad peak at higher temperature region. Broaden $\tan \delta$ can be attributed to the heterogeneity in the network structure. Moreover, homopolymer of **10** has the highest crosslink density and lower M_c value. As expected, a reduction in the mean functionality of the polymerization mixture, caused by involvement of monomer **7** or monomer **4** bearing only one polymerizable group, leads to a loosely crosslink polymer network and higher M_c values. Another result can be stated for these systems is that although photoinitiator concentration (1 wt % or 3 wt % Irgacure® TPO-L) or type (Irgacure® TPO-L or Ivocerin®) does not have a dominant role on the polymerization kinetic, it has a significant effect on the network formation. While the polymers produced in the presence of higher amount on Irgacure® TPO-L or Ivocerin® show higher crosslink density, lower concentration of Irgacure® TPO-L results in a

crosslink network with higher M_c value. The networks containing long alkyl chains substituted by hydroxy groups might be an interesting candidates for adhesive applications due to their green origin.

This work also contributes to better understanding of utilization of biobased epoxy monomers in cationic UV-curing. In this purpose, 9,10-epoxystearic acid methyl ester (**11**) and bis-(9,10-epoxystearic acid) 1,2-ethanediyl ester (**12**) were photopolymerized using aluminate (S2617) and ITX as a PIS. Photokinetic comparison study depicts that the systems derived from biobased epoxides (**11** and **12**) show higher efficiency than the polymerization of cycloaliphatic **13** which can be explained by high viscosity of **13** and limited diffusion process during polymerization. Furthermore, poly-**13** has lower crosslink density compared to the other crosslink systems derived from epoxides. GPC analysis of the soluble poly-**11** shows that it has an oligomer structure with low molecular weight and high dispersity which is generally observed for the polymerization of vegetable oil derivatives. On the other hand, the reactivity of bisphenol-A-diglycidylether (**15**) is significantly higher than that of biobased epoxides **11** and **12**. However, commercial **15** has a limited final conversion which may be caused by significantly higher viscosity of monomer **15**. Additionally, vitrification at short irradiation time may be a reason for the limited final conversion around 50 % in case of monomer **15**. Copolymerization of monomer **12** with monomer **15** results in a higher maximum polymerization rate compared to homopolymerization of **12** and R_p^{\max} increases with higher amount on monomer **15** in the polymerizing sample. This can be explained by higher reactivity of **15** in comparison with **12**. Moreover, the presence of higher amount on biobased epoxide **12** in the copolymerization mixture of **12:15** (mol ratio= 1:5 and 1:9) may increase the mobility in the polymerizing mixture which results in higher final conversion values (80 % or higher). The material obtained from the **12:15** mixture with 1:5 molar ratio exhibits the highest crosslink density which is almost ideal network. It can be concluded that both polymerization kinetic and physical processes such as viscosity have a significant effect on the final material properties. The result obtained also shows that vitrification can be a limitation for final conversion. On the other hand, low glass transition temperature of the poly-**12** was shifted to the higher temperature region as a result of copolymerization with monomer **15**, confirmed by DSC and DMA. Poly-**12** with the properties of high CA and low T_g may have a potential for application in adhesive systems. However, crosslinked copolymers of **12:15** mixtures can be more useful for coating applications as a binder due to the higher T_g values.

Surface characterization by contact angle measurement is crucial parameter for coating applications. It can be linked to hydrophobic/hydrophilic character and wettability of the surface as well as adhesion. In between the all crosslinked materials, poly-**12** has the lowest surface free energy and hydrophobic character. Incorporation of monomer **15** into the polymer network results an increase in both surface free energy and polar component of the surface free energy depending on a decrease in the effect of long alkyl chain. On the other hand, ring opening reaction of monomer **12** and substitution with methacrylate and hydroxy groups brings hydrophilicity to the polymer film of **10** after UV-curing. Therefore, while poly-**12** shows hydrophobic character, the surface produced from biobased monomer **10** gives contact angle lower than 90° in case of water. It displays that poly-**12** may be an interesting candidate to create a surface showing adhesion and water repellent behaviour.

The generated systems based on biobased monomers may be possible candidates to make a contribution to the reduction of carbon footprint or to strength the green label of the materials used in coating or adhesive applications.

References

1. S. Chatani, C. J. Kloxin, C. N. Bowman, The power of light in polymer science: photochemical processes to manipulate polymer formation, structure, and properties, *Polym. Chem.*, 5, **2014**, 2187-2201
2. W. Schnabel, *Polymers and Light: Fundamentals and Technical Applications*, Wiley-VCH Verlag GmbH & Co. KGaA, Weinheim, **2007**, 275-329.
3. A. Gandini, The irruption of polymers from renewable resources on the scene of macromolecular science and technology, *Green. Chem.*, 13, **2011**, 1061-1083.
4. J.M. Raquez, M. Deleglise, M.F. Lacrampe, P. Krawczak, Thermosetting (bio)materials derived from renewable resources: A critical review, *Prog. Polym. Sci.*, 35, **2010**, 487-509.
5. R. Auvergne, S. Caillol, G. David, B. Boutevin, J.P. Pascault, Biobased thermosetting epoxy: present and future, *Chem. Rev.*, 114, **2014**, 1082-1115.
6. V. Vaida, Review article: Sunlight initiated atmospheric photochemical reactions, *International Journal of Photoenergy*, 7, **2005**, 61-68.
7. M. Oelgemöller, C. Jung, M. Jochen, Green photochemistry: Production of fine chemicals with sunlight, *Pure and Applied Chemistry*, 79, **2007**, 1939-1947.
8. P. Douglas, R. C. Evans, H. D. Burrows, *Applied Photochemistry*, Springer, **2013**, 598.
9. M.SI. Veitía, C. Ferroud, New activation methods used in green chemistry for the synthesis of high added value molecules, *Int. J. Energy Environ. Eng.*, 6, **2015**, 37-46.
10. S. Jonsson, P.E. Sundell, J. Hultgren, D. Sheng, C. E. Hoyle, Radiation Chemistry Aspects of Polymerization and Crosslinking. A Review and Future Environmental trends in 'non-acrylate' Chemistry, 27, **1996**, 107-122.
11. S. S. Liow, L. K. Widjaja, V. T. Lipik, M. J. M. Abadie, Synthesis, characterization and photopolymerization of vinyl functionalized poly (-caprolactone), *eXPRESS Polymer Letters*, 3, **2009**, 159-167.
12. M. A. Tehfe, F. Louradour, J. Lalevée, J.P. Fouassier, Photopolymerization Reactions: On the Way to a Green and Sustainable Chemistry, *Appl. Sci.*, 3(2), **2013**, 490-514.
13. K. A. Berchtold et al., Novel Monovinyl Methacrylic Monomers Containing Secondary Functionality for Ultrarapid Polymerization: Steady-state Evaluation, *Macromolecules*, 37, **2004**, 3165-317.
14. R. Dessauer, *Photochemistry, History and Commercial Applications of Hexaarylimidazoles: All about HABIs*, Elsevier, **2006**.

15. J. W. Stansbury, M. J. Idacavage, 3D printing with polymers: Challenges among expanding options and opportunities, *Dental Materials*, 32, **2016**, 54-56
16. G. Yilmaz, Y. Yagci, New Photochemical Processes for Macromolecular Synthesis, *Journal of Photopolymer Science and Technology*, 29, **2016**, 91-98.
17. D. Y. Kim, J. W. Park, D. Y. Lee, K. H. Seo, Correlation between the Crosslink Characteristics and Mechanical Properties of Natural Rubber Compound via Accelerators and Reinforcement, *Polymers*, 12, **2020**.
18. F. Zhao, W. Bi, S. Zhao, Influence of Crosslink Density on Mechanical Properties of Natural Rubber Vulcanizates, *Journal of Macromolecular Science Part B*, 7, **2011**, 1460-1469.
19. G. Hoti, F. Caldera, C. Cecone, A. Rubin Pedrazzo, A. Anceschi, S.L. Appleton, Y. Khazaei Monfared, F. Trotta, Effect of the Cross-Linking Density on the Swelling and Rheological Behavior of Ester-Bridged β -Cyclodextrin Nanosponges, *Materials(Basel)*, 14, **2021**, 478.
20. J. L. Lenhart, W. Wu, Influence of Cross-link Density on the Thermal Properties of Thin Polymer Network Films, *Langmuir*, 19, **2003**, 4863-4865.
21. F. C. Campbell, (Eds), Chapter 3, Thermoset Resins, *Manufacturing Processes for Advanced Composites*, Elsevier Science, **2004**, 63-101.
22. R. Schwalm, *UV Coatings, Basics, Recent Developments and New Applications*, Elsevier Science, **2007**.
23. W. A. Green, *Industrial Photoinitiators: A technical Guide*, CRC Press, **2010**.
24. K. H. Pfoertner, T. Oppenländer, *Photochemistry*, Wiley-VCH, Weinheim, in *Ullmann's Encyclopedia of Industrial Chemistry*, **2012**, 2-45.
25. C. Dietlin, S. Schweizer, P. Xiao, J. Zhang, F. M. Savary, B. Graff, J.P. Fouassier, J. Lalevée, *Polym. Chem.*, 6, **2015**, 3895-3912.
26. R. Podsiadly, K. Podemska, A. M. Szymczak, Novel visible photoinitiators systems for free-radical/cationic hybrid photopolymerization, *Dyes and Pigments*, 91, **2011**, 422-426.
27. C. Noè, S. Malburet, A. Bouvet-Marchand, A. Graillet, C. Loubat, M. Sangermano, Cationic photopolymerization of bio-renewable epoxidized monomers, *Prog. in Org. Coat.*, 133, **2019**, 131-138
28. Lalevée J., Mokbel H., Fouassier, Recent Developments of Versatile Photoinitiating Systems for Cationic Ring Opening Polymerization Operating at Any Wavelengths and under Low Light Intensity Sources, *Polymers*, 20, **2015**, 7201-7221

29. M. Sangermano, Multifunctional UV-Cured Epoxy Coatings, Radtech Report, 3, **2012**, 40-43.
30. Y. Yagci, I. Reetz, Externally stimulated initiator systems for cationic polymerization, Prog. Polym. Sci., 23, **1998**, 1485-1538
31. J.V. Crivello, R. Narayan, Epoxidized triglycerides as renewable monomers in photoinitiated cationic polymerization, Chem. Mater., 4, **1992**, 692-699.
32. S. Chakrapani, J.V. Crivello, Synthesis and Photoinitiated Cationic Polymerization of Epoxidized Castor Oil and Its Derivatives, J. Macrom. Sci., Pure Appl. Chem., A35, **1998**, 1-20.
33. J. Lalevée, M. A. Tehfe, D. Gigmes, J. P. Fouassier, On the Favorable Interaction of Metal Centered Radicals with Hydroperoxides for an Enhancement of the Photopolymerization Efficiency Under Air, Macromolecules, 43, **2010**, 6608-6615.
34. M. Chen, M. Zhong, J. A. Johnson, Light-Controlled Radical Polymerization: Mechanisms, Methods, and Applications, Chem Rev, 116, **2016**, 10167-10211.
35. J.P. Fouassier, J.F. Rabek (Eds.), Laser in Polymer Science and Technology: Applications, CRC Press, Boca Raton, FL, **1990**.
36. C.G. Roffey, Photopolymerization of Surface Coatings, Wiley, New York, **1982**.
37. J.P. Fouassier, Photoinitiation, Photopolymerization, Photocuring, Carl Hanser, Munich, **1995**.
38. J.P. Fouassier, J.F. Rabek (Eds.), Radiation Curing and Polymer Science and Technology, Chapman & Hall, Andover, **1993**.
39. J. W. Stansbury, C. N. Bowman, S. M. Newman, Shining a light on dental composite restoratives, Physics Today, 61, **2008**, 82-83.
40. K. Ikemura, T. Endo, A review of the development of radical photopolymerization initiators used for designing light-curing dental adhesives and resin composites, Dent. Mater. J., 29, **2010**, 481-501.
41. F. A. Rueggeberg, State-of-the-art: Dental photocuring - A review, Dental Materials, 27, **2011**, 39-52.
42. J.P. Fouassier, J. Lalevée, Photoinitiators for Polymer Synthesis Scope, Reactivity, and Efficiency, Wiley-VCH Verlag GmbH & Co. KGaA, Weinheim, **2012**, 21-34.
43. B. Christmas, R. Kemmerer, F. Kosnik, UV/EB Curing Technology: A Short History. In: Seymour R.B., Kirshenbaum G.S. (Eds) High Performance Polymers: Their Origin and Development. Springer, Dordrecht, **1986**.
44. W. Tomal, J. Ortyl, Water Soluble Photoinitiators in Biomedical Applications, Polymers, 12, **2020**, 1073.

-
45. J.-P. Fouassier, X. Allonas, D. Burget, Photopolymerization Reaction under Visible Lights: Principle, Mechanism and Examples of Applications, *Progress in Organic Coatings*, 47, **2003**, 16-36.
46. B. Jędrzejewska, B. Ośmiałowski, Difluoroboranyl derivatives as efficient panchromatic photoinitiators in radical polymerization reactions, *Polym. Bull.*, 75, **2018**, 3267-3281.
47. Y. Yagci, S. Jockusch, N. J. Turro, Photoinitiated Polymerization: Advances, Challenges, and Opportunities, *Macromolecules*, 43, **2010**, 6245-6260.
48. Y. M. Huang, C. P. Jiang, Curl distortion analysis during photopolymerization of stereolithography using dynamic finite element method, *International Journal of Advanced Manufacturing Technology* 21, **2003**, 586-595.
49. Y. M. Huang, C. P. Jiang, Numerical analysis of a mask type stereolithography process using a dynamic finite-element method, *International Journal of Advanced Manufacturing Technology* 21, **2003**, 649-655.
50. G. Bugeđa, M. Cervera, G. Lombera, E. Onate, Numerical analysis of stereolithography processes using the finite element method, *Rapid Prototyping Journal*, 1, **1995**, 13-23.
51. M. T. Carver, U. Dreyer, R. Knoesel, F. Candau, R. M. Fitch, Kinetics of Photopolymerization of Acrylamide in Aot Reverse Micelles, *Journal of Polymer Science Part a-Polymer Chemistry*, 27, **1989**, 2161-2177.
52. J. Ma, X. Mu, C. N. Bowman, Y. Sun, M. L. Dunn, H. J. Qi, D. A. Fang, Photoviscoplastic model for photoactivated covalent adaptive networks, *Journal of the Mechanics and Physics of Solids*, 70, **2014**, 84-103.
53. T. Scherzer, U. Decker, Real-time FTIR-ATR spectroscopy to study the kinetics of ultrafast photopolymerization reactions induced by monochromatic UV light, *Vibrational Spectroscopy*, 19, **1999**, 385-398.
54. Z. Zhao, X. Mu, N. Sowan, Y. Pei, C. N. Bowman, Q. H. Jerry, D. Fang, Effects of oxygen on light activation in covalent adaptable network polymers, *Soft Matter* 11, **2015**, 6134-6144.
55. K. Kambly, Characterization of curing kinetics and polymerization shrinkage in ceramic-loaded photocurable resins for large area maskless photopolymerization (LAMP) M.S. thesis, Georgia Institute of Technology, **2009**.
56. G. Odian, *Principles of Polymerization*. 4 ed., John Wiley & Sons: Hoboken, New Jersey, **2004**.
57. C. E. Hoyle, A. B. Lowe, C. N. Bowmann, Thiol-click chemistry: a multifaceted toolbox for small molecule and polymer synthesis, *Chem. Soc. Rev.*, 39, **2010**, 1355.

58. G. Dossi, G. Storti, D. Moscatelli, Initiation Kinetic in Free-Radical Polymerization: Prediction of Thermodynamic and Kinetic Parameters Based on ab initio Calculations, *Macromol. Theory Simul*, 19, **2010**, 170-178.
59. N. S. Kenning, B. A. Ficek, C. C. Hoppe, A. B. Scranton, Spatial and temporal evolution of the photoinitiation rate for thick polymer systems illuminated by polychromatic light: selection of efficient photoinitiators for LED or mercury lamps, *Polymer International*, 57, **2008**, 1134-1140.
60. F. A. Rueggeberg, M. Giannini, C. A. G. Arrais, R. B. T. Price, Light Curing in Dentistry and Clinical Implications: A Literature Review, *Brazilian Oral Research*, 31, **2017**.
61. D. Neshchadin, A. Rosspeinter, M. Griesser, B. Lang, S. Mosquera-Vazquez, E. Vauthey, V. Gorelik, R. Liska, C. Hametner, B. Ganster, R. Saf, N. Moszner, G. Gescheidt, Acylgermanes: Photoinitiators and Sources for Ge-centered Radicals. Insights into Their Reactivity, *J. Am. Chem. Soc.*, 135, **2013**, 17314-17321.
62. N. Moszner, U. K. Fischer, B. Ganster, R. Liska, V. Rheinberger, Benzoylgermanium Derivatives as Novel Visible-Light Photoinitiators for Dental Materials, *Dent. Mater.*, 24, **2008**, 901-907.
63. M. Bouzrati-Zerelli, J. Kirschner, C. P. Fik, M. Maier, C. Dietlin, F. Morlet-Savary, J. P. Fouassier, J. M. Becht, J. E. Klee, J. Lalevée, Silyl Glyoxylates as a New Class of High Performance Photoinitiators: Blue LED Induced Polymerization of Methacrylates in Thin and Thick Films, *Macromolecules*, 50, **2017**, 6911-692.
64. B. Sanay, B. Strehmel, V. Strehmel, Green Approach of Photoinitiated Polymerization Using Monomers Derived from Oleic Acid and Ionic Liquid, *ChemistrySelect*, 4, **2019**, 10214-10218.
65. J.P. Fouassier, J. Lalevée, Production of Interpenetrating Polymer Networks; Simultaneous Initiation of Radical and Cationic Polymerization Reactions, *Polymers*, 6, **2014**, 2588-2610.
66. N. Arsu, M. Aydin, Y. Yagci, S. Jockusch, N. Turro, One component thioxanthone based Type II photoinitiators, *Photochemistry and UV Curing: New Trends*, 1, **2006**, 17-29.
67. D., Dendukuri, P. Panda, R. Haghgooie, J. M. Kim, T. A. Hatton, P. S. Doyle, Modeling of Oxygen-Inhibited Free Radical Photopolymerization in a PDMS Microfluidic Device, *Macromolecules*, 41, **2008**, 8547-8556.
68. S. Yoshida, Y. Takahata, S. Horiuchi, H. Kurata, M. Yamamoto, Numerical Model of Radical Photopolymerization Based on Interdiffusion, *International Journal of Polymer Science, New York Vol.*, **2014**, 1-8.

-
69. J. Krstina, G. Moad, E. Rizzardo, C. L. Winzor, C. T. Berge, M. Fryd, Narrow polydispersity block copolymers by free-radical polymerization in the presence of macromonomers, *Macromolecules*, **28**, **1995**, 5381-5385.
70. Y. Nakamura, S. Yamago, Termination Mechanism in the Radical Polymerization of Methyl Methacrylate and Styrene Determined by the Reaction of Structurally Well-Defined End Radicals, *Macromolecules*, **48**, **2015**, 6450-6456.
71. C. Decker, Kinetic Study and New Applications of UV Radiation Curing, *Macromolecular Rapid Communications*, **23**, **2002**, 1067-1093
72. L. Gou, B. Opheim, A. B. Scranton, Methods to overcome oxygen inhibition in free radical photopolymerizations, in: J.P. Fouassier (Ed.), *Photochemistry and UV Curing: New Trends*, Research Signpost, **2006**, 301-310.
73. J. G. Qin, W. P. Guo, Z. Zhang, Modeling of the bulk free radical polymerization up to high conversion - three stage polymerization model. II. Number-average molecular weight and apparent initiator efficiency, *Polymer*, **43**, **2002**, 4859-4867.
74. Y. Zhen, L. Bogeng, C. Kun, H. Yuan, P. Zu-ren, Modeling for the diffusion limitation of free radical polymerization, *Journal of Zhejiang University- SCIENCE A*, **1**, **2000**, 148-156.
75. M. R. Gleeson, J. T. Sheridan, Nonlocal photopolymerization kinetics including multiple termination mechanisms and dark reactions, Part I. Modeling. *J. Opt. Soc. Am. B.*, **26**, **2009**, 1736-1745.
76. B. O'Shaughnessy, J. Yu, Autoacceleration in free radical polymerization, *Phys. Rev. Lett.*, **73**, **1994**, 1723-1726.
77. K.D. Belfied, J.V. Crivello, *Photoinitiated Polymerization*, Eds., ACS Symposium Series 847; ACS: Washington, DC, USA, **2003**.
78. S. Davidson, *Exploring the Science, Technology and Application of UV and EB Curing*; Sita Technology Ltd: London, UK, **1999**.
79. Neckers D.C., Jager W., *UV and EB at the Millenium*, Sita Technology, London, UK: **1999**.
80. S.P. Pappas, *UV-Curing: Science and Technology*, Plenum Press; New York, NY, USA: 1992, Tech. Mark. Corp. Stamford, **1986**.
81. A.B. Scranton, A. Bowman, R.W Peiffer, *Photopolymerization: Fundamentals and Applications*;., Eds.; ACS Symposium Series 673, ACS: Washington, DC, USA, **1997**.
82. K. Olldring, R. Holman, *Chemistry & Technology of UV & EB Formulation for Coatings, Inks and Paints*;., Eds.; Wiley and Sita: London, UK, Volume I-VIII, **1997**.

83. J.G. Drobny, Radiation Technology for Polymers; CRC Press: Boca Raton, FL, USA, **2003**.
84. C.G. Roffey, Photogeneration of Reactive Species for UV Curing; Wiley: New York, NY, USA, **1997**.
85. S. I. Schlesinger, Photopolymerization of Epoxides, Photographic Science and Engineering, 18, **1974**, 387-393.
86. J.V. Crivello, J.H.W. Lam, Diaryliodonium Salts. A New Class of Photoinitiators for Cationic Polymerization, Macromolecules, 10, **1977**, 1307-1316.
87. M. Sangermano, I. Roppolo, A. Chiappone, New Horizons in Cationic Polymerization, Polymers, **2018**, 10, 136.
88. J.V. Crivello, J.H.W. Lam, Photoinitiated cationic polymerization with triarylsulfonium salts, J. Polym. Sci. Part A Polym. Chem., 17, **1979**, 977-999.
89. J.V. Crivello, J. Ma, F. Jiang, Synthesis and photoactivity of novel 5-arylthianthrenium salt cationic photoinitiators, J. Polym. Sci. Part A Polym. Chem., 40, **2002**, 3465-3480.
90. J.V. Crivello, The discovery and development of onium salt cationic photoinitiators, J. Polym. Sci. Part A Polym. Chem., 37, **1999**, 4241-4254.
91. M. Sangermano, N. Razza, J.V. Crivello, Cationic UV-curing: Technology and applications, Macromol. Mater. Eng., 299, **2014**, 775-793.
92. M. Tasdelen, Y. Yagci, Aust. J. Chem., Photochemical Methods for the Preparation of Complex Linear and Cross-linked Macromolecular Structures, 64, **2011**, 982-991.
93. A. Hartwig, Influence of moisture present during polymerization on the properties of a photocured epoxy resin, International Journal of Adhesion and Adhesives, 22, **2002**, 409-414.
94. K. Brzezinska, R. Szymanski, P. Kubisa, S. Penczek, Activated monomer mechanism in cationic polymerization. I: Ethylene oxide, formulation of mechanism, Die Makromolekulare Chemie Rapid Communications, 7, **1986**, 1-4.
95. C. Decker, Photoinitiated Crosslinking Polymerization, Progress in Polymer Science 21, **1996**, 593-650.
96. J.V. Crivello, In Photoinitiators for Free-Radical Cationic and Anionic Photopolymerization, G. Bradley (Ed.), John Wiley, New York, **1998**.
97. V. Sipani, A. B. Scranton, Dark-cure studies of cationic photopolymerizations of epoxides: Characterization of the active center life time and kinetic rate constants, Journal of Polymer Science Part A: Polymer Chemistry, 41, **2003**, 2064-2072.

-
98. V. Sipani, A. Kirsch, Scranton, Dark cure studies of cationic photopolymerizations of epoxides: Characterization of kinetic rate constants at high conversions, *Journal of Polymer Science Part A: Polymer Chemistry*, 42, **2004**, 4409-4416.
99. J. V. Crivello, *Nuclear Instruments and Methods in Physics Research Section B: Beam Interactions with Materials and Atoms*, 151, **1999**, 8-21.
100. J. P. Fouassier, D. Burr, J.V. Crivello, Photochemistry and photopolymerization activity of diaryliodonium salts, *J. Macromol. Sci. Pure Appl. Chem.*, A31, **1994**, 677-701.
101. Y. Yagci, A. Kornowski, W. Schnabel, *N*-alkoxy-pyridinium and *N*-alkoxy-quinolinium salts as initiators for cationic photopolymerizations, *J. Polym. Sci. Part A Polym. Chem.*, 30, **1992**, 1987-1991.
102. Y. Yagci, T. Endo, *N*-benzyl and *N*-alkoxy pyridinium salts as thermal and photochemical initiators for cationic polymerization, *Adv. Polym. Sci.*, 127, **1997**, 59-86.
103. Y. Yagci, Photoinitiated cationic polymerization of unconventional monomers, *Macromol. Symp.*, 240, **2006**, 93-101.
104. M. Degirmenci, A. Onen, Y. Yagci, Photoinitiation of cationic polymerization by visible light activated titanocene in the presence of onium salt, *Polymer Bulletin*, 46, **2001**, 443-449.
105. M. A. Tasdelen, J. Lalevée, Y. Yagci, Photoinduced Free Radical Promoted Cationic Polymerization after 40 Years of the Discovery, *Polym. Chem.*, 11, **2020**, 1111-1121.
106. W.D. Cook, S. Chen, F. Chen, M.U. Khreci, Y. Yagci, Photopolymerization of vinyl ether networks using an iodonium initiator. The role of photosensitizers, *J. Polym. Sci. Part A Polym. Chem.*, 47, **2009**, 5474-5487.
107. N. Klikovits, P. Knaack, D. Bomze, I. Krossing, R. Liska, Novel photoacid generators for cationic photopolymerization, *Polym. Chem.*, 8, **2017**, 4414-4421.
108. A. Kocaarslan, C. Kütahya, D. Keil, Y. Yagci, B. Strehmel, Near-IR and UV-LED Sensitized Photopolymerization with Onium Salts Comprising Anions of Different Nucleophilicities, *ChemPhotoChem*, 3, **2019**, 1127-1132.
109. J. V. Crivello, *Radiation Physics and Chemistry*, 63, **2002**, 21-27.
110. E. Andrzejewska, Photopolymerization kinetics of multifunctional monomers, *Progress in Polymer Science*, 26, **2001**, 605-665.
111. J. S. Young, C. N. Bowman, Effect of polymerization temperature and cross-linker concentration on reaction diffusion controlled termination, *Macromolecules*, 32, **1999**, 6073±81.
112. B. Sanay, B. Strehmel, V. Strehmel, Photoinitiated polymerization of methacrylates comprising phenyl moieties, *Journal of Polymer Science*, 58, **2020**, 1-13.

- 113.B. Sanay, B. Strehmel, V. Strehmel, Manufacturing and Photocrosslinking of a New Bio-based Dimethacrylate for Application in Water-Repellent Coating, *Applied Research*, **2021** (submitted).
- 114.B. Sanay, B. Strehmel, V. Strehmel, Formation of Highly Crosslinked Polymer Films in the Presence of Bio-based Epoxy by Photoinitiated Cationic Polymerization, *Prog. Org. Coat.*, **158**, **2021**, 106377.
- 115.T. Brömme, D. Oprych, J. Horst, P. S. Pinto, B. Strehmel, New iodonium salts in NIR sensitized radical photopolymerization of multifunctional monomers, *RSC Advances*, **5**, **2015**, 69915-69924.
- 116.C. Schmitz, A. Halbhuber, D. Keil, B. Strehmel, NIR-sensitized photoinitiated radical polymerization and proton generation with cyanines and LED arrays, *Prog. Org. Coat.*, **100**, **2016**, 32-46.
- 117.H. J. Timpe, B. Strehmel, Lichtinduzierte polymer-und polymerisationsreaktionen, **44**. Zur kinetik der radikalischen photopolymerisation mehrfunktioneller acrylate in polymeren bindemitteln, *Makromol. Chem.*, **192**, **1991**, 779-791.
- 118.H. J. Timpe, B. Strehmel, F. H. Roch, K. Fritzsche, Lichtinduzierte polymer und polymerisationsreaktionen, *Acta Polym.*, **38**, **1987**, 238-244.
- 119.B. Golaz, V. Michaud, J.-A.E. Månson, Photo-polymerized epoxy primer for adhesion improvement at thermoplastics/metallic wires interfaces *Composites: Part A*, **48**, **2013**, 171-180.
- 120.V. Strehmel, S. Berdzinski, L. Ehrentraut, C. Faßbender, J. Horst, E. Leeb, J. Liepert, M.-P. Ruby, V. Senkowski, P. Straßburg, A. Wenda, C. Strehmel, Application of ionic liquids in synthesis of polymeric binders for coatings, *Prog. Org. Coat.*, **89**, **2015**, 297-313.
- 121.D. Swern, H. B. Knight, J. T. Scanlan, W. C. Ault, *Oil & Soap*, Fractionation of tallow fatty acids. Preparation of purified oleic acid and an inedible olive oil substitute, **1945**, 302-304.
- 122.S. Berdzinski, B. Strehmel, V. Strehmel, Photogenerated lophyl radicals in 1-alkyl-3-vinylimidazolium bis(trifluoromethylsulfonyl)imides, *Photochem. Photobiol. Sci.*, **14**, **2015**, 714-725.
- 123.R. M. Joshi, Heats of polymeric reactions. Part I. Construction of the calorimeter and measurements on some new monomers, *J. Polym. Sci.*, **56**, **1962**, 313-338.
- 124.J. N. Cardenas, K. F. O'Driscoll, High-conversion polymerization. I. Theory and application to methyl methacrylate, *J. Polym. Sci. Polym. Chem. Ed.*, **14**, **1976**, 883.

-
- 125.M. Stickler, D. Panke, A. E. Hamielec, Free-radical polymerization kinetics of methyl methacrylate at very high conversions, *J. Polym. Sci. Polym. Chem. Ed.*, **22**, **1984**, 2243.
- 126.E. Abuin, E. A. Lissi, Methyl Methacrylate Polymerization at High Conversion. II. Factors Determining the Onset of the Gel Effect, *J. Macromol. Sci. Chem. A*, **11**, **1977**, 287.
- 127.V. Strehmel, D. Strunk, M. Heinz, S. Walther, A Green Step to New Monomers and Their Polymerization, *ChemistrySelect*, **5**, **2020**, 12109.
- 128.R. Anastasio, W. Peerbooms, R. Cardinaels, LCA van Breemen, Characterization of Ultraviolet-Cured Methacrylate Networks: From Photopolymerization to Ultimate Mechanical Properties, *Macromolecules*, **52**, **2019**, 9220-9231.
- 129.E. Mark, *Physical Properties of Polymers Handbook*, AIP Press, Woodbury, New York **1996**.
- 130.P. K. Shah, J. W. Stansbury, C. N. Bowman, Application of an Addition-Fragmentation-Chain Transfer Monomer in Di(meth)acrylate Network Formation to Reduce Polymerization Shrinkage Stress, *Polym Chem.*, **8**, **2017**, 4339-4351
- 131.M. Krzeminski, M. Molinari, M. Troyon, X. Coqueret, Characterization by Atomic Force Microscopy of the Nanoheterogeneities Produced by the Radiation-Induced Cross-Linking Polymerization of Aromatic Diacrylates, *Macromolecules*, **43**, **2010**, 8121-8127.
- 132.J. Park, J. Eslick, Q. Ye, A. Misra, P. Spencer, The influence of chemical structure on the properties in methacrylate-based dentin adhesives, *Dent Mater.*, **27**, **2011**, 1086-1093.
- 133.K. Hodd, *Epoxy Resins*, *Comprehensive Polymer Science and Supplements*, 1st ed., G. Allen, J. C. Bevington (Eds), Oxford, **5**, **1989**, 667-699.
134. G. Gibson, Chapter 27: Epoxy Resins, *Brydson's Plastic Materials*, 8th ed., M. Gilbert (Ed), Elsevier, Oxford, **2017**, 773-797.
- 135.T. Vidil, F. Tournilhac, S. Musso, A. Robisson, L. Leiblera, Control of reactions and network structures of epoxy thermosets, *Prog. Polym. Sci.*, **62**, **2016**, 126-179.
- 136.Z. Liu, S. Z. Eran, Ring-Opening Polymerization of Epoxidized Soybean Oil, *J Am Oil Chem Soc*, **87**, **2010**, 437-444.
- 137.Z. S. Petrovi, Polyurethanes from Vegetable Oils, *Polymer Reviews*, **48**, **2008**, 109-155.
- 138.R. Wang, T. P. Schuman, Vegetable oil-derived epoxy monomers and polymer blends: A comparative study with review, *eXPRESS Polymer Letters*, **7**, **2013**, 272-292.

- 139.R. T. Olsson, H. E. Bair, V. Kuck, A. Hale, Thermomechanical Studies of Photoinitiated Cationic Polymerization of a Cycloaliphatic Epoxy Resin, In Photoinitiated Polymerization, K. D. Belfield, J. V. Crivello (Eds.), ACS Symposium Series 847, **2003**, 317-329.
- 140.A. P. Gupta, S. Ahmad, A. Dev, Modification of Novel Bio-Based Resin-Epoxidized Soybean Oil by Conventional Epoxy Resin, Polym. Eng. Sci., 51, **2011**, 1087-1091.
- 141.P. Niedermann, G. Szebènyi, A. Toldy, Effect of Epoxidized Soybean Oil on Curing, Rheological, Mechanical and Thermal Properties of Aromatic and Aliphatic Epoxy Resins, J. Polym. Environ., 22, **2014**, 525-536.
- 142.S. K. Sahoo, S. Mohanty, S. K. Nayak, Synthesis and Characterization of Bio-based epoxy Blends from Renewable Resource Based Epoxidized Soybean Oil as Reactive Diluent, Chinese J. Polym. Sci., 33, **2015**, 137-153.
- 143.S. Kumar, S. K. Samal, S. Mohanty, S. K. Nayak, Epoxidized Soybean Oil-Based Epoxy Blend Cured with Anhydride-Based Cross-Linker: Thermal and Mechanical Characterization, Ind. Eng. Chem., 56, **2017**, 687-698.
- 144.S. Kumar, S. K. Samal, S. Mohanty, S. K. Nayak, Curing kinetics of bio-based epoxy resin-toughened DGEBA epoxy resin blend, J. Thermal Analysis and Calorimetry, 137, **2019**, 1567-1578.
- 145.P. Hidalgo, S. Álvarez, R. Hunter, A. Sánchez, Epoxidation of Fatty Acid Methyl Esters Derived from Algae Biomass to Develop Sustainable Bio-Based Epoxy Resins, Polymers, 12, **2020**, 2313.
- 146.A.X.H. Yong, G.D. Sims, S.J.P. Gnaniah, S.L. Ogin, P.A. Smith, Heating rate effects on thermal analysis measurement of T_g in composite materials, Adv. Manufacturing Polym. Composite Sci., 3, **2017**, 43-51.
- 147.J. G Williams, The Beta Relaxation in Epoxy Resin-Based Networks, J. Appl. Polym. Sci., 23, **1979**, 3433-3444.
- 148.M. M. Charlesworth, Effect of Crosslink Density on the Molecular Relaxations in Diepoxide-Diamine Network Polymers, Part 1. The Glassy Region, Polym. Eng. Sci., 28, **1988**, 221-229.
- 149.F. Román, P. Colomer, Y. Calventus, J.M. Hutchinson, Study of Hyperbranched Poly(ethyleneimide) Polymers of Different Molecular Weight and Their Interaction with Epoxy Resins, Materials, 11, **2018**, 410.
- 150.D. K. Owens, R. C. Wendt, Estimation of the Surface Free Energy of Polymers, J. Appl. Polym. Sci., 13, **1969**, 1741-1747.

-
151. Paints and varnishes – Wettability – Part 2: Determination of the free surface energy of solid surfaces by measuring the contact angle, DIN 55660-2: 2011-12.
152. T. S. Chung, W. Y. Chen, Y. Lin, K. P. Pramoda, Surface Free Energy of Ladderlike Polyepoxysiloxane-Diamine Reaction System, *J. Polym. Sci. B Polym. Phys.* 38, **2000** 1449-1460.
153. M. P. K. Turunen, T. Laurila, J. K. Kivilahti, evaluation of the Surface Free Energy of Spin-Coated Photodefinable Epoxy, *J. Polym. Sci. B Polym. Phys.* 40, **2002** 2137-2149.

This page contains personal information and has been removed from the document.

This page contains personal information and has been removed from the document.

Attachment

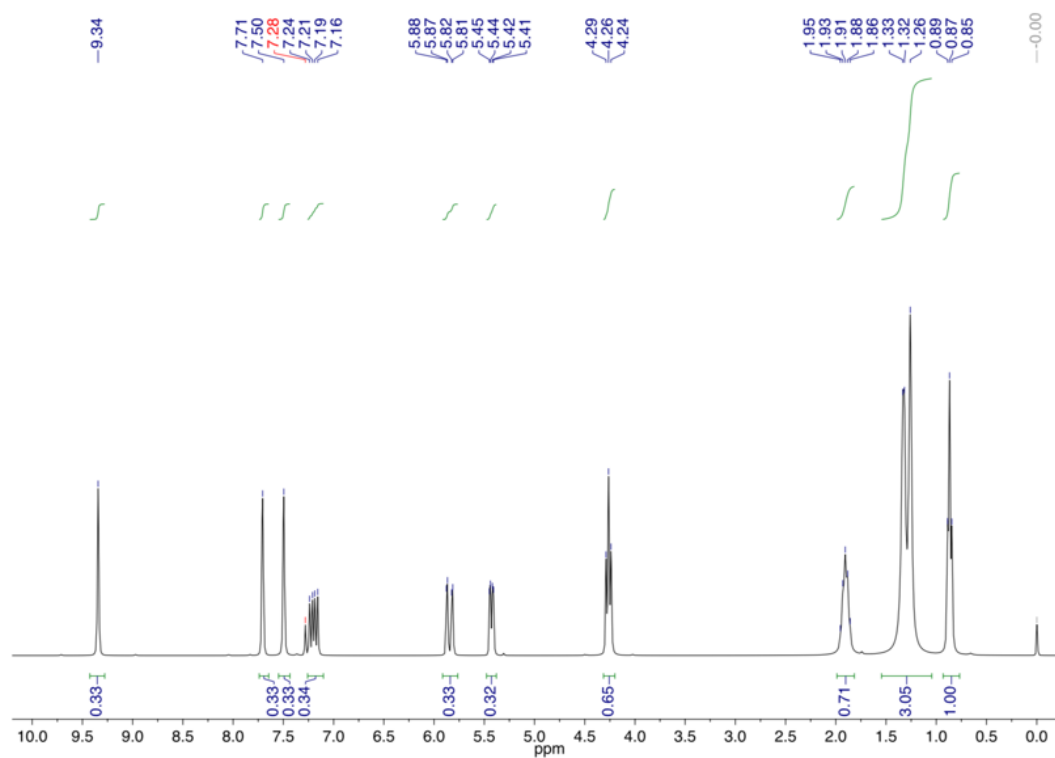


Figure S01: ¹H-NMR spectra of *N*-octyl-*N'*-vinylimidazolium NTf₂ (**1a**) taken at 300 MHz in CDCl₃.

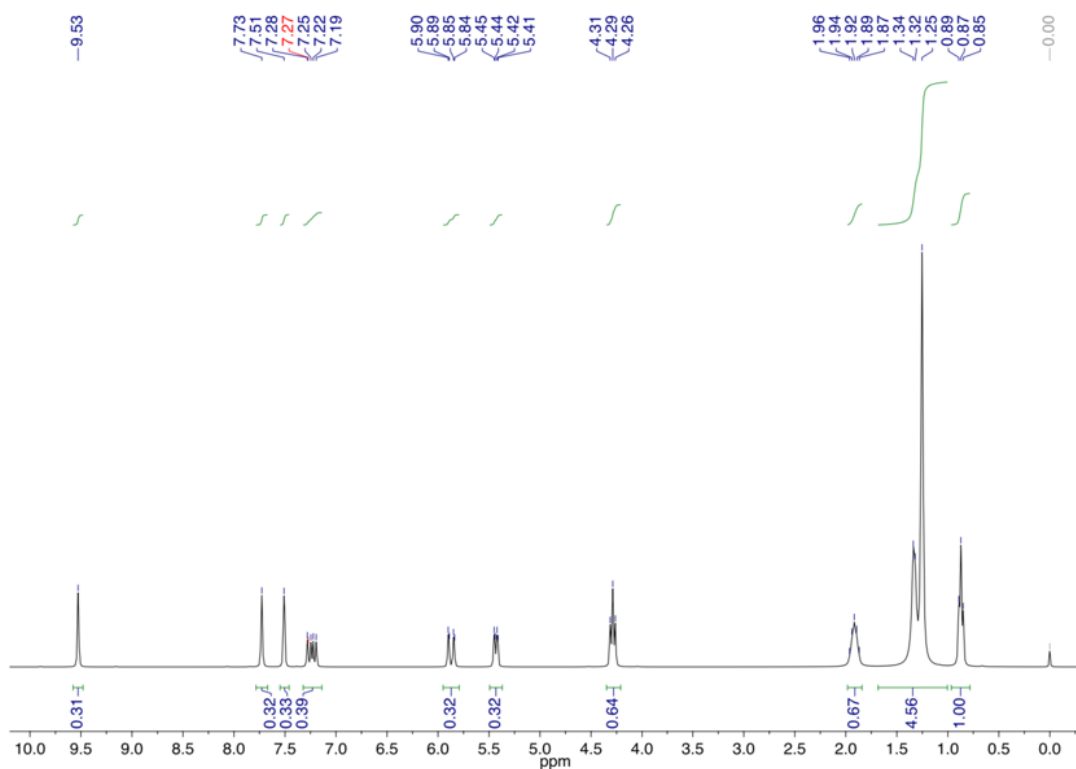


Figure S02: ¹H-NMR spectra of *N*-decyl-*N'*-vinylimidazolium NTf₂ (**1b**) taken at 300 MHz in CDCl₃.

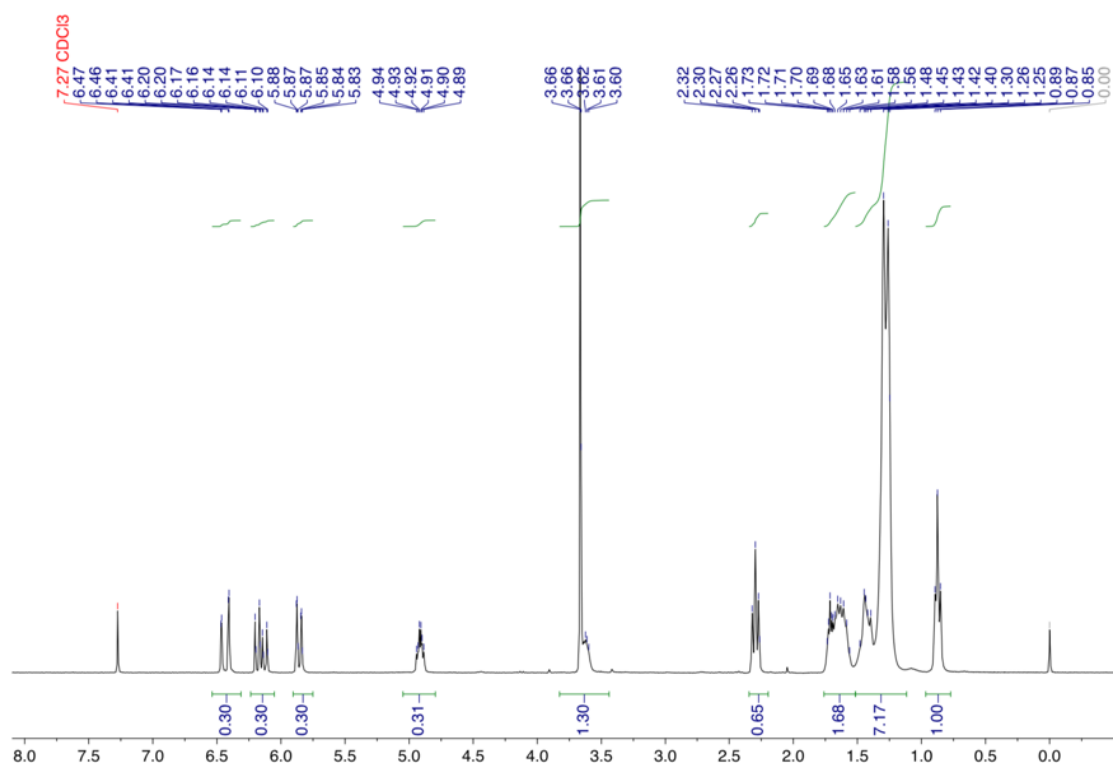


Figure S03: ¹H-NMR spectra of methyl 9-(acryloyloxy)-10-hydroxyoctadecanoate / methyl 9-hydroxy-10-(acryloyloxy)octadecanoate mix (**2**) taken at 300 MHz in CDCl₃.

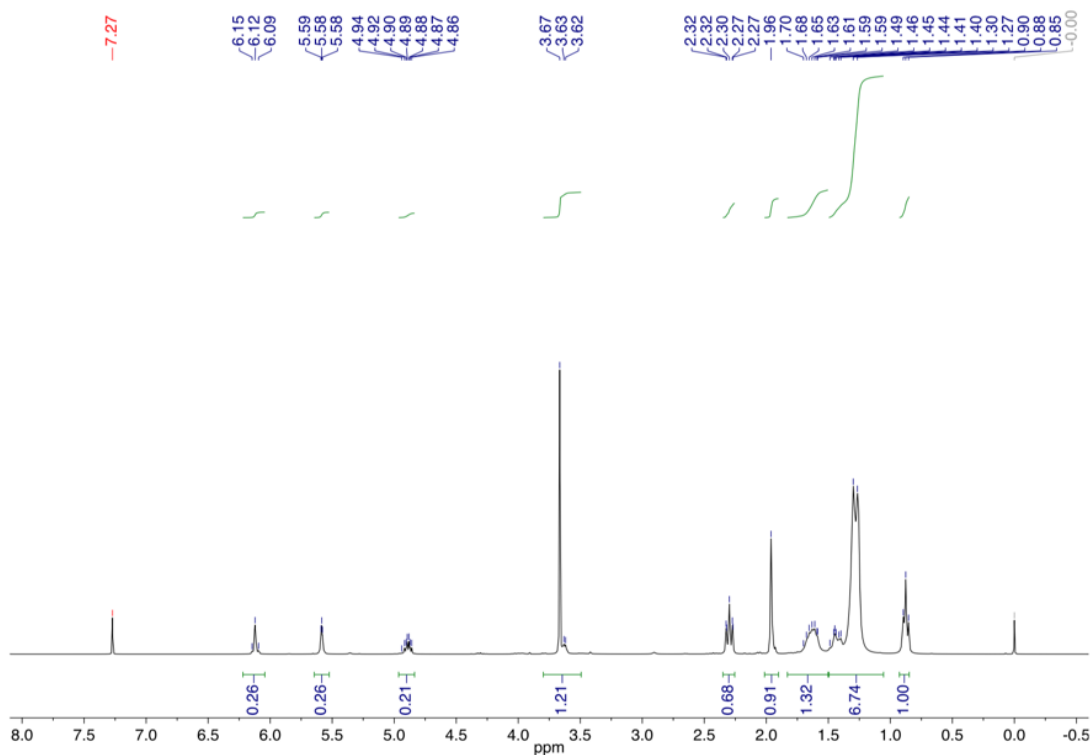


Figure S04: ¹H-NMR spectra of methyl 9-(methacryloyloxy)-10-hydroxyoctadecanoate / methyl 9-hydroxy-10-(methacryloyloxy)octadecanoate mix (**3**) taken at 300 MHz in CDCl₃.

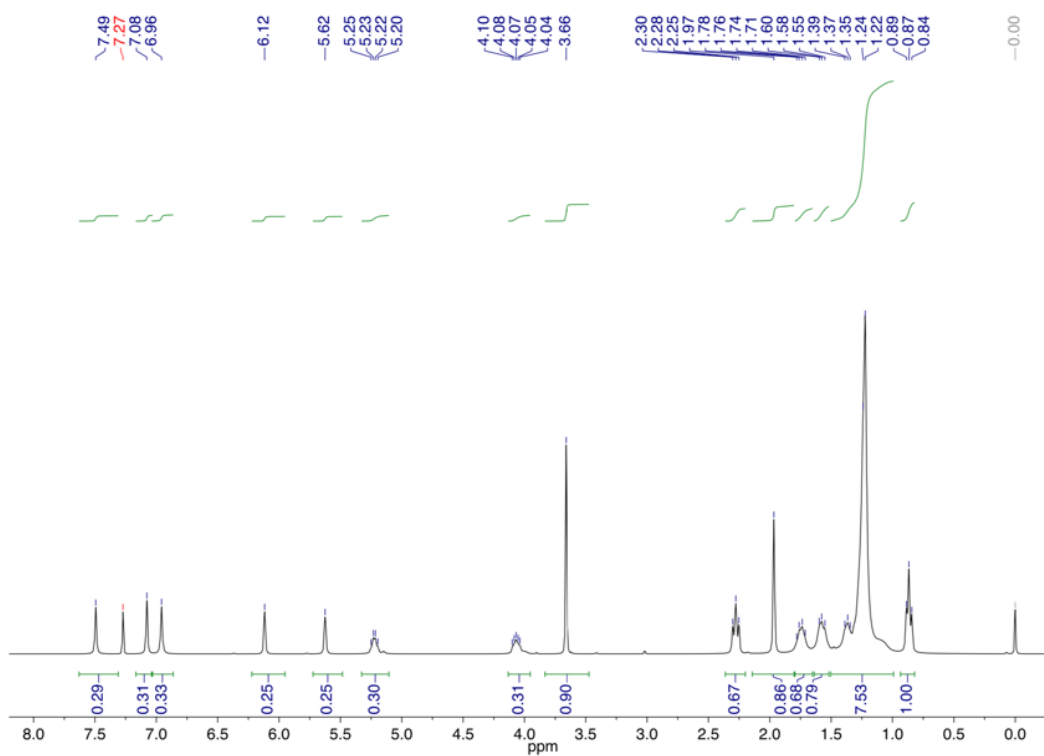


Figure S05: $^1\text{H-NMR}$ spectra of methyl 9-(1H-imidazol-1-yl)-10-(methacryloyloxy)octadecanoate / methyl 9-(methacryloyloxy)-10-(1H-imidazol-1-yl)octadecanoate mix (**4**) taken at 300 MHz in CDCl_3 .

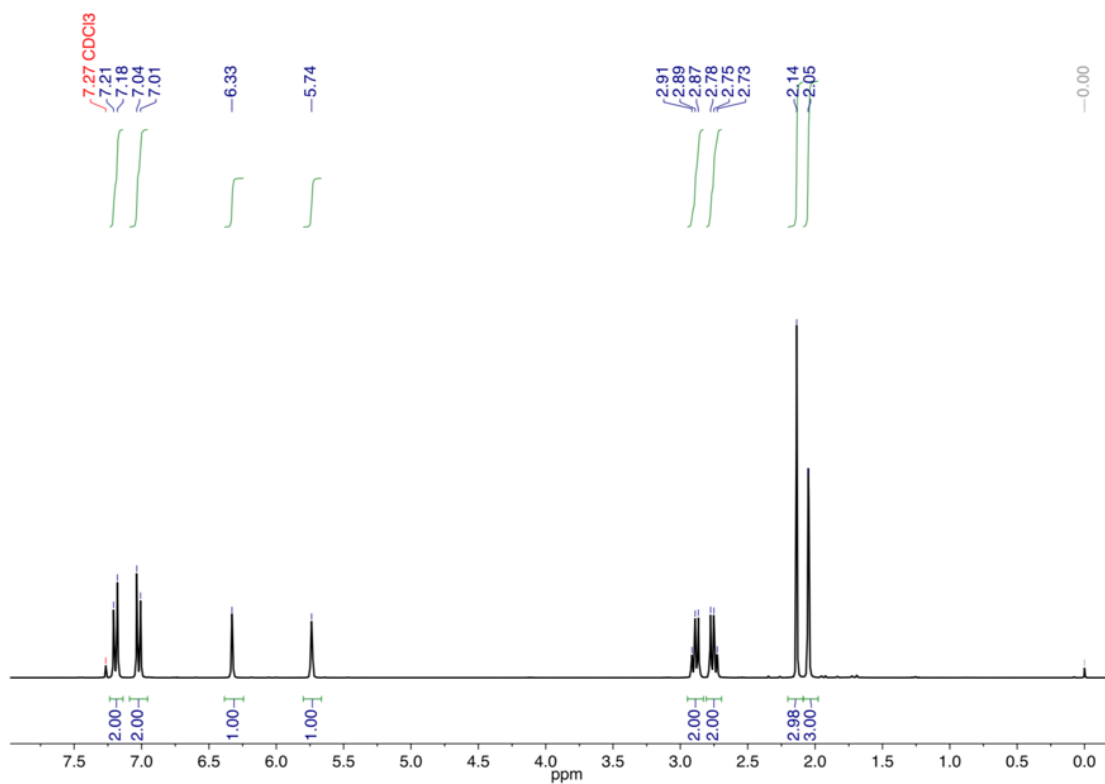


Figure S06: $^1\text{H-NMR}$ spectra of 4-(4-methacryloyloxyphenyl)-butan-2-one (**7**) taken at 300 MHz in CDCl_3 .

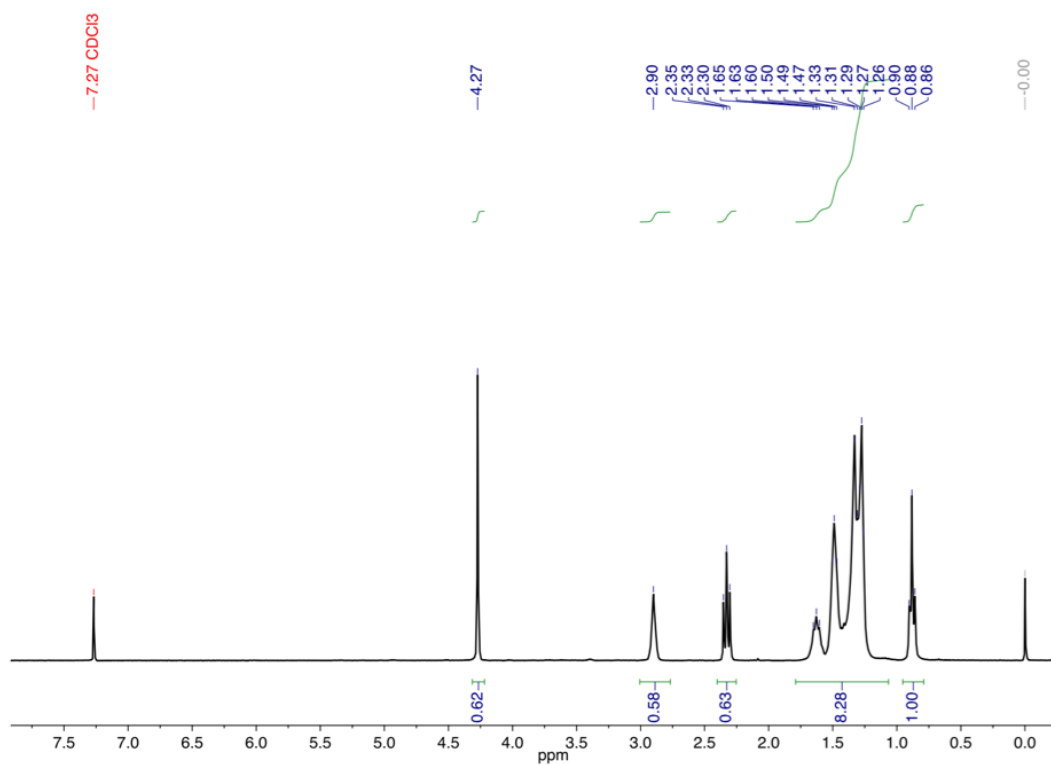


Figure S07-a): ¹H-NMR spectra of bis-(9,10-epoxystearic acid) 1,2-ethanediyl ester (**12**) taken at 300 MHz in CDCl₃.

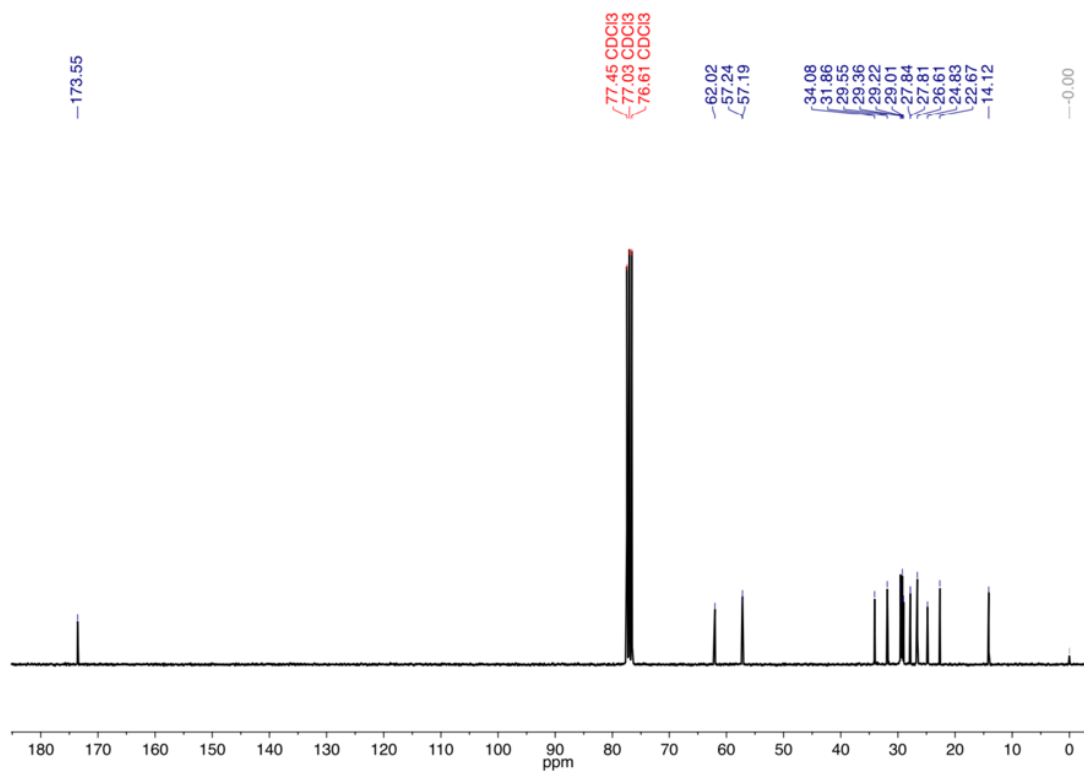


Figure S07-b): ¹³C-NMR spectra of bis-(9,10-epoxystearic acid) 1,2-ethanediyl ester (**12**) taken at 300 MHz in CDCl₃.

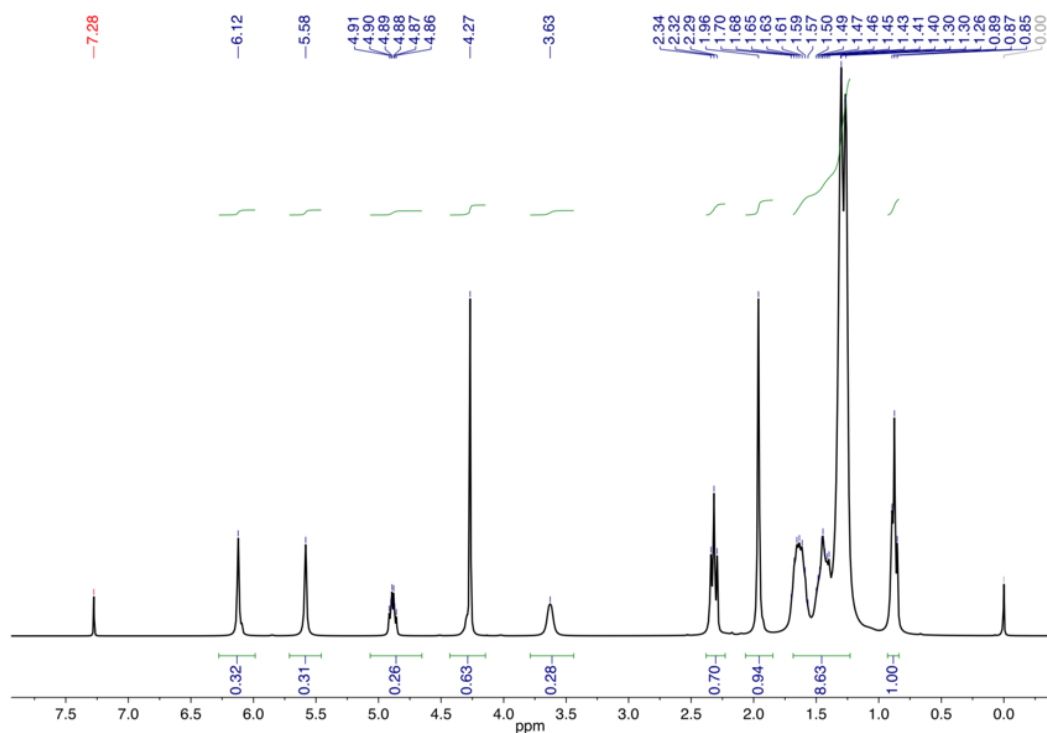


Figure S08-a): ^1H -NMR spectra of ethane-1,2-diyl bis(9-methacryloyloxy-10-hydroxy octadecanoate) / ethane-1,2-diyl 9-hydroxy-10-methacryloyloxy-9'-methacryloyloxy-10'-hydroxy octadecanoate / ethane-1,2-diyl bis(9-hydroxy-10-methacryloyloxy octadecanoate) (**10**) taken at 300 MHz in CDCl_3 .

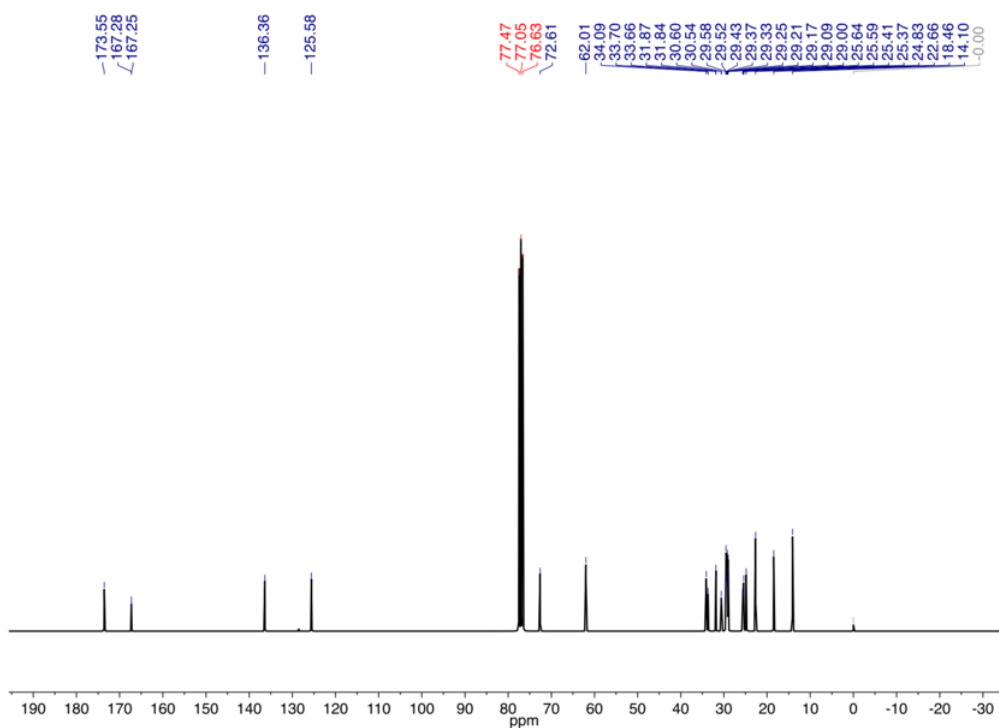


Figure S08-b): ^{13}C -NMR spectra of ethane-1,2-diyl bis(9-methacryloyloxy-10-hydroxy octadecanoate) / ethane-1,2-diyl 9-hydroxy-10-methacryloyloxy-9'-methacryloyloxy-10'-hydroxy octadecanoate / ethane-1,2-diyl bis(9-hydroxy-10-methacryloyloxy octadecanoate) (**10**) taken at 300 MHz in CDCl_3 .

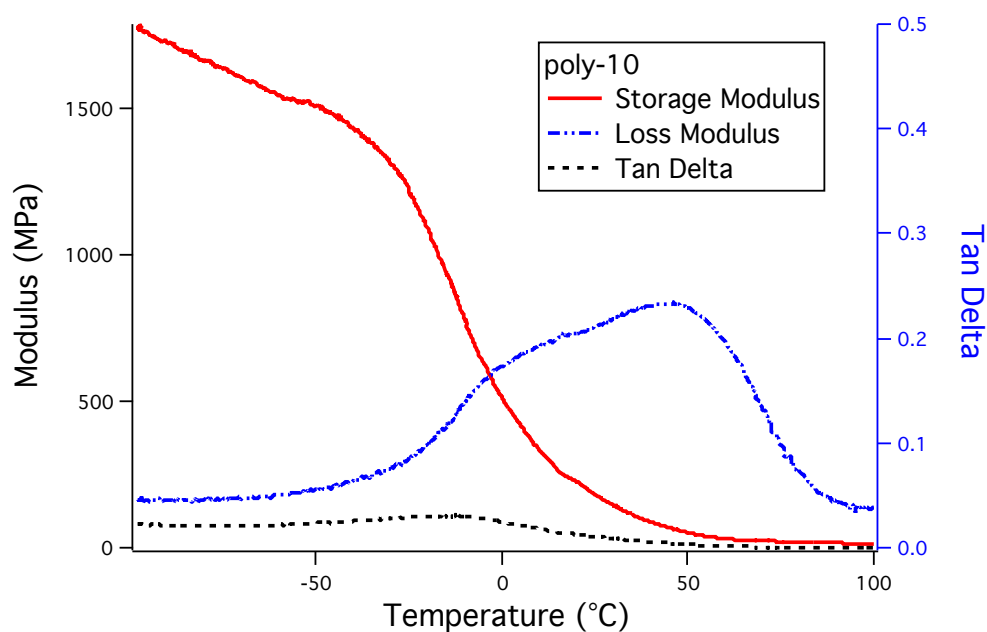


Figure S09: Storage modulus, loss modulus, and $\tan \delta$ obtained from DMA analysis of poly-**10** by photoinitiated polymerization from ethane-1,2-diyl bis(9-methacryloyloxy-10-hydroxy octadecanoate) / ethane-1,2-diyl 9-hydroxy-10-methacryloyloxy-9'-methacryloyloxy-10'-hydroxy octadecanoate / ethane-1,2-diyl bis(9-hydroxy-10-methacryloyloxy octadecanoate) (**10**) in the presence of 3 wt % Irgacure® TPO-L.

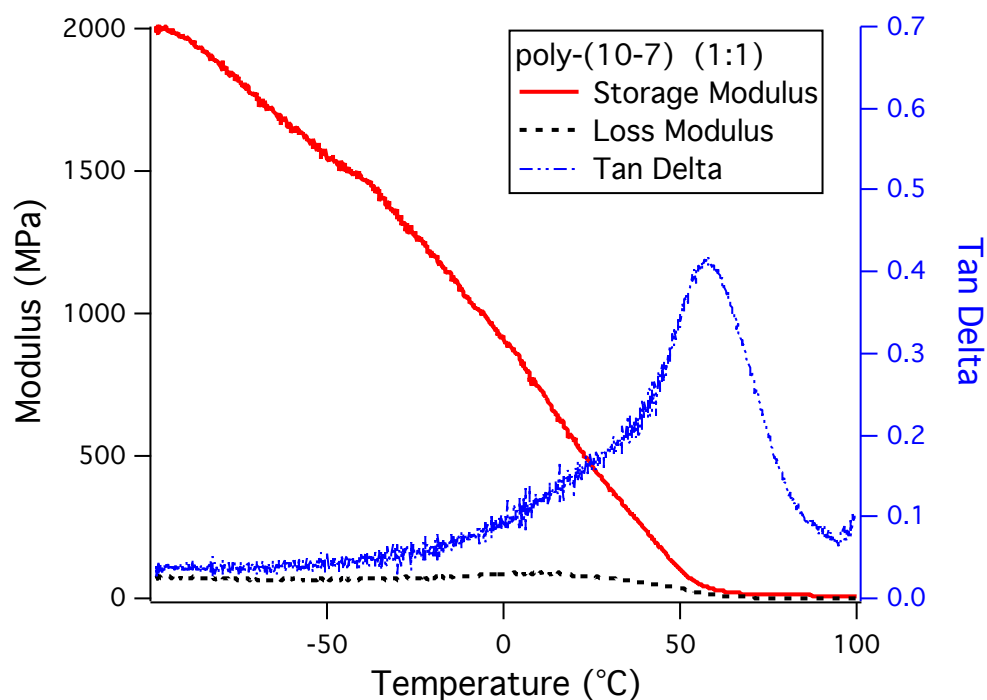


Figure S10: Storage modulus, loss modulus, and $\tan \delta$ obtained from DMA analysis of co-(**10-7**) by photoinitiated polymerization from a 1:1 mixture of ethane-1,2-diyl bis(9-methacryloyloxy-10-hydroxy octadecanoate) / ethane-1,2-diyl 9-hydroxy-10-methacryloyloxy-9'-methacryloyloxy-10'-hydroxy octadecanoate / ethane-1,2-diyl bis(9-hydroxy-10-methacryloyloxy octadecanoate) (**10**) and 4-(4-methacryloyloxyphenyl)-butan-2-one (**7**) in the presence of 3 wt % Irgacure® TPO-L.

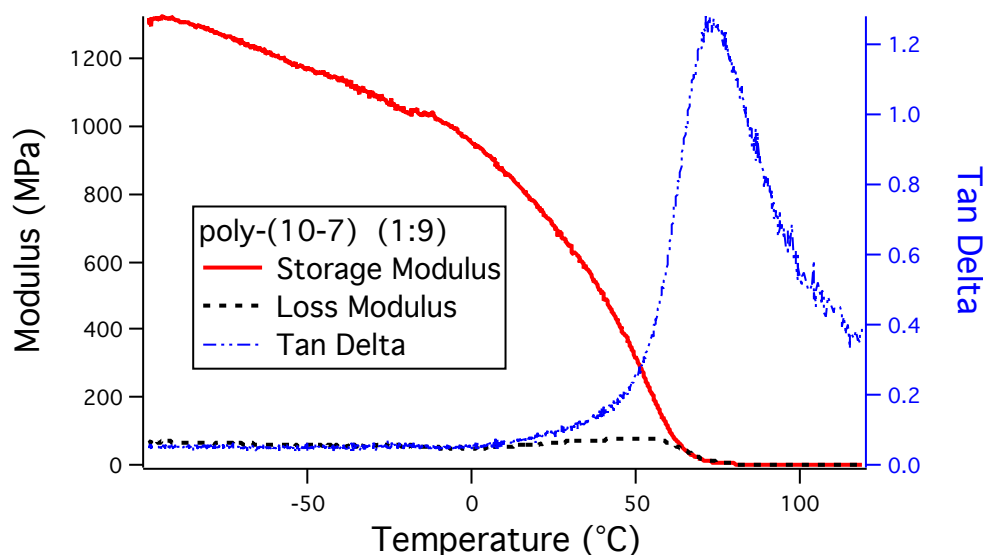


Figure S11: Storage modulus, loss modulus, and $\tan \delta$ obtained from DMA analysis of co-(**10-7**) by photoinitiated polymerization from a 1:9 mixture of ethane-1,2-diyl bis(9-methacryloyloxy-10-hydroxy octadecanoate) / ethane-1,2-diyl 9-hydroxy-10-methacryloyloxy-9'-methacryloyloxy-10'-hydroxy octadecanoate / ethane-1,2-diyl bis(9-hydroxy-10-methacryloyloxy octadecanoate) (**10**) and 4-(4-methacryloyloxyphenyl)-butan-2-one (**7**) in the presence of 3 wt % Irgacure® TPO-L.

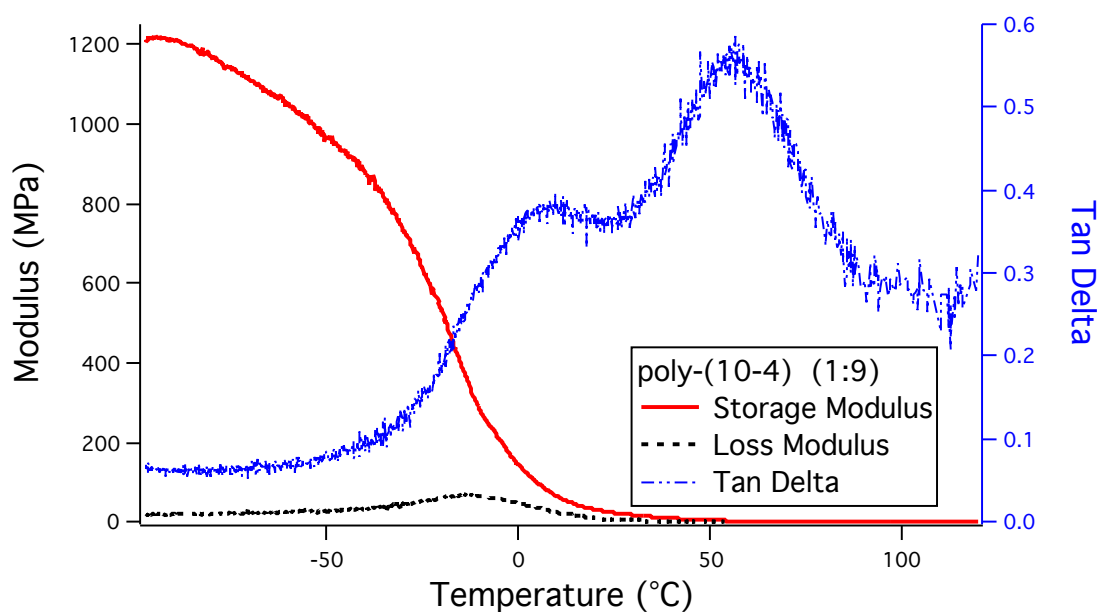


Figure S12: Storage modulus, loss modulus, and $\tan \delta$ obtained from DMA analysis of co-(**10-4**) by photoinitiated polymerization from a 1:9 mixture of ethane-1,2-diyl bis(9-methacryloyloxy-10-hydroxy octadecanoate) / ethane-1,2-diyl 9-hydroxy-10-methacryloyloxy-9'-methacryloyloxy-10'-hydroxy octadecanoate / ethane-1,2-diyl bis(9-hydroxy-10-methacryloyloxy octadecanoate) (**10**) and methyl 9-(1H-imidazol-1yl)-10-(methacryloyloxy)octadecanoate / methyl 9-(methacryloyloxy)-10-(1H-imidazol-1yl)octadecanoate (**4**) in the presence of 3 wt % Irgacure® TPO-L.

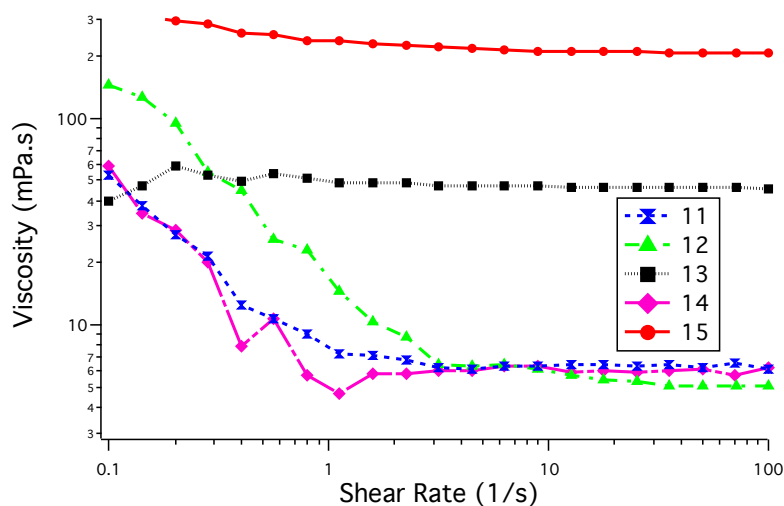


Figure S13: Viscosity of the monomers (**11**, **12**, **13**, **14** and **15**) measured at 60°C as function of shear rate.

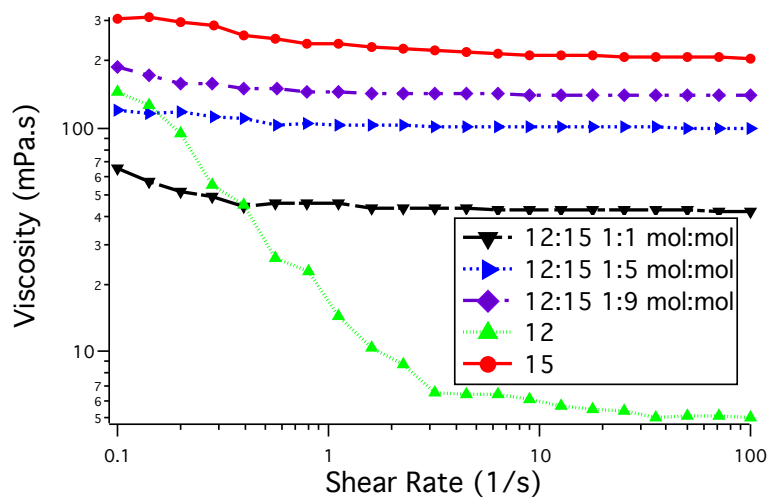


Figure S14: Viscosity of monomer mixtures (molar ratio **12**: **15** = 1 : 1; 1 : 5; and 1 : 9) in comparison with the pure monomers measured at 60°C as function of shear rate.

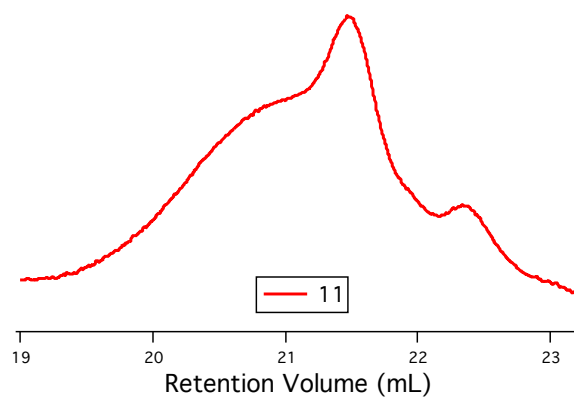


Figure S15: GPC chromatogram of the polymer made of 9,10-epoxystearic acid methyl ester (**11**) (poly-**11**: $M_n = 2050 \text{ g} \cdot \text{mol}^{-1}$; $M_w = 4300 \text{ g} \cdot \text{mol}^{-1}$; $\bar{D} = 2.1$).

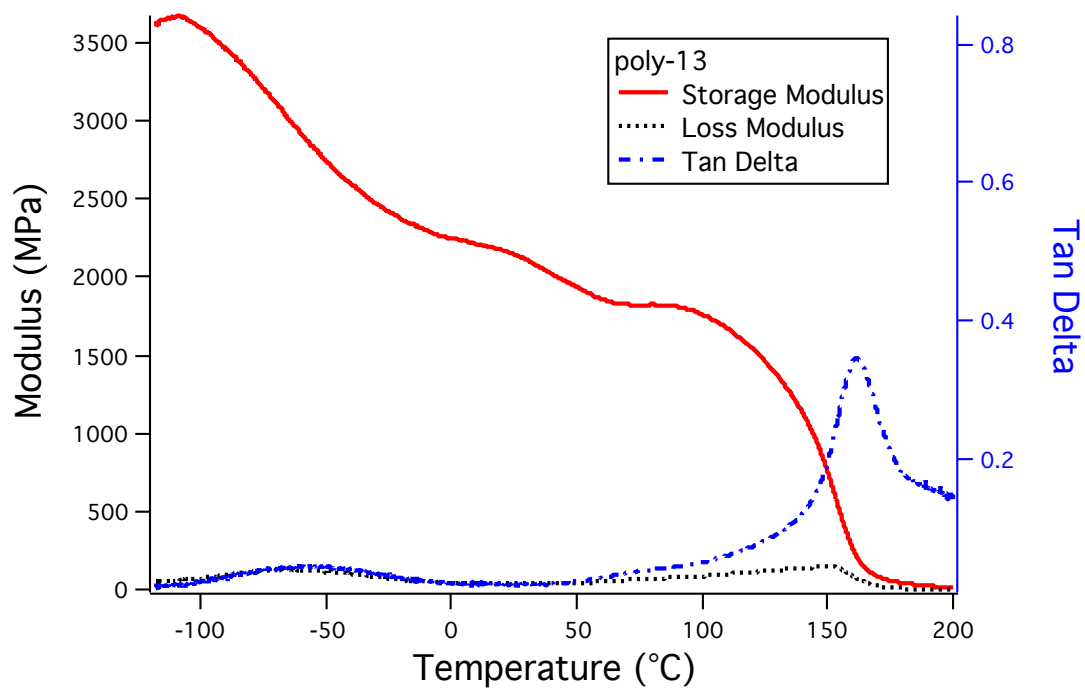


Figure S16: DMA measurement of the poly-13.

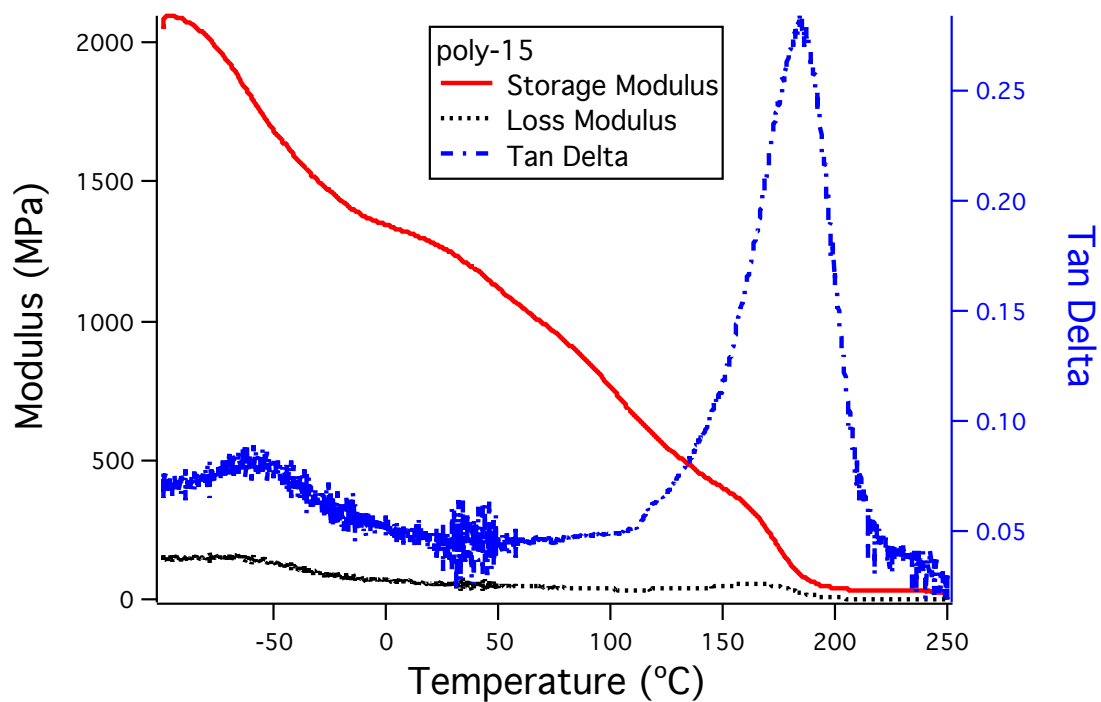


Figure S17: DMA analysis of poly-15.

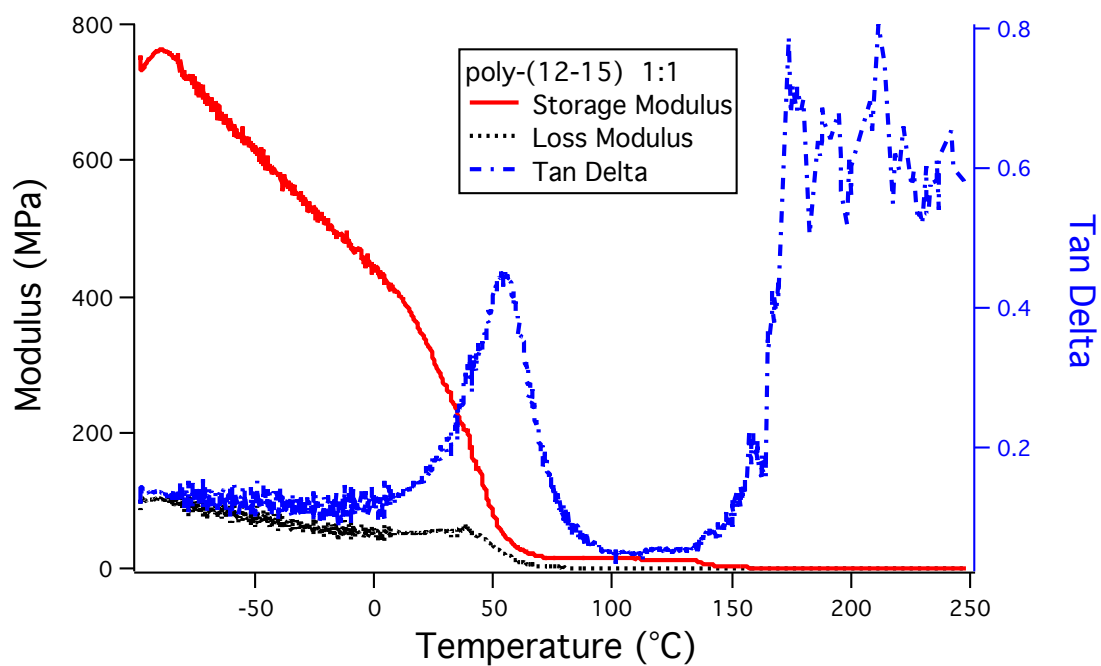


Figure S18: DMA measurement of copolymer of 12: 15 (1:1, mol:mol).

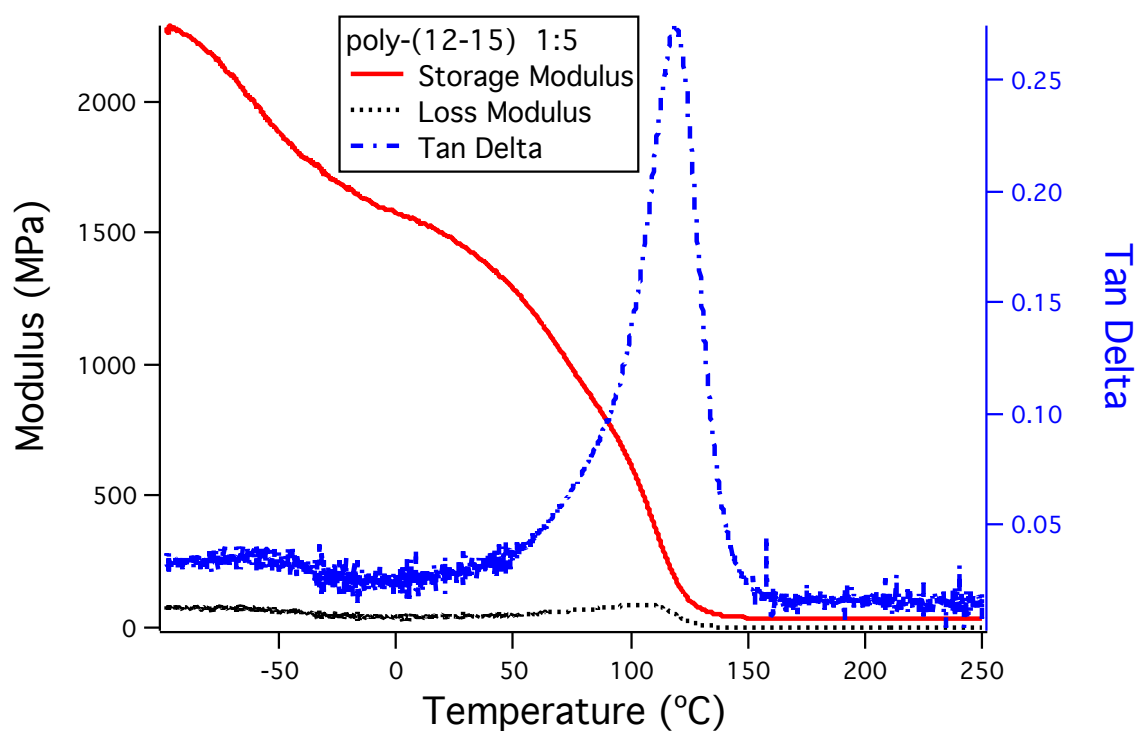


Figure S19: DMA measurement of copolymer of 12: 15 (1:5, mol:mol).

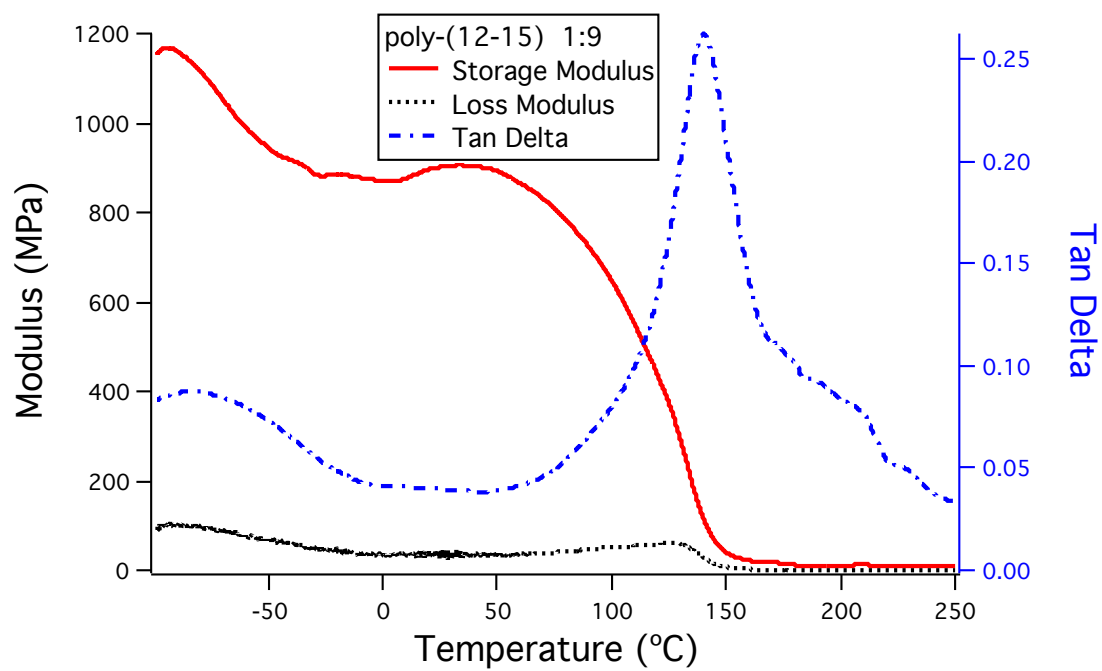


Figure S20: DMA measurement of copolymer of **12: 15** (1:9, mol:mol).